Assessment and Control of Virological Risk in Reclaimed Water Treated by Soil Aquifer Treatment

Thuangsit DENPETKUL

2016

Abstract

This study was performed to estimate the potential of human enteric viruses especially enteric adenovirus (AdVF) and rotavirus (RV) in the reclaimed water treated by soil aquifer treatment (SAT) with short retention time. The operation of SAT under a short retention time (up to 2 months) is more practical in the limited space area, but challenging. Interestingly, previous study showed that chemical pollutants, dissolved organic carbon (DOC) and fecal coliform were effectively removed even in short retention time of SAT. However, no information of human enteric virus reduction in SAT under a short retention time has been reported. Then, the board objective of this study is to quantify the viral risk of reclaimed water treated by SAT with short retention time.

The first specific objective was to study the effects of temperature, virus type and soil type on virus inactivation and adsorption by soil in batch experiments. Batch experiments of virus adsorption and inactivation were tested with treated sewage and sand or weathered granite soil and control sample (only treated sewage). Results showed that AdVF adsorption was higher than RV in both soil types (sand and weathered granite soil). It is due to the isoelectric point of virus that brings about higher adsorption of AdVF. Nevertheless, present study reveal that overall virus removal under the different temperature ranged between 4 and 37 ˚C was similar (p=0.05), indicating temperature effect on virus removal was less significant in this study. For virus inactivation experiments, AdVF and RV followed the first order decay rate. The inactivation rate of RV in sand was fairly higher and ranges between 0.075 and 0.114 day^{-1}. Interestingly, results indicate that RV was more inactivated than AdVF under almost conditions either in sand, weathered granite soil or treated sewage. In addition, another observation showed that inactivation of both viruses in samples with soil seemed to be lower than the water sample that without soil (control sample) this might reveal that sand and weathered granite soil could protect AdVF and RV from inactivation process.

The second specific objective was to investigate the removal and inactivation of AdVF and RV during SAT with short retention time. A pilot plant column of SAT has been set up closed to A2O wastewater treatment plant. SAT was operated at constant rate of around 46 mL/min corresponding to 28-day of hydraulic retention time (HRT). This SAT column was directly and continuously fed with treated A2O water. The influent and effluent of SAT were taken twice a month for over 2 years. The concentrations of AdVF and RV in samples were detected by q-(RT)-PCR and ICC-(RT)-PCR. Results showed that few infectious AdVF and RV were detected in SAT effluent samples. In terms of virus reduction based on genomic detection, the removal of AdVF and RV of this pilot-scale SAT are in the range of 0.09 to 2.24 $\log_{10}$ (mean 0.72-log10) and 0.00 to 1.45 $\log_{10}$ (mean 0.15-log10), respectively. However, the overall removal are slightly increase when integrate the removal from inactivation. For example, the overall reduction of AdVF is approximately 1.28-2.03 $\log_{10}$ and of RV is approximately 0.43-0.96 $\log_{10}$. The key findind, including virus concentration and inactivation coefficient, are integrated into one- and two- dimensional virus transport model as input parameters in later objective in order to simulate the virus transport in SAT at the target area.

The third specific objective was to simulate the virus reduction profile of SAT located at Katsura River Basin, Kyoto, Japan by using the numerical virus transport model. The 2-D virus transport model was used as a predictive tool for simulating the virus reduction in SAT from treated municipal wastewater through SAT at Katsura River Basin. The conditions (injection flow rate, distance between pumping and abstraction) of SAT were varied into 9 cases for virus reduction simulation. The model required the specific input data (specific condition of virus, water and soil type and groundwater velocities) to make an accurate prediction of the virus reduction in SAT. The virus inactivation coefficient was obtained from batch experiment, whereas the virus irreversible removal coefficient is estimated by one-dimensional transport model, which calibrated from the data of the column experiment. Subsequently, these parameters, including, simulated groundwater velocity in the target area, virus concentration, virus inactivation and removal coefficients were incorporated to perform predictive simulation by 2-D model. Results showed that the best simulation case in terms of the highest virus reduction was in the case of 200 m with 500-m^3/day injection flow rate corresponding to approximately 6 months of HRT. From this case, the model provided a highest virus reduction at the withdrawal point (7.12 $\log_{10}$ and 7.23 $\log_{10}$ of AdVF and RV, respectively). However, in terms of application the long HRT may be not practical for Japan. Thus the case of 50 m and 500-m^3/day injection flow rate seem to be more appropriate, good virus reduction (1.52 $\log_{10}$ and 1.54 $\log_{10}$ of AdVF and RV, respectively), having short HRT (25 days), and providing acceptable water recovery.

The forth specific objective was to perform the virological risk assessment in the reclaimed water by applying QMRA approach. This consists of viral risk assessment of reclaimed water by QMRA obtained the data from virus transport model, yearly infection risk of viruses in the reclaimed water, uncertainty analysis according to the unit of dose harmonization and the additional water treatment requirements for human safety. The results of AdVF and RV yearly infection risks in reclaimed water treated by SAT when implemented in the Katsura River Basin seem to be over the acceptable risk in all selected cases. Therefore, to achieve the acceptable risk level of drinking water, an additional water treatment must be integrated. For example, typically, advance oxidation processes are carried out for the reclaimed water. Nevertheless, UV treatment and chlorination may be more interesting because of lower energy consumption and simple processes.

This study introduced that the numerical transport model and viral risk assessment are very useful tools to provide significant information for a decision maker of SAT project. Even though this study suggests that Reclaimed water from Soil Aquifer Treatment system with short HRT could not completely meet the acceptable level of 10^{-4} infection/person/year in QMRA, SAT is still be a good alternative technology for water reclamation. From this perspective, the development and improvement of SAT is obviously required.

Acknowledgements

I would like to express my deepest thanks to my supervisor, Prof. Sadahiko Itoh for his kindness and thoughtful guidance and giving me several valuable comments. Also, I am really thankful for giving me a lot of opportunities attending international conferences. The lessons I have learnt from him might be useful for my future.

I would like to express my special thanks to Assoc. Prof. Shiya Echigo and Assoc. Prof. Yumiko Ohkouchi for their useful and valuable advice me and teaching me when I met some obstacles. I am so thankful to my sub-supervisor, Assist. Prof. Yasuhiro Asada, for valuable advice, patience and taking a great care of me all along. My research cannot complete without his help. Without their guidance, my research also cannot be successful completion. I am obliged to you for your patience and invaluable advice.

I wish to thank my committee members Prof. Minoru Yoneda and Assoc. Prof. Fumitake Nishimura for their useful advices in my research. Also, I would like to express my sincere thanks to Prof. Shigeo Fujii who introduced me to Kyoto University.

My Ph.D work has never come to successful completion without the contributions of my colleagues and the members of Itoh laboratory: Mr. Keita Kunimoto, Mr. Tatsuya Yamaguchi, Mr. Shingo Ito, Mr. Takashi Sakakibara, Mr. Yumeto Utsnomiya and Mr. Kosuke Nagai for their exchange of scientific knowledge and other support. I will never forget the friendship of all these people. I also would like to thank other members who usually support me and but I did not mention here. I am so thankful to Miss Kaori Kawai, Dr. Songkeart Phattarapattamawong, Dr. Suphia Rahmawati, Dr Liang Zhou, Mr. Vu Kiem Thuy, Mr. Kai He and Mr. Tomohiro Nakanishi, Mr. Yosuke Tanoue, and Miss Xinyi Zhou for their comfort communication and support me in some daily needs.

My research was financial supported by CREST project and I would like to thank the Toba Water Environment Conservation Center in Kyoto city for providing the space for SAT pilot plant for our research. I also thank to Japanese government that provide me a scholarship for my Ph.D. level in Japan.

Last but not lease I am indebted to my entire family. Without their supports, it would have been simply impossible for me to overcome so many difficulties, many more than I had expected before. A million of thanks to all of them, I love our family and life with them is full of happiness and blessing. Thank you so much for doing your best to support me in all my needs.

Table of Contents

List of Figures

List of Tables

Chapter 1

Introduction

1.1 Background

Clean water supply is a fundamental element for every our day life. However, water deterioration and depletion have become increasingly severe in a global scale as a result of an accelerated population growth, rapid urbanization, and climate change. Therefore, water reclamation and reuse have become important to solve the problems of water stress and water shortage in many areas, especially in urban areas. Water reclamation has been introduced as an important multidisciplinary component in water resource development and management. There are several successful reclaimed water cases in California, USA and NEWater, Singapore from treated municipal wastewater to indirect potable purposes (Rodriguez et al., 2009). However, these processes typically consume high energy and, in many cases, produce excess treatment) (Lazarova et al., 2013).

This introduces a practical water reuse concept of the combination of Wastewater Treatment Plant (WWTP)- Soil-Aquifer Treatment (SAT)- Drinking Water Treatment Plant (DWTP) as shown in Figure 1.1. WWTP and DWTP are well-known for water purification depending on the source of water treatment and water standards. SAT is the natural system-related technology. It is considered as an attractive technology to enhance the reclaimed water quality because of not only its cost-effectiveness, but also its reliability for water purification. That is, sorption and biodegradation process in SAT can remove a large number of contaminants including chemicals and pathogenic microorganisms in water environment.

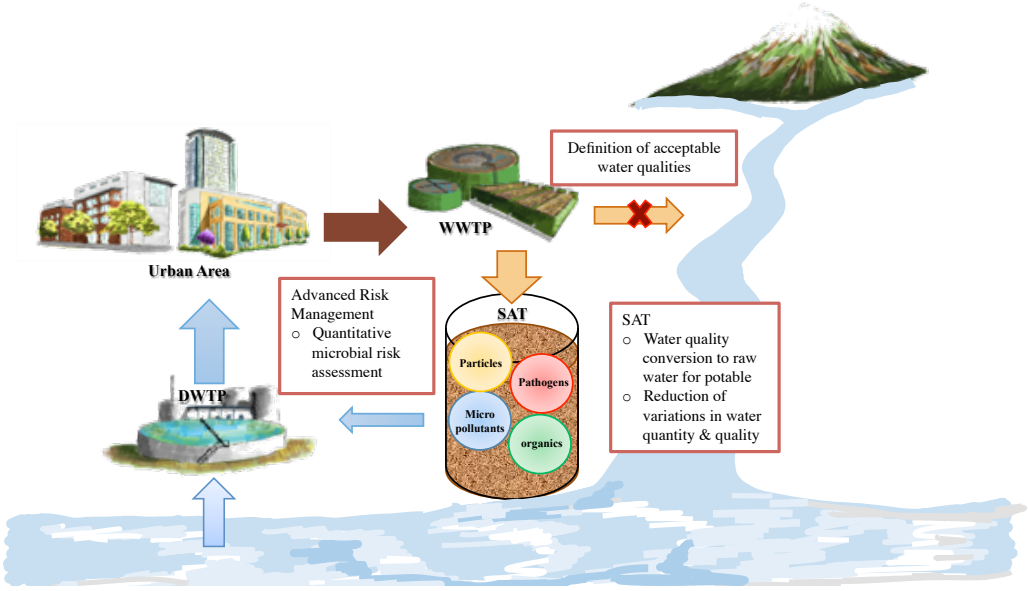

Figure 1.1: Conceptual diagram of WWTP-SAT-WTP for water reclamation

Figure 1.1 illustrates the key concept of the water reclamation system by the combination of WWTP-SAT-WTP. Based on the definition of acceptable water qualities, reclaimed water concerns contaminants such as enteric pathogens and micro-pollutants in the treated water, especially in municipal treated wastewater. Although SAT plays a significant role in purifying water and reduces the variation of water quality and quantity, the advanced risk assessment (quantitative microbial risk assessment (QMRA)) is also necessary to examine the safety of the reclaimed water process for human consumption.

As previously mentioned, SAT has been used to purify treated wastewater to provide potable water worldwide (Amy et al., 2007). Adequate travel times and distance are considered to be the crucial factors to ensure production of safe drinking water (Schijven & Hassanizadeh, 2000). Typically, a long retention time (≥6 months) is recommended to ensure efficient removal of treatment, which requires a large area. Therefore, it may not be practical for a limited space (i.e. in Japan). The operation of SAT with a short retention time has a potential as a treatment step, but is challenging in the control of chemicals and pathogens removal. For SAT with short retention time (≤2 months (Fox, 2001)), chemical pollutants such as Pharmaceuticals and Personal Care Products (PPCPs), Dissolved Organic Carbon (DOC) were effectively removed

(Echigo et al., 2015 and Takabe et al., 2014). Moreover, bacteria such as fecal coliform also were effectively inactivated (Yasukawa et al., 2014). However, there is a lack of information on human enteric virus reduction in SAT.

1.2 Research goals and objectives

This study aims to quantify the potential risk of human enteric virus in reclaimed water through the SAT system with short retention time approximately 1 month. Target pathogens are enteric adenovirus and rotavirus. They were chosen because among human enteric viruses, rotavirus (RV) and adenovirus F (AdVF) are the leading agents of gastroenteritis in children (Cruz et al., 1990). Also, AdVF is abundant in the sewage and secondary treated sewage, turning it into a potential health risk in the water reuse system (Haramoto et al., 2007).

The experiments were set up in batch and pilot scales, in order to collect all the data for achieving the viral risk assessment, including the concentration of virus occurrence in treated effluent from wastewater treatment plant combined with pilot-scale SAT, the virus inactivation rate coefficient quantified during the batch experiment and the virus removal rate coefficient obtained from the pilot-scale SAT will be applied to estimate the virus reduction in the implemented area. Then, the virus profile in the effluent is simulated by a numerical transport model. Subsequently, quantitative microbial risk assessment (QMRA) is performed to estimate the viral risk in the treated water via the SAT.

The specific objectives of this study are:

1. To study the effects of temperature, virus type and soil type on virus inactivation and adsorption by soil in batch experiments.
2. To investigate the removal and inactivation of AdVF and RV during SAT with short retention time.
3. To predict the virus reduction profile in a hypothetical SAT in Katsura River Basin, Kyoto, Japan by using the numerical virus transport model.
4. To perform the virological risk assessment of the reclaimed water by QMRA approach.

1.3 Framework of the study

The purpose of this research is to evaluate the viral risk in the reclaimed water as mentioned previously. Thus, the removal and inactivation of human enteric viruses (AdVF and RV) in the pilot plant of SAT system were estimated, at Toba wastewater treatment plant in Kyoto City, over one-year period. The pilot plant SAT, aimed at evaluating its treatment capability with short retention time, (approximately one month) is connected subsequently to treated A2O system. The pathogens and biogeochemical parameters such as temperature and soil type are analyzed. While the correlation among virus removal, temperature and soil types are examined under batch experiments. Then all parameters are incorporated into a virus transport model in order to simulate the virus concentration profile at the extraction point. Subsequently, this information is applied to the risk assessment, based on the QMRA framework. Finally, the virological risks associated with the water reclamation treated by SAT are discussed. The overall steps such as virus concentration, detection techniques, virus transport model and viral risk assessment model are shown in Figure 1.2.

This dissertation contains the following chapters: the current chapter describes the background information and addresses the research conducted, including the objectives of the study and study framework. The relevant literature reviews is described in Chapter 2 were explained regarding the current of water reclamation around the world, Soil Aquifer Treatment (SAT), Removal of pathogens in SAT, virological risk control in reclaimed water by SAT and required data for the virological risk assessment in this study. In Chapter 3, the virus adsorption and inactivation in batch experiments are conducted in order to explore the adsorption and inactivation kinetics coefficient based on isotherms and model. In Chapter 4, the virus concentration in the SAT influent and effluent samples are measured including genome based concentration and infectious concentration. Then, the virus removal and inactivation are estimated. Chapter 5 studies the virus transport model and their concentration profile in the Katsura River basin. All input parameters from the previous chapters are put into the model and the estimation of virus concentration output is conducted by Python and Mathematica. In Chapter 6, the characterization of the parameters is investigated to fulfill the numerical modeling of adenovirus and

rotavirus removal during the SAT. Subsequently, the human health risk related to rotavirus and adenovirus in the drinking water process is evaluated. Finally, Chapter 7 summaries the major findings of this study.

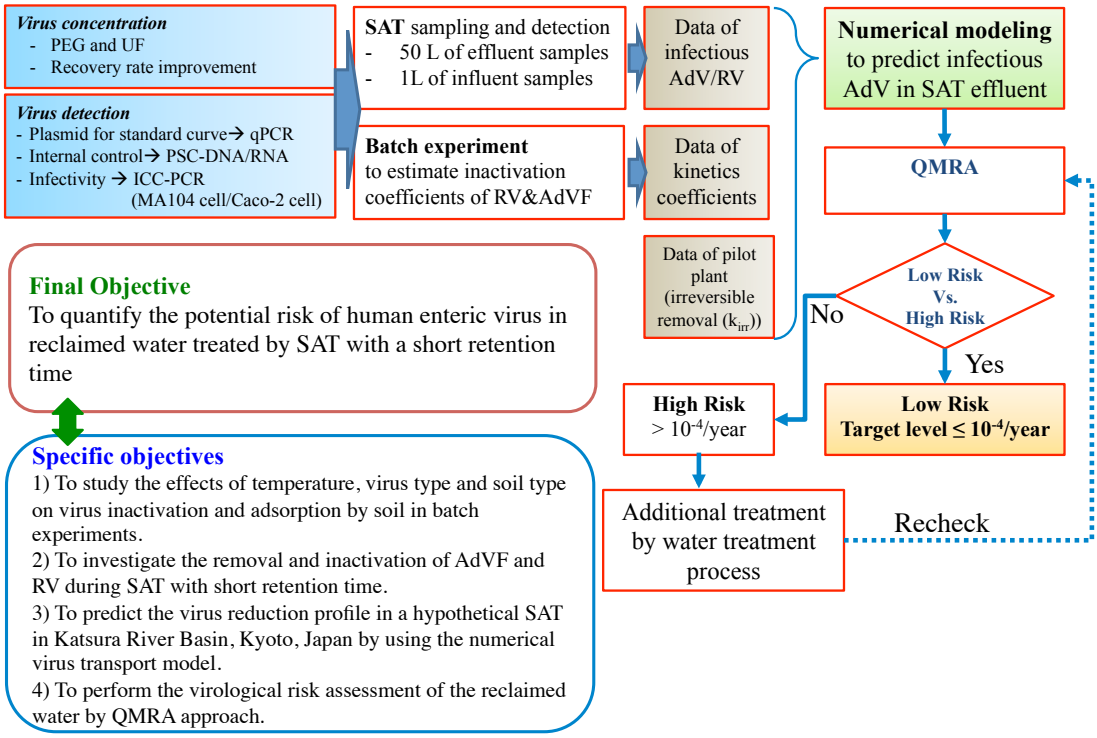

Figure 1.2: the overall framework of this study

References

Cruz J. R., Caceres P., Cano F., Flores J., Bartlett A. & Torun, B. 1990 Adenovirus types 40 and 41 and rotavirus associated with diarrhea in children from Guatemala. Journal of Clinical Microbiology, 28(8), 1780-1784.

Echigo S., Nakatsuji M., Takabe Y. & Itoh S. 2015 Effect of preozonation on wastewater reclamation by the combination of ozonation and soil aquifer treatment. *Water Science & Technology: Water Supply,* **15**(1), 101-106.

Haramoto E., Katayama H., Oguma, K. & Ohgaki S. 2007 Quantitative analysis of human enteric adenoviruses in aquatic environments. *Journal of Applied Microbiology,* **103**(6), 2153-2159.

Lazarova V., Asano T., Bahri A. & Anderson J. 2013 Milestones in water reuse: the best success stories. *Water Intelligence Online,* **12**, 9781780400716.

Rodriguez C., Van Buynder P., Lugg R., Blair P., Devine B., Cook A., & Weinstein P. 2009 Indirect potable reuse: a sustainable water supply alternative. *International Journal of Environmental Research and Public Health,* **6**(3), 1174-1203.

Schijven J. F. & Hassanizadeh S. M. 2000 Removal of viruses by soil passage: Overview of modeling, processes, and parameters. *Critical Reviews in Environmental Science & Technology,* **30**(1), 49-127.

Sharma S., Harun C. & Amy G. 2008 Framework for assessment of performance of soil aquifer treatment systems. *Water Science & Technology,* **57**(6).

Takabe Y., Kameda I., Suzuki R., Nishimura F. & Itoh S. 2014 Changes of microbial substrate metabolic patterns through a wastewater reuse process, including WWTP and SAT concerning depth. *Water Research,* **60**, 105-117.

Yasukawa T., Asada Y., Kunimoto K., Ojkouchi Y. & Itoh S. 2014 An estimation of disability adjusted life years associated with indirect potable reuse based on the occurrence of *Campylobacter Jejuni*. *Journal of Japan Society of Civil Engineering, Ser. G Environmental Research,* **70**(7), 285-294.

Chapter 2

Literature Review

2.1 The purpose of this chapter

This chapter introduces the current state of water reclamation as an essential element of sustainable water use. Among water reclamation technologies, Soil Aquifer Treatment (SAT) system has been considered as an alternative and are been used worldwide. However, waterborne pathogen, especially viruses, are a major concern of water reclamation technology. Therefore, the overview of virus transport through SAT and the primary factors influencing virus transport will be described in this chapter. After that an overview of the numerical modeling of virus transport in the SAT will be reviewed. This numerical modeling is an essential tool for conducting the quantitative microbial risk assessment (QMRA). Moreover, the overview of QMRA for the reclaimed water treated by the SAT in this study is described.

2.2 Current issue of water reclamation in the world

2.2.1 Issues of water reuse

Water shortage has become a serious problem in global scale, caused by fast population growth and freshwater deterioration in many areas. Over 50 per cent of European countries are facing with water stress issues. In 2025, the world population may reach to around 2.4 billion (Zeman et al., 2006), and this will cause an extremely severe water stress problem in many areas (Zeman et al., 2006). To solve this problem, water reclamation and reuse may play an important role in water management, which will probably account for 25 to 60% of the water demand in the next 100 years (Levine & Asano, 2004). Treated municipal wastewater has been considered to be a good alternative water resource for water reuse and reclamation for two reasons: firstly, such treated wastewater has to meet the water quality standard before disposal into environment according to the regulation and reducing of environmental impact: secondly, the amount of treated wastewater is proportional to the population, and managed water reuse could fulfill the water demand of such an area in a sustainable way.

2.2.2 Wastewater reuse and reclamation

Wastewater reclamation is the treatment of wastewater to improve its quality suitability for reuse in various purposes. Reclaimed water may be used either directly or indirectly. The direct reuse requires conveyance facilities to redirect the treated wastewater back to use. Whereas indirect reuse is usually employed by discharging a treated effluent into receiving water and subsequent withdrawals in downstream. Indirect reuse has been used for several decades. However, most of these applications have not been planned, which resulted in water streams with no condition control. Nevertheless, at the present the implementation of water reclamation is focusing only on planned direct and indirect water reuse. For example, the reclaimed water may be blended or diluted with raw water prior to treatment in the water treatment plant.

Originally, the existing standards for drinking water have been developed under the condition that raw water has high quality. Therefore, only significant parameters are monitored and controlled. On the other hand, reclaimed water may contain various contaminants, including microorganism and trace compounds, which could affect directly human health (Ahuja, 2014). Therefore, water reclamation from sewage and treated sewage should be concerned about the risk of contaminants.

2.2.3 Water reuse system cases

Water recycling around the world: there are many places around the world that recycled water is added to their drinking water supplies. The key difference between the methods is where they put the recycled water. Advanced water treatment technologies have been incorporated into the water reclamation system, such as ultrafiltration (UF), nanofiltration (NF) and reverse osmosis (RO). The water recycle cases around the world are shown in Table 2.1.

Table 2.1: The water recycle cases around the world modified from Po et al., (2003); Jimenez & Asano, (2008)

Recycle water project	Country	Treatment	Source
Western Corridor	Queensland, Australia	micro-filtration, reverse osmosis and ultraviolet disinfection with hydrogen peroxide disinfection (advanced oxidation)	domestic and industrial wastewater
Groundwater Replenishment System	California, The USA	aquifer treatment, micro-filtration, reverse osmosis and ultraviolet disinfection with hydrogen peroxide disinfection (advanced oxidation)	domestic and industrial wastewater
Windhoek	Namibia	ozonation, activated carbon filtration, ultrafiltration and chlorination	domestic and industrial wastewater
NEWater	Singapore	ultrafiltration and microfiltration, reverse osmosis and ultraviolet disinfection	domestic and industrial wastewater
Hampton Water treatment works-London	England	advanced water treatment using rapid gravity filters, ozone treatment and sand filters	water from the River Thames, stormwater and industrial wastewater

2.2.4 the problems of RO and AOP system for water reuse

Basically, the conventional drinking water system consists of a series of treatment units to remove contaminants from water. For instance, the filtration and coagulation units may effectively remove the protozoa and some enteric pathogenic bacteria. Then conventional processes end up with a disinfection unit, such as chlorination. However, for a very small size of virus particles, these treatment processes may not completely remove the viruses form water. Advances in water treatment technologies have been incorporated into the water reclamation system, such as ultrafiltration (UF), nanofiltration (NF) and reverse osmosis (RO). Even though these advanced membrane treatment systems can effectively remove not only toxic pollutants but also the essential minerals, due to the high initial cost to and the high-energy consumption to have them functioning, their implementation is highly constrained.

The use of advanced techniques (e.g., RO) tends to result in over treatment. This is especially true for developed countries. A typical example is the combination of RO and advanced oxidation process (AOP) for water reclamation in the southern California (Po et al, 2003). The system is safe and achieves the drinking water standard level, but the system requires, high cost and high energy consumption. Another example is NEWater project in Singapore where highly purified water produced from treated wastewater using advanced membrane technology. The NEWater factories combine many stages of treatment involving micro-filtration (MF) or ultra-filtration (UF) continued to RO and UV disinfection. (Lazarova et al., 2013). The NEWater currently constitutes 30% of Singapore's total water demand and is for direct non-potable use. It is more expensive to produce NEWater than the common drinking water treatment plant. In Singapore, the NEWater factories consume 0.72-0.92 kWh/m^3 to produce drinking water from municipal effluent (Bodik & Kubaská, 2013). However, the cost for treating and transporting potable water is approximately 0.52 KWh/m^3.

The main concept of pathogens control has been changed. That is to increase the safety and reliability of reclaimed water quality for potable use, multiple barriers have been applied, rather than relying on a single process (Metcalf et al., 2007). The reason for this is related to the fact that in an event of the failure of one unit, another unit will still be available to provide the adequate quality of water. A few decades ago, most efforts were aimed into finding sustainable processes that relied on natural treatments. Recently, it has been recognized that a natural treatment system such as soil aquifer treatment (SAT) could remove several kinds of pollutants, including pathogens, from treated wastewater. Therefore, this technology is more attractive, when compared with advanced membrane filtration, due to the fact that it requires less energy and avoids overtreatment.

2.3 Soil aquifer treatment (SAT)

SAT is a geo-purification technology that relies on natural processes. SAT involves a variety of mechanisms that effectively improve water quality when secondary treated wastewater percolates through soil layer and subsequent storage and transport in the underlying aquifer (Bdour et al., 2009). It can provide satisfactory quality water when combined with other suitable wastewater treatment system (Sharma et al., 2008).

Several pollutants, including organic compounds, suspended solid (SS), heavy metals, bacteria and viruses can be effectively attenuated or transformed by sorption, chemical reaction, biotransformation, die-off and predation processes during SAT. A previous study revealed that passing treated wastewater through SAT could minimize groundwater pollution (Martin & Koerner, 1984).

SAT has been operated in many areas for indirect potable reuse, followed by tertiary filtration. It has been acknowledged that the quality of SAT treated effluent for reusing secondary wastewater was probably equal to or even better than that of a conventional tertiary wastewater treatment plant (Amy et al., 1993). Moreover, SAT can have a major advantage for the underground storage of reclaimed water for future use (Asano & Cotruvo, 2004). Therefore water reclamation using SAT has been proposed as an alternative technology for our future. The chemical can be removed by adsorption and biodegradation in SAT system. Several studies have shown that total organic carbon (TOC) in effluent is significantly reduced by SAT (Quanrud et al., 2003). Moreover, it also removed DOC more than 90 % especially in the vadose zone (Quanrud et al., 2003). Estrogenic compounds such as estriol and 17β-estridiol) are mainly removed by 80-90% by adsorption, but some chemicals such as nonionic-surfactants (APECs) are need more than 6 months for its removal (Drews et al., 2003)

With respect to pathogenic microorganisms including protozoa, bacteria and virus, although past studies revealed that some pathogens could be removed during soil passage (Asano & Cotruvo, 2004; Schijven & Hassizadeh, 2000) the mechanism of pathogen removal is not clearly known yet. For instance, the enteric viruses such as rotavirus are removed in a small amount level by the SAT, whereas MS-2 (bacteriophage) can be inactivated under unsaturated conditions (Jin & Yates, 2002). Moreover, pathogens especially viruses are not permanently immobilized on soil particles, as they can be remobilized, due to a change of water quality. Previous studies revealed that a major factor involved in pathogen removal in soil aquifer treatment is the retention time during transport throughout soil layer. Factors influencing the microorganisms transport are complicated and site-specific, This is the main reason why pathogen removal is different among various soil surfaces, vadose zones and saturated aquifers. Generally, the retention time more than 6 month is

recommended to ensure the pathogen removal especially virus in the SAT (Metcalf et al., 2007).

The long retention time as mentioned required a large area; however, it may not be practical for a limited area such as Japan. The removal of chemicals during SAT was studied in several studies. SAT with 1-month retention time showed an effective removal of DOC (Takabe et al., 2014). Similarly, the considerable removal of several chemicals such as pharmaceutical personal care products (PPCPs) and 1,4-dioxane in treated sewage through SAT without ozonation were achieved under a short HRT (7 days) (Echigo et al., 2015), resulting in safe water for drinking purpose. For the microorganisms, most bacteria were effectively removed by SAT with a short retention time (Yasukawa et al., 2014). Yasukawa (2014) found that fecal coliform could be removed by more than 6-$\log_{10}$ in SAT with an HRT of one month. However, there is a lack of information on human enteric virus reduction in SAT, especially with a short retention time. Thus, it is very important to study the viral removal and its risk of the reclaimed water and to understand the virus removal mechanism

2.4 Removal of pathogens in SAT

2.4.1 Pathogens reduction in the SAT system

Past studies suggest that most pathogen removal occurs near soil surface and it decreases in deeper layers, which described as a power function (Pang, 2009). Previous studies in a laboratory scale suggested that the effective column length for virus removal is at least one meter and if the column below one meter is exploited, the virus removal rate can be unreliable (Pang, 2009). Table 2.2 includes the pathogen reduction by SAT in the various studies.

Table 2.2 Pathogenic microorganism attenuation in SAT

	Microorganisms	Column condition	Log removal	Length of column	Log removal /meter	Reference
bacteria	*Campylobacter* spp.	Sand, saturated	>6.0	-	-	Page et al. (2010)
	E.coli	Sand, saturated	4.1-4.8	0.5	8.2-9.6	Hainan et al. (2005)
	Bacteria	Sand, saturated	2.0	0.5	4.0	Deflaun et al. (1997)
	Bacteria	Sand, saturated	4.7	0.02	235	Deflaun et al. (1997)
	Fecal coliform	Sand, unsaturated	5.1-6.8 (average=5.6)	2.4	2.3	Yasukawa 2014
protozoa	Cryptsporidium	Sand, saturated	0-0.9 (average0.4)	-	-	Page et al (2010)
	protozoa	Sand, saturated	2.9	3.6	0.81	Harvey et al. (1995)
	protozoa	Sand, saturated	2.9	0.6	4.87	Harvey et al. (1995)
virus	rotavirus	Sand, saturated	0-0.8 (average 0.2)	-		Page et al. (2010)
	MS2 bacteriophage	Sand, saturated	1.3-3.4	0.5	2.6-6.8	Hijnen et al. (2005)
	MS2 bacteriophage	Sand, saturated	3.3	3.8	0.87	Schijven et al. (1999)
	MS2, PRD1 bacteriophage	Sand, unsaturated	2.0-3.0	0.6	3.3-5.0	Van Cuyk et al. (2004)
	Coliphage	Sand, unsaturated	1.0	1.0	1.0	Quanrud et al. (2003)
	F-RNA phages and coliforms	Coarse and fine gravel with sand	4.0	15	0.27	Medema et al. (2000)

The type of soil, infiltration, type of virus and the degree of soil saturation are most important parameters controlling virus transport and removal. Thus SAT requires a large area or sufficient retention time to ensure the contaminants prevention (Metcalf et al., 2007). Retention time is the time interval during the reclaimed water augmentation till the time of withdrawal for intended use. For pathogen prevention, a retention time of more than 6 months is recommended by the US artificial recharge guidelines (Metcalf et al., 2007). In a similar example, California's guideline suggested that retention time for reclaimed water introduced to aquifer by directly injection on the basin, should be 6 and 12 months, respectively. Nevertheless, this requirement may not be practical in a limited space. This seems to be the major constraint for SAT to remove pathogens under short retention time.

Previous studies revealed that most bacteria and protozoa could be trapped in soil particles during passing through subsurface environment (Pedley et al., 2006). It

means that the process to remove bacteria and protozoa are filtration and adsorption that can occur rapidly. Thus, HRT with a short retention time should provide a high efficiency to remove bacteria and protozoa. Yasukawa (2014) studied the fecal coliform and *Campylobacter* removal during SAT with 1-month retention; the bacteria could be removed by more than 6-$\log_{10}$. For protozoa, their sizes (4-15 μm) are larger than bacterial (4-15μm) and virus (80 nm) (Abbaszadegan et al., 2003). Bacteria can be removed more than 6-$\log_{10}$; therefore, protozoa could be removed effectively in SAT as well.

For virus, their sizes are really small as shown in Figure 2.1. Thus, virus particles could move easily through the soil layer to groundwater. That is, it is more difficult to remove virus than other pathogens in SAT process. Moreover, ingestion of viruses can lead to illness. For these reasons, enteric viruses are likely to be of greater concern than bacteria and protozoa, and it is necessary to evaluate the health risk association with viruses in the water treated by SAT. The major concern of using the SAT is how to control the viral risks associated with water reuse system especially with a short retention time.

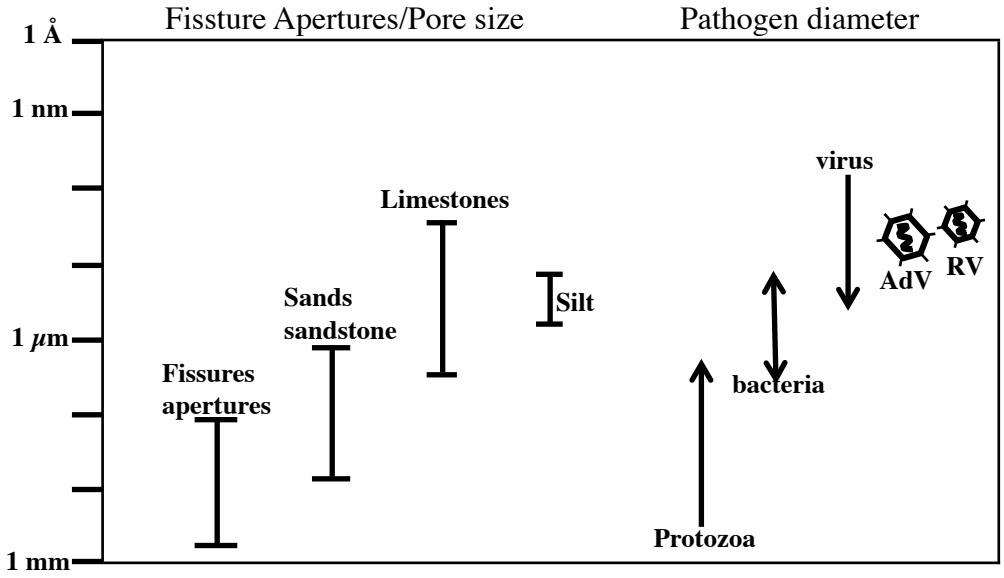

Figure 2.1: The size of pathogens (logarithmic scale) in relation to the properties of geological media (WHO, 2006)

2.4.2 Adsorption and inactivation of viruses in soils

By the point of view of pathogens transport in soil especially on viruses, the adsorption and inactivation rate are very important parameters.

a) Virus adsorption

Adsorption of virus in soil or subsurface depends on several factors. It may be influenced by changes in temperature, pH and presence of cations and anions in the surrounding medium and pathogen species (Matthess et al., 1988). The reversible process of pathogen adsorption is often described by the Freundlich isotherm (Burge & Enkiri, 1978; Matthess & Pekdeger, 1981; Tim et al., 1988). The Freundlich isotherm equation is shown as follows:

$$q = k_f C^{1/n} \tag{2.1}$$

where q = amount (microorganisms) adsorbed per unit mass of adsorbent (soil) C = equilibrium concentration of adsorbate (microorganisms) in solution after adsorption .k_f = empirical constants, n the term 'reversible' implies that adsorbed microorganisms may detach from the surfaces of soil particles and desorb in water. They may subsequently be readsorbed.

Other mechanisms that influence the virus reduction are sedimentation, trapping and filtration. Jin et al., (1997) suggested these terms could be denoted as extra sink term or irreversible removal of virus. It can be estimated by first order reduction equation.

b) Virus inactivation

Virus inactivation is the damage of genetic material that helps virus to replicate in the host environment. Virus structures have a nucleic acid and protein coat, that, when damaged or if degradation of the nucleic acid occurs, lead to virus inactivation as shown in Figure 2.2. Owing to protein deformation, virus loses its ability to bind the host receptor site, making it unable to reproduce itself in the host (Anders & Chrysikopoulous, 2005; Harvey & Ryan, 2004; Azadpour-Keeley et al, 2003).

Virus may have different inactivation rates when attached to the soil or subsurface. The degradation process may decrease due to the attachment of the microbe to the soil that protects the pathogen from the adverse condition in soil and helps it to go into and prolong its survival rate. However, in the case of strong binding between the virus

and soil, the damage of the virus structure may occur, leading to inactivation (Harvey & Ryan, 2004).

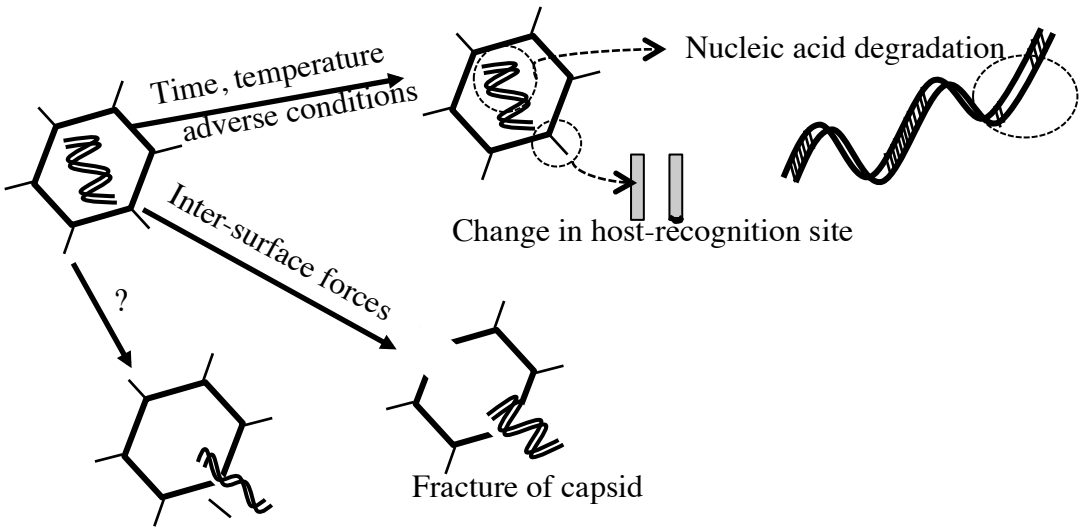

Figure 2.2: potential mechanisms of pathogens inactivation due to loss of genetic material (Harvey & Ryan, 2004).

Inactivation of virus is generally described as the time dependent first order decay with a constant rate coefficient (Harvey & Ryan, 2004), and can be shown as the exponential decay equation below:

$$C_t = C_0 e^{-\mu t} \quad or \qquad \ln\left(\frac{C_t}{C_0}\right) = -\mu t \quad or \qquad \log_{10}\left(\frac{C_t}{C_0}\right) = -\frac{\mu}{2.3} t \tag{2.2}$$

where C_t is the concentration of virus present after time t and C_0 is the initial concentration of the virus. μ is the inactivation rate coefficient (WHO, 2006).

The inactivation rate coefficients vary under the different conditions of subsurface, which results in viruses that have a varying inactivation under the different experimental conditions (WHO, 2006). Most literature data used in the numerical transport model is based on the first order inactivation constant rate of pathogens to estimate the pathogen removal or adequate retention time (Anders &

Chrysikopoulous, 2005). The literature data of pathogen inactivation rate constants for bacteria, virus and protozoa in groundwater are shown in Table 2.3.

Table 2.3 Pathogen inactivation rates in groundwater

Pathogens	**Inactivation rate constant (day^{-1})**
Bacteria	**0.044-1.700**
E.coli	0.044-0.980
Fecal Streptococci	0.066-0.850
Salmonella spp.	0.190-0.500
Shigella spp.	0.620-1.700
Klebsiella spp.	0.030-0.072
Virus	**0.010-1.600**
Poliovirus	0.010-1.600
Echovirus	0.019-1.400
Coxsackievirus A and B	0.012-0.490
Hepatitis A	0.038-0.410
Rotavirus	0.360-0.830
Protozoa cysts and spores	**Can survive in the environment for long (>70 weeks)**
Bacilus subtilis spores and *Clostridium perfringens* spores	0.071-0.138

2.5 Virological risk control in reclaimed water by SAT for its implementation

The risk assessment in the reclaimed water has been conducted in many studies for various target pathogens. For example, Toze et al., (2010) performed QMRA using the methodology described in the Australia Water recycling Guidelines (NRMMC, 2006), and published data for pathogen numbers in secondary treated wastewater in the unconfined aquifer recharge for irrigation. The study conceptual model was cooperated with the input data that is necessary for model input. The requirement input data such as the pathogens concentrations in the secondary treated effluent, the decay rate of the pathogens, the condition of the native groundwater in the area (dilution) needed to be added or assumed. Toze's study needed the *Campylobacter* and *Cryptosporidium* and rotavirus concentration in the secondary treated sewage water and their decay rates. The model was assumed that there was no mixing of the reclaimed water with native groundwater and no filtration and adsorption of the pathogens. The stochastic data on pathogen decay rates and aquifer residence times were derived in that study and then the pathogen risk assessment was estimated (Toze et al., 2010).

The present study also uses the same concept of Toze (2010) study. Thus, the pathogen concentration in the secondary treated sewage and decay rates are needed.

However, to increase the model accuracy for implementation, the virus transport model was used. It was not only decay rate or inactivation rate of virus but also focused on virus adsorption and irreversible removal (sedimentation and filtration) and the advection and dispersion effect in the groundwater that needed to add into the model input. Then the virus reduction in the SAT was simulation. After the virus transport model was conducted, the virus output data after SAT system continued to estimate the viral risk assessment by QMRA.

2.5.1 Model of microbial transport in soil or subsurface

The virus transport model generally accounts for virus inactivation and linear local equilibrium adsorption combined with the advection and dispersion equation, like solute transport in porous media (Chrysikopoulos et al., 1990). There are several model equations depending on the assumption. In this study, the advection, dispersion, irreversible removal and inactivation described by Schijven and Hassabuzadeh, 2000; Gitis et al., (2011) was selected with an assumption of one-dimensional, homogenous, steady-state water flow, saturated porous medium. The model definition and equation are described as below:

$$\frac{\partial C}{\partial t} = D\frac{\partial^2 C}{\partial x^2} - v\frac{\partial C}{\partial x} - k_{irr}C - \mu C \qquad (2.3)$$

where C (virus/L) is the spatially averaged concentration of viruses in the suspension; D (cm^2/day) is the coefficient of longitudinal dispersion; t (day) is time; v (cm/day) is Darcy velocity; x (cm) is the distance along the vertical axis, and virus irreversible removal rate k_{irr} (day^{-1}) and virus inactivation rate μ (day^{-1}) are the adsorption and inactivation rate constants, respectively.

2.5.2 Quantitative microbial risk assessment (QMRA)

QMRA was a powerful tool as described in the Australia Water recycling guidelines (NRMMC, 2006), and it was used for estimating the pathogen risks in secondary treated wastewater. As part of the four steps of this framework, including: Hazard identification, exposure assessment, dose-response assessment, and risk characterization. The output from each of these steps is fed into risk management, which is one of the key components of the risk analysis process. The Risk assessment is considered as a new scientific-based approach that allows the risk manager or policy maker to understand the probability of the occurrence of hazard events, as well

as, the probable adverse effect that such events will have. So far the risk assessment is increasingly applied for a wide range of activities not only for the economy and finance, but also the environment and health.

The QMRA was firstly introduced in the early 90's (Regli et al., 1991). The QMRA has been used to address the human health impacts of waterborne hazard, including viruses. The QMRA involves the infection risk that comes from the exposure to water-borne pathogens due to water consumption, recreational water activities, or eating aquatic food contaminated with pathogens. To conduct QMRA, four basic elements, explained below, need to be taken into account: Hazard Identification, Exposure Assessment, Effect Assessment (Dose Response) and Risk Characterization (WHO, 2004) as described followings.

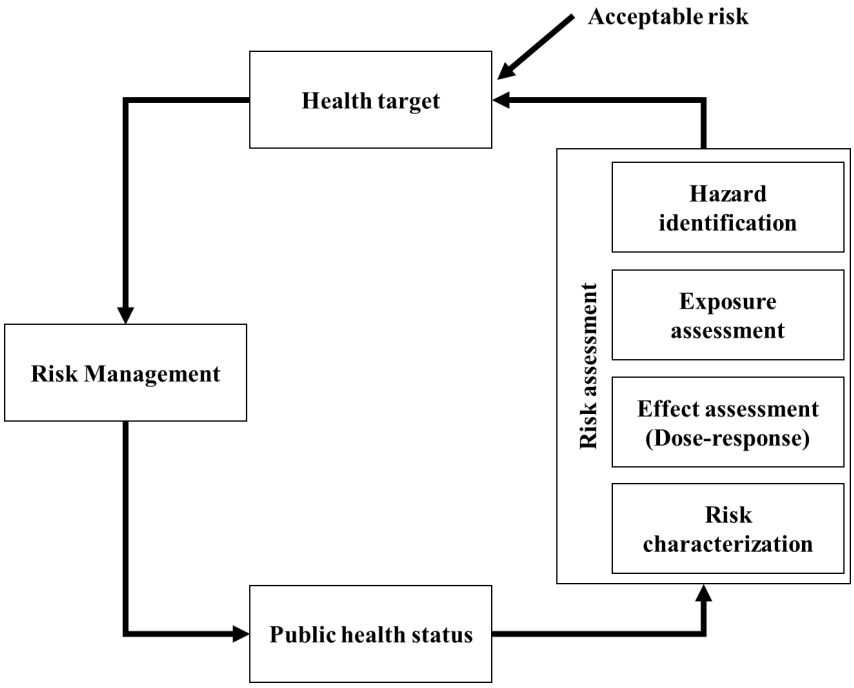

Figure 2.3: Risk assessment diagram (Microrisk, 2006)

Hazard Identification: The main purpose of hazard identification is to characterize the problem. In an example of waterborne pathogens, the characteristics of the specific pathogens related to waterborne transmission are described, such as the survival and persistency of pathogens in water and environment. Next, the primary transmission route related to waterborne outbreak should be described. In addition, the hazard identification also includes the description of illness, duration of illness and the susceptible group, caused by the pathogens.

Exposure Assessment: The purpose of an exposure assessment is to determine the microbial dose typically consumed by drinking water. Basically, exposure assessment requires the quantitative assessment of the pathogen levels (concentration) in source water and the probability of exposure to those waterborne pathogens. In assessing exposure, there are several factors involved, including the amount of virus in drinking water, the volume of consumption, the frequency and duration of the exposure. For example, to estimate the amount of ingested pathogens per exposure, a default value of drinking water consumption per person per day is 2 L, whereas, the occurrence of pathogens in a water source is collected in a catchment survey.

Dose-Response: the dose refers to the amount of viruses and the resulting adverse health effects. Dose-response model is developed from human and animal studies and estimated and predicted with mathematical models. There are two mathematical models, exponential and the beta-Poisson, which are commonly used to assess the risk of virus infection. Both mathematical models assume that the viruses are randomly distributed in the exposure.

Risk Characterization: the combined data in the previous steps are necessary to calculate the risk in this step. It is necessary to use Monte Carlo Analysis to estimate the full range of possible risk. Monte Carlo analysis is a simulation tool that provides the probability distributions for each parameter instead of point estimate.
The outcomes of previous steps have shown the result in distribution. It is necessary to use Monte Carlo Analysis to estimate the full range of possible risk. Based on these risk estimations, the advance treatment unit or recommendation may suggest the use of reclaimed water for indirect potable purpose. This result can make a decision for a policy maker or to require more treatment.

2.5.3 Application of QMRA in this study

1) Hazard Identification

Hazard Identification is comprised by the target pathogens and their concentration in the environmental media.

Target pathogens

Pathogens in the system could cause human illness and the type of illness should be gastroenteritis illness. QMRA focuses on a proper "index pathogens" that cover a range of health risk (Medema & Ashbolt, 2006). Viruses are significantly smaller than bacteria, and may move faster in SAT. The leading agents of gastroenteritis in children particularly are composed by viruses that are rotavirus (RV) and adenovirus-F (AdVF) (Cruz et al., 1990). In Japan, the gastroenteritis epidemic data reported that 70% of children under 2 years of age got infected by RV group A during the period from 2010 to 2013 (National Institute of Infectious Diseases (NIID) 2014). When applying a water reuse system, the health risk of RV group A for children may increase. AdVF has a potential health risk in water reuse system because AdVF is abundant in secondary treated sewage (Haramoto et al., 2007). Thus they were selected as the target pathogens in this study.

a) Adenovirus

Adenoviridae are a family of viruses that infect both humans and animals. The viruses are ~100 nm in diameter, have an icosahedral structure containing double stranded DNA, and do not possess a membrane. 52 serotypes of human adenoviruses are recognized and divided in 7 subgroups, designated from A to G, on the basis of their ability to agglutinate red blood cells (Percival et al., 2013). Generally, adenovirus type 40 and 41 from subgroup F infect the gastrointestinal tract. Incubation periods vary according to the serotypes and the site of infection. Respiratory illness and gastrointestinal disease can occur after a few days. Serotypes 40 and 41 are transmitted via fecal-oral spread. Their lack membrane gives adenoviruses the ability to resist ether and chloroform, but they are inactivated by chlorine (Thurston-Enriquez et al., 2003). The adenovirus is more resistant to UV light than enteroviruses (Hijnen et al., 2006; Medema, 2006). The viruses are stable in a pH range from 3 to 10 (Fong & Lipp 2005). Soil often has a pH 5 to 10, meaning that adenoviruses are stable in environmental soil. Furthermore, the viruses are resistant to intestinal enzymes and replicate in the epithelial cells of the intestine. The virus is an obligate intracellular parasite, and it is not able to replicate in the environment.

Previous studies detected adenoviruses in sewage water, and shellfish throughout the year in most of the investigated samples (Puig et al., 1994 and Pina et al., 1998). The

adenovirus is associated with the failure of the chlorination system in wastewater treatment plants.

b) Rotavirus

Reoviridae are a family of viruses that infect both humans and animals. The viruses are 75 nm in diameter, have an icosahedral structure containing double stranded RNA, and do not possess a membrane. Rotaviruses are classified base on the inner shell antigen (VP6), termed the groups antigen. Based on the VP6 antigen, there are seven groups of rotaviruses, designated group A-G, humans are primarily infected by species A, B and C. The most important species causing infection in humans is the one in Group A Rotavirus (Alam et al., 2007; Yang et al., 2004).

The WHO lists rotavirus as: being highly significant regarding to incidence and severity of illness; having an ability to persist in water supplies for periods over a month; moderately resistant to conventional chlorine disinfection parameters; and a high infectivity of 1-100 viral particles. Rotavirus was most commonly detected in sewage samples in Beijing during the winter and spring months (He et al., 2011; Li et al., 2011; He et al., 2008). One study noted that rotavirus was detected in all of the sewage treatment plant influent samples collected in the period of October-January but not detected in any samples collected in August and September (He et al., 2008). Rotavirus genomes have been detected in similar numbers in raw and treated wastewater treated by settling, activated sludge, and phosphorus removal indicating inefficient removal (Lodder & de RodaHusman, 2005).

2) Exposure assessment

The exposure assessment is the exposure of consumers with reclaimed water, which is estimated depending on the amount of drinking water a day. The virus concentration in the reclaimed water varies because of the prevalence of each disease is variable throughout the year.

3) Dose-response data

A single pathogen can cause a physiological response. The physiological response to a given pathogen dose may be described with reference to two potential stages: infection and illness. As we are interested in the risk of getting ill from drinking

reclaimed water, the dose-response relationships with the amount of drinking have been investigated. Several dose-response relationships have been established to describe the physiological response for different pathogens. Adenovirus dose response model was described by exponential model as shown in the equation 2.4 and 2.5. The dose response study involved human inhalation of small-particle aerosols of adenovirus 4 with respiratory illnesses as health outcome that is the only one available for adenovirus (Cabtree et al., 1997).

$$P_d = 1\text{-}e^{\text{-}rD} \tag{2.4}$$

$$P_d(Adenovirus) = 1 - e^{(-0.4172xD)} \tag{2.5}$$

With r equal to 0.4172 and D representing the number of organism ingested or inhaled.

Regli (1991) described the rotavirus dose-response model with β-Poisson distribution. The β-Poisson model for rotaviruses is the dominant dose response model as showed in the equation 2.6. Owing to the fact that rotaviruses are the type of enteric virus with the lowest infections dose. The hypothesis of an independent action of single organisms forms the base for the β-Poisson model. The β-Poisson model was first used for drinking water and food technology and is an appropriate model to assess virus ingestion and the probability of infection (Rose and Gerba 1991; Tanaka et al. 1998).

$$P_d = 1\text{-}(1\text{-}D_I/\beta)^{\text{-}\alpha} \tag{2.6}$$

where P_d is daily probability of infection through ingestion of pathogens; D is daily consumed dose of contaminant (in virus/days); β is the β-Poisson distribution coefficient; and α is a model parameter (α=0.26 and β =0.42 for rotavirus; Regli et al., 1991).

$$P_d(Rotavirus) = 1 - (1 + \frac{D}{0.42})^{-0.26} \tag{2.7}$$

Subsequently, for both dose-response relationships, the annual risk (P_a) is based on equation 2.8, with P_d as the daily risk of getting ill and t as the amount of exposure events in days per year.

$$P_a = 1\text{-}(1\text{-}P_d)^{365} \tag{2.8}$$

4) Risk characterization

The risk characterization of a QMRA integrates the information form hazard identification, exposure assessment, and dose response model into a single mathematical model to calculate the risk of an outcome like infection, illness or death. Since exposure and effect assessment will not provide a single value, but a distribution of values, the risk needs to be calculated for all values across this distribution. This done via the Monte Carlo analysis, will result in a full range of possible risks, including the minimum, average and worst-case scenarios. Based on these risk estimations, the advance treatment unit may be suggested for the reclaimed water.

Past applications of QMRA on the risk of adenovirus and rotavirus in water were summarized in Table 2.4. Several studies attempted to evaluate the risk assessment of adenovirus and rotavirus because the viruses are the first and second leading agents for gastroenteritis illness in children. As can be seen many studies reported the yearly risk of infection for adenovirus and rotavirus were really high in the water environment. Adenovirus and rotavirus is also needed to study in reclaimed water.

Table 2.4: QMRA studies on the risk of adenovirus and rotavirus in water

Authors	Exposure assessment	Dose response	Outcome	Type	Probability of Yearly infection
Crabtree et al., 1997	AdV in drinking water (1 IU/1000L and 1 IU/100 L ; IU = infectious unit (4L/day)	Exponential model r = 0.4172 from AdV4	Risk of infection	Point estimation	$2.63x10^{-1}$ $9.52x10^{-1}$
Crabtree et al., 1997	AdV in recreation water (0.118 MPN/100L and 12.8 MPN/100L) infectious unit (30L/day)	Exponential model r = 0.4172 from AdV4	Risk of infection	Point estimation	$1.48x10^{-4}$ in 10 days $1.59x10^{-2}$ in 10 days
Heerden et al., 2005	AdV in drinking water using PCR and make quantitative results by Poission distribution Fraction of detected HAds that is capable of infection = 1 (2L /day)	Exponential model r = 0.4172 from AdV4	Risk of infection	Point estimation	$1.01x10^{-1}$ at A plant and $1.70x10^{-1}$ at B plant
Kundu 2013	AdV in the Collegues creek focusing on three groups of swimmer , qPCR data, swimmers Volume intake using pert distribution	Exponential model r = 0.4172 from AdV4	Individual illness risk (IIR) predicted illness risk 3 groups (children, Adults and secondary	Distribution	IIR
McBride et al., 2013	AdV in recreation water from stormwater: target group swimmers using qPCR data harmonized with genome:PFU ~ 1000 Only inhalation exposure pathway Min,mode,max intake rate 10,50,100	Exponential model r = 0.4172 from AdV4	Individual illness risk (IIR) Short-term predicted illness risk	Cumulative frequency distribution	IIR
Chigor et al 2014	AdV in the Buffalo River and three sources of water dams using qPCR data estimated with infectious ration: qPCR (1/2)	Exponential model r = 0.4172 from AdV4	Probability of infection	Point estimates and estimated risk of morbidity and mortality	1 in all water media
Chigor et al 2014	RV in the Buffalo River and three sources of water dams Using qPCR data estimated with infectious ration: qPCR (1/10)	Beta poisson model α= 0.2531 β= 0.4265	Probability of infection	Point estimates and estimated risk of morbidity and mortality	ND and 1 in the river in town
McBride et al., 2013	RV in recreation water from stormwater: target group swimmers Using qPCR data harmonized with genome:FFU ~ 1900	Beta poisson α= 0.2531 β= 0.4265	Individual illness risk (IIR) Short-term predicted illness risk	Cumulative frequency distribution	IRR
Prez et al., 2015	RV in recreation rivers (Xanaes and Suquia) from Cordoba, Argentina usng qPCR results 10 mL for people swimming and playing in the river	Beta poisson from Haas et al., 1999: α= 0.2531 and N50 =6.17	Probability of infection	Distribution	Median =1 in Suquia river, median =0.7010 in Xanaes river

2.6 Required data for the virological risk assessment in this study

2.6.1 Data input for the virological risk assessment

In order to perform the viral risk assessment in the reclaimed water treated by SAT implemented in a target area, the hydraulic parameters of soil-aquifer treatment are necessary for the virus transport model. Also, the virus concentration and its reduction efficacy in the reclaimed water are very important for the risk assessment model. The hydraulic parameters such as groundwater velocity and virus inactivation and sorption rate coefficients are used for the virus concentration profile prediction. Then the output concentrations are used for viral risk assessment. The required data for the virological risk assessment in this study are listed bellow as:

- Virus concentration in the SAT influent and effluent (genome base and infectious virus)
- The removal rate constant of virus during SAT system
- The inactivation rate constant of virus during the SAT system
- The ground water velocity in the implemented area
- The water consumption of people in Japan

To obtain those data, a virus detection method is required. There are several virus detection techniques that can be divided into two groups of detection.

2.6.2 Selection of virus detection methods

Cell culture base method: Traditional cell culture methods employ the appropriate host cell lines of either human or primate origin for detecting the infection of the virus sample. The positive results of cytopathic effects (CPEs), a morphology change, represent the infectivity of virus particles. This test can be performed either as a plaque assay (immobilized cell on agar) or as a liquid culture assay (suspended cell in a liquid medium). The first assay relied on the visual observation of the formation of plaques, the area of dead and damaged cell. The result will be reported as “plaque forming units per milliliter (PFU/mL). Unlike plaque assay, liquid culture assay employs as statistical analysis, called most probable number: MPN, for the quantification of viral infectivity. The presence or absence of CPE, by visual examination in replicated serial dilutions of samples, will be scored and calculated. This technique is used, due to the fact that the virus particles could replicate in the infected cell and then spread into culture supernatant, resulting in the infection of

neighboring cells. Even though this technique provides less precise quantitative result, it can detect culturable viruses at lower concentrations.

During the 1980s, culture methods using the Buffalo Green Monkey Kidney cell line (BMGK) for the detection of waterborne enteroviruses was developed, later the US Environmental Protection Agency adopted this assay as a standardized method for detection of several viruses, known as the total cultivable virus assay (TCVA). Nevertheless, with this technique it may not be possible to distinguish the virus type from the morphological characteristics of CPE, because it is highly similar among virus types. Even though cell culture method has been commonly used for detection of infectious viruses, this method may not succeed well in some viruses because not all types of viruses exhibit CPEs during a certain time of an experiment. For instance, Rotaviruses need more than 1 week to produce obvious CPE (Dan Li et al., 2010), which is labor intensive and time consuming. Moreover, there was a deterioration of inoculated cell culture before the observation of distinctive CPE, leading to an unreliable and non-reproducible result.

PCR method: The PCR is emerging very rapidly as a method for virus detection in environmental samples. Compared to cell culture, the main advantages of PCR methods for virus detection include fast results, high specificity and sensitivity, and the ability to detect those difficult to culture or non-culturable such as noroviruses. The main disadvantage of PCR methods is that they do not provide a measure of infectivity and there are problems associated with the detection limits and inhibition of PCR detection.

Conventional PCR can amplify and detect virus-specific DNA sequences in the presence of DNA from many other sources. Gel electrophoresis is needed afterwards in order to visualize the results. Normally conventional PCR is not a quantitative assay, but quantitative results can be generated by using dilutions and the most probable number (MPN) method. Reverse transcription PCR (RT-PCR) is used to produce a complementary strand (cDNA) for ribonucleic acid (RNA) viruses such as enteroviruses and noroviruses. Nested PCR generally has two sets of primers, one set nested within the nucleic acid defined by the second primer pair. An amplicon is generated by the outer primers, while the target sequence of DNA is amplified by

inner primers. In multiplex PCR, multiple DNA sequences are targeted simultaneously.

Real-time PCR (qPCR) is a quantitative assay in which target sequences are simultaneously amplified and quantified. In addition to primers, a set of probes with attached dyes is involved in real-time PCR. During amplification, the dyes are released from the probes and fluoresce. The fluorescence signal can be detected and by using a standard curve, the number of viral genome copies is quantified. When combined with cell culture, PCR can be employed to determine the infectivity of viruses using a procedure called integrated cell culture PCR (ICC-PCR).

A simplified schematic of virus detection method in environmental media is shown in Figure 2.4. Sample collection and pretreatment is a critical element of all environmental analysis. Virus concentration in natural water bodies is usually low, and pre-concentration of viruses is often the most important step for effective detection (Xagorarake et al., 2014).

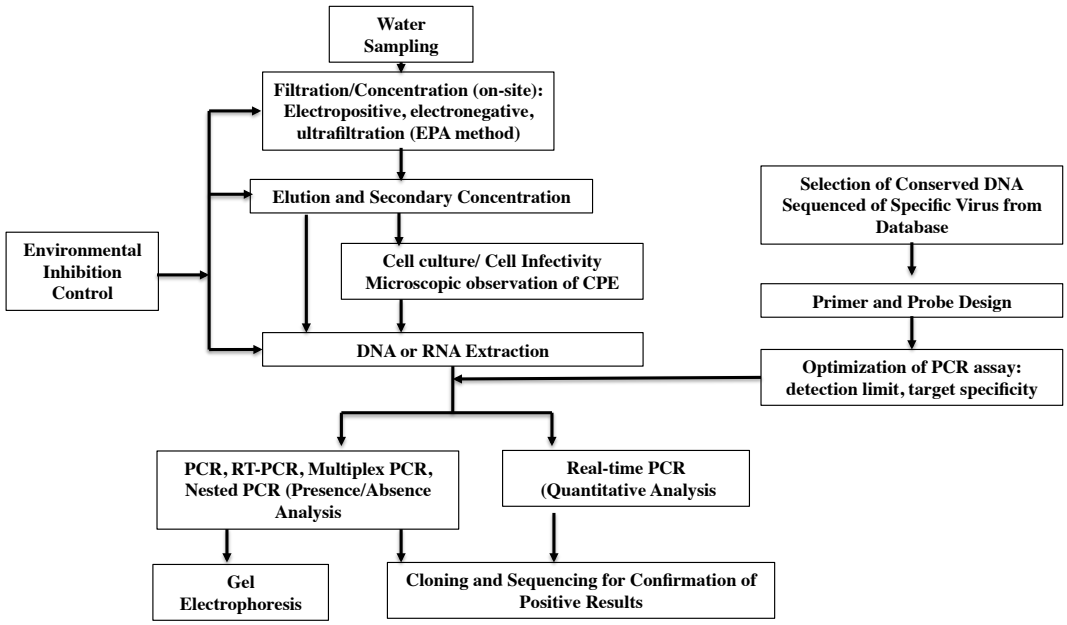

Figure 2.4: Diagram of virus detection in water (Xagorarake et al., 2014)

2.7 Summary

In this chapter, water reclamation from treated sewage through SAT with the special focus on pathogen risk was addressed. Then, the pathogen removal and inactivation

during the SAT are reviewed. To estimate the pathogen risk, the QMRA is usually applied. The data of QMRA required for the exposure evaluation on the reclaimed water thus the target pathogens concentration and the SAT reduction of the target pathogens was quantified. Findings obtained in this chapter are as follows:

Reclaimed water from treated sewage through SAT was shown to be one effective option to solve instability in quality and quantity of future water resources. Among pathogens, viruses are the most difficult to remove by SAT because of their small size and low inactivation. Moreover, little information is known on the enteric viruses reduction during SAT especially with short retention time. It is strongly believed that the reduction of enteric viruses during short retention time SAT is really interesting and they have been chosen as the topic of this study. The viral risk assessment is required to confirm the viral risk after the water has been treated by SAT.

References

Abbaszadegan M., Lechevallier M. & Gerba C 2003 Occurrence of viruses in US groundwaters. *American Water Works Association Journal,* **95**(9), 107.

Ahuja S. 2014 *Water Reclamation and Sustainability*: Elsevier.

Alam M., Kobayashi N., Ishino M., Ahmed M., Ahmed M., Paul S. & Naik T. 2007 Genetic analysis of an ADRV-N-like novel rotavirus strain B219 detected in a sporadic case of adult diarrhea in Bangladesh. *Archives of Virology,* **152**(1), 199-208.

Amy G., Wilson L. G., Conroy A., Chahbandour J., Zhai, W. & Siddiqui M. 1993 Fate of chlorination byproducts and nitrogen species during effluent recharge and soil aquifer treatment (SAT). *Water Environment Research,* **65**(6), 726-734.

Anders, R. & Chrysikopoulos C. 2005 Virus fate and transport during artificial recharge with recycled water. *Water Resources Research,* **41**(10).

Asano T. & Cotruvo J. A. 2004 Groundwater recharge with reclaimed municipal wastewater: health and regulatory considerations. *Water Research,* **38**(8), 1941-1951.

Azadpour-Keeley A., Faulkner B. R. & Chen J.-S. 2003 Movement and longevity of viruses in the subsurface. EPA/540/S-03/500. USEPA, Washington, DC.

Bdour A. N., Hamdi M. R. & Tarawneh Z. 2009 Perspectives on sustainable wastewater treatment technologies and reuse options in the urban areas of the Mediterranean region. *Desalination,* **237**(1), 162-174.

Bodik I. & Kubaská M. 2013 Energy and sustainability of operation of a wastewater treatment plant. *Environment Protection Engineering,* **39**(2), 15-24.

Burge W. & Enkiri N. 1978 Virus adsorption by five soils. *Journal of Environmental Quality,* **7**(1), 73-76.

Crabtree K. D., Gerba C. P., Rose J. B. & Haas C. N. 1997 Waterborne adenovirus: a risk assessment. *Water Science and Technology,* **35**(11), 1-6.

Chigor V. N., Sibanda T. & Okoh A. I. 2014 Assessment of the risks for human health of adenoviruses, hepatitis a virus, rotaviruses and enteroviruses in the buffalo river and three source water dams in the eastern cape. *Food and Environmental Virology,* **6**(2), 87-98.

Chrysikopoulos C. V., Kitanidis P. K. & Roberts P. V. 1990 Analysis of one-dimensional solute transport through porous media with spatially variable retardation factor. *Water Resour. Res,* **26**(3), 437-446.

Crabtree K., Gerba C., Rose J. & Haas C. 1997 Waterborne adenovirus: a risk assessment. *Water Science and Technology,* **35**(11), 1-6.

Cruz J. R., Caceres P., Cano F., Flores J., Bartlett A. & Torun B. 1990 Adenovirus types 40 and 41 and rotaviruses associated with diarrhea in children from Guatemala. *Journal of Clinical Microbiology,* **28**(8), 1780-1784.

DeFlaun M. F., Murray C. J., Holben W., Scheibe T., Mills A., Ginn T. & Wilson, J. L. 1997 Preliminary observations on bacterial transport in a coastal plain aquifer. *FEMS Microbiology Reviews,* **20**(3-4), 473-487.

Drewes J. E., Reinhard M. & Fox P. 2003 Comparing microfiltration-reverse osmosis and soil-aquifer treatment for indirect potable reuse of water. *Water Research,* **37**(15), 3612-3621.

Echigo S., Nakatsuji M., Takabe Y. & Itoh S. 2015 Effect of preozonation on wastewater reclamation by the combination of ozonation and soil aquifer treatment. *Water Science and Technology: Water Supply,* **15**(1), 101-106.

Fong T.-T. & Lipp E. K. 2005 Enteric viruses of humans and animals in aquatic environments: health risks, detection, and potential water quality assessment tools. *Microbiology and Molecular Biology Reviews,* **69**(2), 357-371.

Gitis V., Dlugy C., Gun J. & Lev O. 2011 Studies of inactivation, retardation and accumulation of viruses in porous media by a combination of dye labeled and native bacteriophage probes. *Journal of Contaminant Hydrology,* **124**(1), 43-49.

Haramoto E., Katayama H., Oguma K. & Ohgaki S. 2007 Quantitative analysis of human enteric adenoviruses in aquatic environments. *Journal of Applied Microbiology,* **103**(6), 2153-2159.

Harvey R. W., Kinner N. E., Bunn A., Macdonald D. & Metge D. 1995 Transport behavior of groundwater protozoa and protozoan-sized microspheres in sandy aquifer sediments. *Applied and Environmental Microbiology,* **61**(1), 209-217.

Harvey R. W. & Ryan J. N. 2004 Use of PRD1 bacteriophage in groundwater viral transport, inactivation, and attachment studies. *FEMS Microbiology Ecology,* **49**(1), 3-16.

He X., Cheng L., Zhang D., Xie X., Wang D. & Wang Z. 2011 One-year monthly survey of rotavirus, astrovirus and norovirus in three sewage treatment plants (STPs) in Beijing, China and associated health risk assessment. *Water Science and Technology,* **64**(6).

He X. Q., Cheng L., Li W., Xie X. M., Ma M. & Wang Z. J. 2008 Detection and distribution of rotavirus in municipal sewage treatment plants (STPs) and surface water in Beijing. *Journal of Environmental Science and Health Part A,* **43**(4), 424-429.

Heerden J., Ehlers M. M., Vivier J. C. & Grabow W. O. K. 2005 Risk assessment of adenoviruses detected in treated drinking water and recreational water. *Journal of Applied Microbiology,* **99**(4), 926-933.

Hijnen W., Beerendonk E. & Medema G. J. 2006 Inactivation credit of UV radiation for viruses, bacteria and protozoan (oo) cysts in water: a review. *Water Research,* **40**(1), 3-22.

Jiménez B. & Asano T. 2008 Water reuse: an international survey of current practice, issues and needs. *Water Intelligence Online,* **7**, 9781780401881.

Jin Y. & Yates M. V. 2002 *Virus Behavior in Saturated and Unsaturated Subsurface Media*: American Water Works Association.

Jin Y., Yates M. V., Thompson S. S. & Jury W. A. 1997 Sorption of viruses during flow through saturated sand columns. *Environmental Science and Technology,* **31**(2), 548-555.

Kundu A., McBride G. & Wuertz S. 2013 Adenovirus-associated health risks for recreational activities in a multi-use coastal watershed based on site-specific quantitative microbial risk assessment. *Water Research,* **47**(16), 6309-6325.

Lazarova V., Asano T., Bahri A. & Anderson J. 2013 Milestones in water reuse: the best success stories. *Water Intelligence Online,* **12**, 9781780400716.

Levine A. D. & Asano T. 2004 Peer reviewed: recovering sustainable water from wastewater. *Environmental Science and Technology,* **38**(11), 201A-208A.

Li D., Gu A., Zeng S. Y., Yang W., He M. & Shi H. C. 2011 Monitoring and evaluation of infectious rotaviruses in various wastewater effluents and receiving waters revealed correlation and seasonal pattern of occurrences. *Journal of Applied Microbiology,* **110**(5), 1129-1137.

Li D., Gu A. Z., Yang W., He M., Hu X.-h. & Shi H.-C. 2010 An integrated cell culture and reverse transcription quantitative PCR assay for detection of infectious rotaviruses in environmental waters. *Journal of Microbiological Methods,* **82**(1), 59-63.

Lodder, W. & de Roda Husman A. 2005 Presence of noroviruses and other enteric viruses in sewage and surface waters in The Netherlands. *Applied and Environmental Microbiology,* **71**(3), 1453-1461.

Martin J. P. & Koerner R. M. 1984 The influence of vadose zone conditions in groundwater pollution: Part II: Fluid movement. *Journal of Hazardous Materials,* **9**(2), 181-207.

Matthess G., Pekdeger, A. & Schroeter J. 1988 Persistence and transport of bacteria and viruses in groundwater—a conceptual evaluation. *Journal of Contaminant Hydrology,* **2**(2), 171-188.

McBride G. B., Stott R., Miller W., Bambic D. & Wuertz S. 2013 Discharge-based QMRA for estimation of public health risks from exposure to stormwater-borne pathogens in recreational waters in the United States. *Water Research, 47*(14), 5282-5297.

Medema G. & Ashbolt N. 2006 *QMRA: its value for risk management*. Retrieved from http://www.camra.msu.edu/documents/QMRA_framework.pdf

Medema G.J., Juhasz-Holterman M.H.A. & Luijten J.A. 2000 Removal of micro-organisms by bank fi ltration in a gravel-sand soil. p. 161–168. In W. Jülich and J. Schubert (ed.) Proc. of the Int. Riverbank Filtration Conf., Dusseldorf, Germany. 2–4 Nov. 2000. IAWR, Rhein-Themen 4.

Metcalf E., Asano T., Burton F., Leverenz H., Tsuchihashi R. & Tchobanoglous G. 2007. Water Reuse: Issues, Technologies, and Applications: Mc-Graw Hill. NewYork, USA.

Microrisk 2006. Microbiological risk assessment: a scientific basis for managing drinking water safety from source to tap. EU project under 5FP. (http://www.microrisk.com/publish/cat_index_11.shtml)(visited 08.08.15)

NRMMC E. 2006 AHMC, Australian Guidelines for Water REcycling: Managing Health and Environmental Risks (Phase 1). *Natural Resource Ministerial Management Council, Environment Protection and Heritage Council and Australian Health Ministers*.

Page D., Dillon P., Toze S., Bixio D., Genthe B., Cisneros B. E. J. & Wintgens T. 2010 Valuing the subsurface pathogen treatment barrier in water recycling via aquifers for drinking supplies. *Water Research,* **44**(6), 1841-1852.

Pang L. 2009 Microbial removal rates in subsurface media estimated from published studies of field experiments and large intact soil cores. *Journal of Environmental Quality,* **38**(4), 1531-1559.

Pedley S., Yates M., Schijven J., West J., Howard G., Barrett M. & Chorus I. 2006 *Pathogens: health relevance, transport and attenuation*: World Health Organization.

Percival S. L., Yates M. V., Williams D., Chalmers R. & Gray, N. 2013 *Microbiology of waterborne diseases: Microbiological Aspects and Risks*: Academic Press.

Pina S., Puig M., Lucena F., Jofre J. & Girones R. 1998 Viral pollution in the environment and in shellfish: human adenovirus detection by PCR as an index of human viruses. *Applied and Environmental Microbiology, 64*(9), 3376-3382.

Po M., Nancarrow B. E. & Kaercher J. D. 2003 Literature review of factors influencing public perceptions of water reuse.

Prez V. E., Gil P. I., Temprana C. F., Cuadrado P. R., Martínez L. C., Giordano M. O. & Barril, P. A. 2015 Quantification of human infection risk caused by rotavirus in surface waters from Córdoba, Argentina. Science of the Total Environment, **538**, 220-229.

Puig M., Jofre J., Lucena F., Allard A., Wadell G. & Girones R. 1994 Detection of adenoviruses and enteroviruses in polluted waters by nested PCR amplification. *Applied and Environmental Microbiology,* **60**(8), 2963-2970.

Quanrud D. M., Hafer J., Karpiscak M. M., Zhang J., Lansey K. E. & Arnold R. G. 2003 Fate of organics during soil-aquifer treatment: sustainability of removals in the field. *Water Research,* **37**(14), 3401-3411.

Regli S., Rose J. B., Haas C. N. & Gerba C. P. 1991 Modeling the risk from Giardia and viruses in drinking water. *Journal American Water Works Association*, 76-84.

Rose J. B. & Gerba C. P. 1991 Use of risk assessment for development of microbial standards. *Water Science and Technology,* **24**(2), 29-34.

Schijven J. F. & Hassanizadeh S. M. 2000 Removal of viruses by soil passage: Overview of modeling, processes, and parameters. *Critical Reviews in Environmental Science and Technology,* **30**(1), 49-127.

Schijven J. F., Hoogenboezem W., Hassanizadeh M. & Peters J. H. 1999 Modeling removal of bacteriophages MS2 and PRD1 by dune recharge at Castricum, Netherlands. *Water Resources Research,* **35***(4)*, 1101-1111.

Sharma S., Harun C. & Amy G. 2008 Framework for assessment of performance of soil aquifer treatment systems. *Water Science and Technology,* **57**(6).

Takabe Y., Kameda I., Suzuki R., Nishimura F. & Itoh S. 2014 Changes of microbial substrate metabolic patterns through a wastewater reuse process, including WWTP and SAT concerning depth. *Water Research,* **60**, 105-117.

Tanaka H., Asano T., Schroeder, E. D. & Tchobanoglous G. 1998 Estimating the safety of wastewater reclamation and reuse using enteric virus monitoring data. *Water Environment Research,* **70**(1), 39-51.

Thurston-Enriquez J. A., Haas C. N., Jacangelo J., Riley, K. & Gerba C. P. 2003 Inactivation of feline calicivirus and adenovirus type 40 by UV radiation. *Applied and Environmental Microbiology,* **69**(1), 577-582.

Tim U. S. & Mostaghimi S. 1991 Model for predicting virus movement through soils. *Ground Water,* **29**(2), 251-259.

Toze S., Bekele E., Page D., Sidhu J. & Shackleton M. 2010 Use of static quantitative microbial risk assessment to determine pathogen risks in an unconfined carbonate aquifer used for managed aquifer recharge. *Water Research,* **44**(4), 1038-1049.

Van Cuyk S., Siegrist R. L., Lowe K. & Harvey R. W. 2004 Evaluating microbial purification during soil treatment of wastewater with multicomponent tracer and surrogate tests. *Journal of Environmental Quality,* **33**(1), 316-329.

WHO. 2004 *Guidelines for drinking-water quality: recommendations* (Vol. 1): World Health Organization.

WHO. 2006 *Protecting Ground Water for Health-Managing the Quality of Drinking-water Sources*: World Health Organization.

Xagoraraki I., Yin Z. & Svambayev Z. 2014 Fate of viruses in water systems. *Journal of Environmental Engineering,* **140**(7), 04014020.

Yang H., Makeyev E., Kang Z., Ji S., Bamford D. & Van Dijk A. 2004 Cloning and sequence analysis of dsRNA segments 5, 6 and 7 of a novel non-group A, B, C adult rotavirus that caused an outbreak of gastroenteritis in China. *Virus Research,* **106**(1), 15-26.

Yasukawa T., Asada Y., Kunimoto K., Ojkouchi Y. & Itoh S. 2014 An estimation of disability adjusted life years associated with indirect potable reuse based on the occurrence of *Campylobacter Jejuni. Journal of Japan society of Civil Engineering, Ser. G (Environmental research)*(**70**(7)), 285-294.

Zeman C., Rich, M. & Rose, J. 2006 World water resources: Trends, challenges, and solutions. *Reviews in Environmental Science and Biotechnology,* **5**(4), 333-346.

Chapter 3

Adsorption and inactivation of the enteric viruses in the presence of soils by batch experiments

3.1 Introduction

Adsorption and inactivation are the main processes for virus control by soil passage. Several researches have studied the factors affecting adsorption and inactivation of viruses in soils (Schijven & Hassanizadeh, 2000). Virus adsorption is influenced by pH, virus types, temperature, soil types, organic matter (OM), and the presence of cations or anions in the surrounding medium (Matthess et al., 1988). Because these factors (i.e., pH, DOC) are relatively stable in treated wastewater, the important factor for virus adsorption is the type of viruses. Similarly to virus adsorption, virus inactivation depends on several factors (e.g., pH, soil types), Among these factors, it highly depends on temperature (Bertrand et al., 2012; Powelson et al., 1990; Yates et al., 1985). While several studies investigated the adsorption and inactivation of bacteriophages, such as MS2 and PRD1, little information on those of human enteric viruses is known. This study aims to investigate the adsorption and inactivation of the human enteric viruses in soils collected in Japan. For this purpose, batch experiments on adsorption and inactivation of RV and AdVF in the presence of soil or sand were performed under various conditions (i.e., temperature, 4, 15, 25, 37 ˚C; soil type, sand and weathered granite soil). In addition to removal efficiencies at equilibrium, adsorption and inactivation kinetics were discussed.

3.2 Materials and Methods

3.2.1 Preparation of viruses, soils and treated A2O water

Enteric adenovirus serotype 40 (AdVF 40) strain Dugan (VR-931) and Human Rotavirus Wa strain (VR-2018^{TM}) were purchased from the American Type Culture Collection (ATCC). Sand and weathered granite soil were collected in Shiga prefecture, Japan. Table 3.1 shows their physical and chemical properties. Both materials were passed through a sieve with ϕ 1 mm openings, and transferred into polyethylene bottles and stored at room temperature.

Table 3.1: Physical and chemical properties of sand and weathered granite soil used in this study

Soil type	Sand	Weathered granite soil
Ignition loss (%)	1.36	2.74
TOC (%)	0.0094	0.0159
Porosity (%)	43.5	29.07
Cation exchange capacity (meq/100 mg-dry)	2.39	15.6
Anion exchange capacity (meq/100 mg-dry)	1.49	3.33
Water content (%)	0.567	1.1
Specific surface (m^2/g)	2.40	5.95
Soil pH	6.64	7.41
Soil density (kg/L)	1.46	1.39

Treated Anaerobic-Anoxic-Oxic (A2O) water was taken from Toba Wastewater Environment Conservation Center, Kyoto city, Japan. The water quality parameters were means of 3.52 mg/L, 3.34 mgC/L, and 6.4 of TOC, DOC and pH, respectively in treated A2O water.

3.2.2 Laboratory-scale batch tests

The adsorption of virus with soils was studied with short-term and long-term batch tests and the inactivation of virus with soils was investigated only with long-term batch tests.

a) Short-term batch tests

For batch experiments for adsorption kinetics, AdVF and RV were spiked into the autoclaved treated A2O water at 10^5 copies/μL and 10^3 copies/μL, respectively. The batch adsorption experiments started by adding the soil samples (weathered granite soil or sand) to the 10 mL of sterilized glass bottle, viruses, and autoclaved A2O water together. For each batch 1 g of soil was put into 6 mL of A2O water with virus. The contents of the test tubes were mixed with a rotated 360-action shaker at 60 rpm at room temperature. At specific time intervals (10, 20, 30, 60, 90, and 120 min), the tube was centrifuged at 1000 × g for 10 minutes. Centrifugation separated the soil and virus adsorbed onto the soil from the free virus particles in the water. One milliliter of supernatant was taken for real-time (RT)-PCR analysis for virus detection.

The isotherm experiment determined the adsorption capacity within 3 hours at the equilibrium time. The initial virus concentration was varied (every 10-fold dilution 10^5,10^4,10^3,10^2,10^1,10^0 copies/μL for AdVF and every 5-fold dilution 10^4, $5x10^3$, 10^3, $5x10^2$, 10^2, $5x10^1$,10^1 copies/μL for RV) with the same amount of soils. The amounts

of A2O water and soils were the same as the kinetic test. All the bottles were rotated at 60 rpm until equilibrium. Then, the bottles were centrifuged at 1000 g for 10 min and 1 mL of supernatant was collected for real-time (RT)-PCR detection. The control samples (only A2O with viruses) were run in both the kinetic and isotherm experiments.

b) Long-term batch tests

The long-term batch experiments until 56-day incubation was set up. The virus stock solutions were added into autoclaved A2O water in 10 mL glass bottle. All glass bottles were sterilized before use. So that the concentrations of AdVF and RV in spiked samples were $5x10^5$ MPN/mL and $5x10^3$ MPN/mL, respectively. Six milliliters of spiked water sample and 4 grams of weathered granite soil or sand were added to sterilized glass bottles. The control test (only A2O water with the spiked viruses) was performed at the same time. Then the bottles sets of sand, weathered granite soil and only A2O water were arranged into four temperature conditions (4, 15, 25 and 37 °C) and stored until 56-day. At the selected time (1, 3, 7, 14, 21, 28, 35, 42, 49 and 56 days) one bottle of each set was chosen randomly for sampling. The AdVF and RV in the supernatants were detected by ICC-(RT)PCR (indicated infectious viral particles to observe the viruses inactivation) and by real-time (RT)PCR (indicated all viral genome copies to observe the virus removal).

3.2.3 Viruses detection methods

a) Real-time PCR Analysis

Viral nucleic acid was extracted from 200 µL of concentrated samples using High Pure Viral Nucleic Acid kit (Roche Diagnostic). For AdVF (Adenovirus serotype F), the primers described in Lion et al. (2003) were used. Each reaction tube contained 10 µL of environmental master mix 2, 1.8 µL of each primer (10 µM), 1 µL of probe (Taqman probe with a FAM™ dye label) and 3.4 µL of nuclease-free water and 2 µL of template in a total volume of 20 µL. The real-time PCR was performed with condition for 10 minutes at 95 ℃, 40 cycles of 15 seconds at 95 ℃ and 1 minute at 60 ℃ using StepOnePlus™ Real-Time PCR System (Applied Biosystems). For RV, quantification by real-time reverse transcription assay was adopted (Zeng, 2008). Taqman probe with a FAM™ dye label was also used. Each reaction tube contained 10 µl of 2x Buffer, 0.8 µL of each primers (10 µM), 0.4 µl of probe and 4.5 µL of

nuclease-free water, 0.5 μL of 40x enzyme mix and 3 μL of template in a total volume of 20 μL. Amplification was carried out on StepOnePlusTM Real-Time PCR System (Applied Biosystems) programmed for 30 minutes at 48 °C, 10 minutes at 95 °C, 40 cycles of 15 seconds at 95 °C and 1 minute at 60 °C. The mixture of AdVF and RV and the sequence of primers and probes were shown in Table 3.2 and Table 3.3.

Table 3.2 q(RT)-PCR of AdVF and RV detection mixture

Mixtures of AdVF detected by qPCR		**Mixtures of RV detected by q-RT-PCR**	
Chemicals	**Volume (µL)**	**Chemicals**	**Volume (µL)**
Nuclease-free water	3.4	2xBuffer	10
Environmental Master Mix2.0	10	Forward Primer (10µL)	0.8
Forward Primer (10µL)	1.8	Reverse Primer (10µL)	0.8
Reverse Primer (10µL)	1.8	RV-Probe (10µL)	0.4
Probe (5µM)	1	Nuclease-free water	3.5
DNA Template	2	40x Enzyme mix	0.5
Total	**20**	RNA Template	4
		Total	**20**

Table 3.3 qPCR primers and probes sequences

Virus	**Primer/Probe**	**Sequence**	**Target**	**Reference**
AdV-F	Forward primer (AdVF-F)	5'-COPIESA GGA CGC CTC GGA GTA-3'	Hexon gene	Lion (2003)
	Reverse primer (AdVF-R	5'-TGT CTG TGG TTA CAT CGT GGG T-3'		
	Probe (AdVF-P)	FAM-TAC TTC AGC CTG GGG AAC AAG TTC AGA AA-NFQ-MGB		
RV	Forward primer (Rota-NSP3-F)	5'-ACC ATC TAC ACA TGA CCC TCT ATG AG-3'	NSP3	Zeng (2008)
	Reverse primer (Rota-NSP3-R	5' GGT CAC ATA ACG CCC CTA TAG C-3'		
	Probe (NSP3-P)	FAM-AGT TAA AAG CTA ACA CTG TCA AA-MGB		

b) Integrated cell culture-PCR (ICC-(RT)-PCR) method

ICC-(RT)PCR detection was applied to detect infectious viral particles in water samples. For cell preparation, human carcinoma cell line CaCO-2 was chosen due to its high susceptibility to enteric virus in water samples (Pintó et al. 1995). Human carcinoma cell line CaCO-2 (RBRC-RCB0988) was purchased from the Riken BRC Cell Bank. The Monkey kidney cell line MA104 (RCB0994) purchased from the Riken BRC Cell bank for the infectivity assay of RV. The Infectivity assay methods were modified from those by Pintó et al. (1994) for AdVF and Li et al., (2010) for

RV. The CaCO-2 cells and MA104 cells were seeded at 6×10^4 cells in 24-well plates and cultured until 70-80% confluent separately. On the day before infection, the cells were pre-incubated overnight in MEM medium without FBS in both of CaCo-2 cells and MA104 cells.

For virus preparation and inoculation, the virus suspension was reactivated with 10 μg/mL trypsin at 37℃ for 30 min, and provided for infection assay after 10- and 100-fold dilutions. The cell layers were washed with sterilized PBS (pH 7.2), and then 80 μL diluted virus solution was inoculated onto the cells. Three wells were used for each dilution with concentrated water samples of 72, 7.2, and 0.72 μL, respectively. Plates were incubated for 1 hr at 37 °C in a 5% CO_2 incubator. Plates were gently rocked every 15 min (Straub et al., 2011). After 1 hr, the concentrated sample of virus solution was removed as much as possible, and the cells were incubated with MEM medium without PBS at 37℃ for 7 days. After a 7-day incubation, the virus particles inside cells in the remaining solution were released by three freeze–thaw cycles. The virus nucleic acids were extracted using High Pure Viral Nucleic Acids Extraction kit (Roche Diagnostic) in both of CaCO-2 cells and MA104 cells. The nucleic acid samples were stored at -80℃ until PCR detection.

For the detection of AdVF DNA, PCR using the primer pair for AdVF adopted by Lion et al., (2003) was performed in PCR Thermal Cycler Dice (Takara Bio Inc.) by using the following steps: mixing 2 μL of extracted DNA with 18 μL of reaction mixture containing an appropriate buffer; then 200 μM each dNTP, 0.4 mM each forward and reverse primer, and 0.25 U Takara Ex Taq. The process of the PCR cycling conditions was carried by the follows; initial denaturation at 95 ℃ for 5 minutes, 35 cycles of 95 ℃ for 30 seconds, 55 ℃ for 30 s, and 72 ℃ for 30 s, final extension at 72 ℃ for 10 min. For detection of rotavirus RNA, PCR Thermal Cycler Dice (Takara Bio Inc.) was also used for the detection of RV RNA using the primer pair adopted from Zheng et al. (2008). The 2 μL of extracted RNA was mixed with 18 μL of reaction mixture containing an appropriate buffer QIAGEN Onestep RT-PCR Kit. The steps of PCR cycling conditions include: reverse transcription 50 ˚C, 30 minutes, initial denaturation at 95℃ for 15 minutes, 30 cycles of 95 ℃ for 1 minute, 60 ℃ for 1 min, and 72 ℃ for 1 min, final extension at 72 ℃ for 10 min. The PCR

products were visualized in 2% agarose gel with ethidium bromide after separation by electrophoresis. All results were calculated as most probable number (MPN) unit.

3.2.4 Theoretical calculation of virus adsorption and inactivation

Generally, the pathogen adsorption is described by the Freudlich isotherm (Gerba and Landce, 1978). The Freundlich isotherm is an empirical equation that has been frequently applied to describe attachment of viruses to soil (Chrysikopoulos and Aravantinou, 2012). The Freundlich equation is

$$q_e = k_f C^{1/n} \tag{3.1}$$

Where q is the number of mass of adsorbate per mass of adsorbent (q is the number of virus per gram soil), k_f is the constant related to the enthalpy of adsorption which indicated the adsorption capacity, C is the concentration of the adsorbate, $1/n$ is a measure of the affinity of adsorption. Typically, the equation can be linearized by a log-log plot version as

$$\log q_e = \log k_f + \frac{1}{n} \log C \tag{3.2}$$

Inactivation rate coefficient for free viruses in water (μ_l), and inactivation rate coefficient for free viruses in suspension with soil (μ_{eff}) were calculated as a time dependent first order reduction with a constant rate coefficient (μ) (Hiatt. 1964) as

$$\mu = -\frac{1}{t} \ln\left(\frac{C}{C_0}\right) \tag{3.3}$$

3.2.5 Statistical analysis

Results were statistically analyzed using ANOVA to determine any significant differences between the temperature conditions (4-37˚C) regarding to the virus inactivation rate. Correlation and determination factors were also used to evaluate if the various parameters tested were correlated. Regression analysis and ANOVA with a confidence level of 95% were used to confirm or deny the correlation.

3.3 Results of virus adsorption and inactivation by batch experiment

3.3.1 Virus adsorption isotherm

The adsorption characteristics of AdVF and RV were evaluated in the short-term batch test. The results revealed that the time to reach apparent equilibrium in all tests was less than 10 min (results was shown in Appendix A). The $\log_{10}$-$\log_{10}$ plots of q versus C were showed in Figure 3.1. These parameters were described in Eq. 3.2 regarding to virus adsorption in soil by real-time (RT)PCR data. It can be said that adsorption results of both virus types were described by Freundlich isotherm because the adsorption mechanism is typically governed by chemical interaction between virus and adsorbent surface (John and Rose 2005). The log k_f and $1/n$ were obtained from the y-interception and the slope of the graph $\log_{10}$-$\log_{10}$ plots of q versus C, respectively. Freundlich constant or k_f of AdVF in sand and weathered granite soil were calculated from the graph in Figure 3.1 to be 16 and 125 mL/g, respectively. The k_f values of RV in sand and weathered granite soil were estimated to be 16 and 40 mL/g, respectively. The $1/n$ values represented the degree of adsorption and $1/n$ values of RV with 1.0 were lower than that of AdVF with 1.7 in both cases of sand and weathered granite soil. Thus, those of weathered granite soil samples were higher than that of sand samples for both cases of RV and AdVF adsorption.

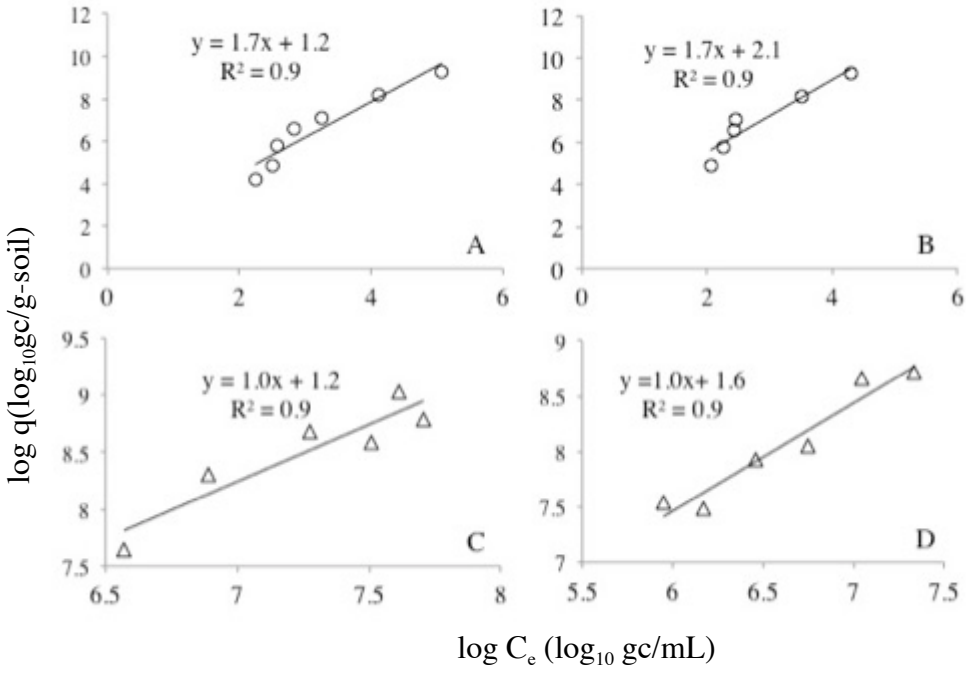

Figure 3.1: The Freudlich isotherm of AdVF in sand (A) and weathered granite soil (B) and RV in sand (C) and weathered granite soil (D)

3.3.2 Effect of temperature on virus adsorption

To investigate the effect of temperature on virus adsorption, the contact time of the batch experiments was extended to approximately 56 days. Figure 3.2 shows $\log_{10}$ removals of RV and AdVF quantified by real-time (RT)PCR in different temperatures. Both virus adsorptions in the weathered granite soil were better than in the sand. These differences of virus adsorption onto soils were statistically significant ($p<0.05$, two-tailed t-test). Many studies agree with the concept that the viruses tend to adsorb to a surface fraction of soils, which have higher cation exchange capacity (CEC) (Burge and Enkiri, 1978), exchangeable iron (Gerba et al., 1981) and higher specific area (Moore et al., 1982). In this study, the adsorption experiments possibly showed that major factor of virus adsorption were virus type and soil type. The viruses (AdVF and RV) adsorption in weathered granite soil was higher than in the sand, because CEC and specific area and organic matter in the weathered granite soil are higher than in the sand. On the other hand, for the same soil type, the removals at various temperature conditions tended to be similar for both viruses. The removals of AdVF and RV were slightly affected by temperature ranging from 4 to 37 °C.

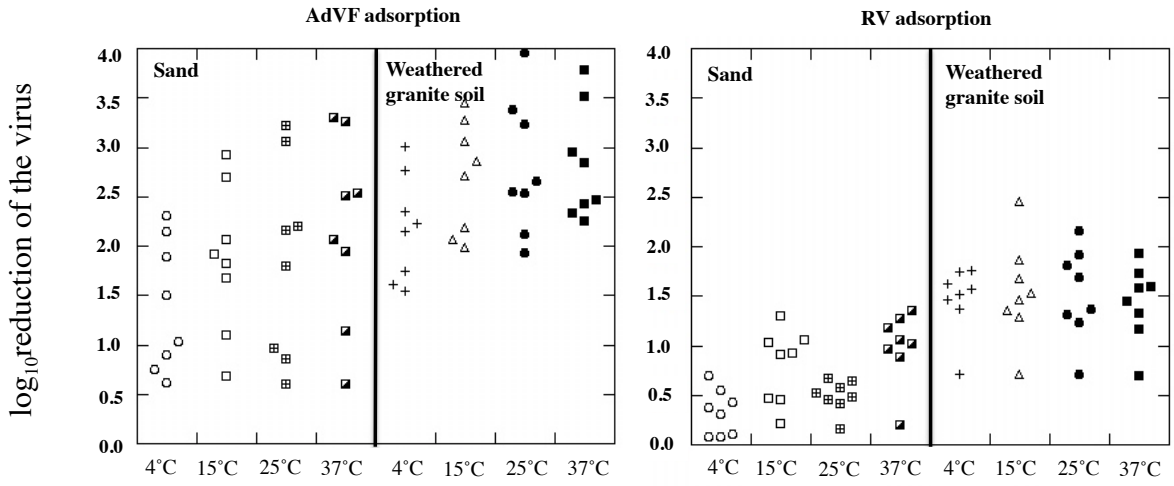

Figure 3.2: AdVF adsorption and RV virus adsorption: the left side is the AdVF adsorption onto sand and weathered granite soil at 4˚C, 15˚C, 25˚C and 37˚C, respectively. The right side is the RV adsorption onto sand and weathered granite soil at 4˚C, 15˚C, 25˚C and 37˚C, respectively.

3.3.3 Virus inactivation results

3.3.3.1 Modified integrated cell culture with PCR for infectious virus detection

For the modified method of infectious AdVF detection by ICC-PCR, the proper conditions such as incubation time for the infectious virus detection was determined. Firstly, the stock of AdVF was diluted into 10^{-2}-fold to 10^{-7}-fold and added to the Caco-2 cell with 2-day incubation. The result was shown in Figure 3.3.

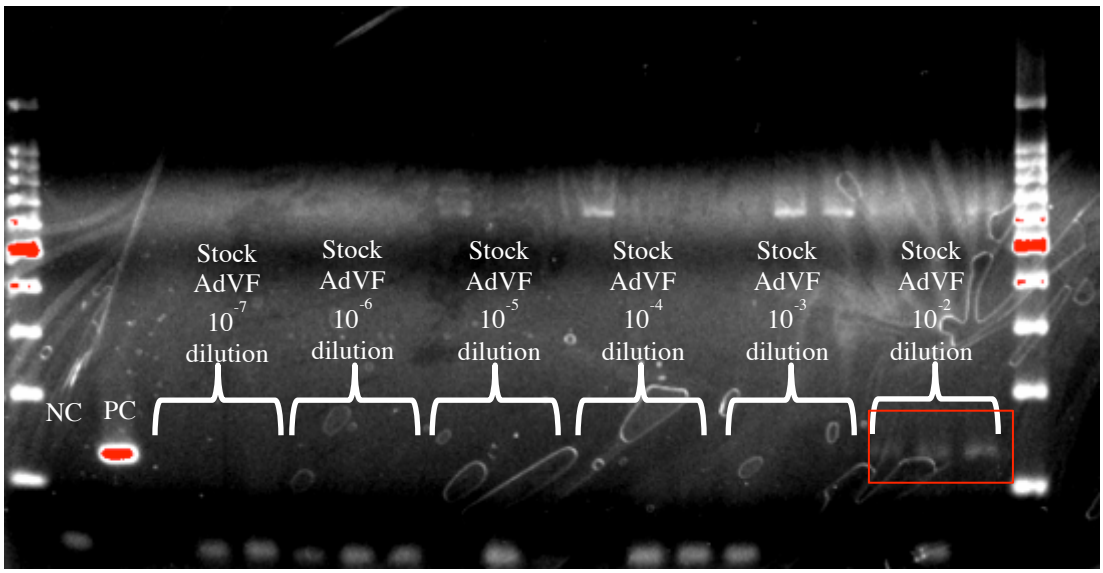

Figure 3.3: Infectious AdV40 detection by ICC-PCR with different dilutions of stock AdV40

The result showed the detection of infectious AdVF only for 100 times dilution. This means that it may not be enough to detect in a lower concentration of AdVF. For improving the sensitivity of infectious virus detection, the increase of the incubation time is one important factor. However, Caco-2 was damaged over 8 days. Thus, the experiment with the incubation time of 5-7 days was examined with the stock AdV40 10^{-1} to 10^{-4} dilution.

The detection method of infectious RV was described by Farkas (2013). That study suggested a 7-day incubation for RV. Moreover, the MA104 cell was totally damaged over 8 days. Thus, the infectious RV detection with the incubation time of 5-7 days was examined with the stock RV 10^{-1} to 10^{-4} dilution.

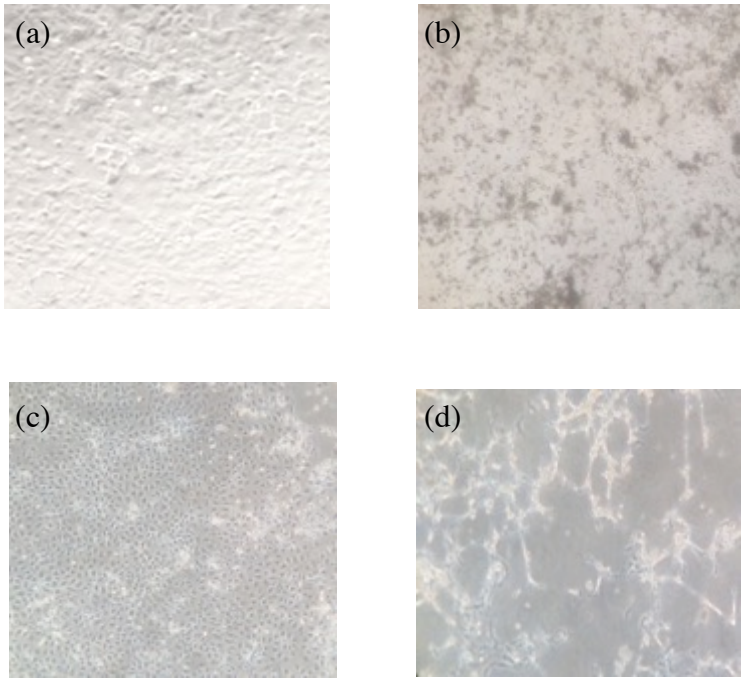

Figure 3.4: Caco-2 cell and MA104 cell morphology change. (a) the Caco-2 cell in good condition (control), (b) the Caco-2 cell with cytopatic effect after 7 day-incubation, (c) the MA104 in good condition control, (d) the MA 104 cell after 7-day incubation with all cytopatic effect.

Figure 3.4 shows the cytopathic changes associated with the culture of adenovirus and rotavirus in susceptible cells. Uninfected cells in the control appear as a confluent monolayer. Cells infected with adenovirus typically become degraded and detach of the monolayer can be observed. The cells infected with rotavirus that become damaged may be observed. The experiment was incubated using a 7 day-incubation period but 100% of cell was lost and damaged. Thus, the 7 day-incubation seems to be the limit of virus incubation after post infection. The ICC-(RT)-PCR was selected to detect infectious viruses; however, the suitable post-incubation time after the virus adsorbed to the cell should be quantified. The MPNIU can be calculated from the positive results with a different three dilution. The results were expressed as MPNIU/L, and only one MPN value was obtained for each sample due to the high labor intensiveness of replication of the MPNIU cell culture experiments. The positive flasks were used for the ICC-PCR assay to determine the occurrence of infectious AdVF and RV in water samples. The results were shown in Table 3.4.

Table 3.4: the results of infectious viruses detection by ICC-(RT)-PCR with different post incubation time

Dilution	10^{-4}	10^{-3}	10^{-2}	10^{-1}	MPNIU/mL
AdVF					
5-day	0/3	0/3	3/3	3/3	300
6-day	0/3	0/3	3/3	3/3	300
7-day	0/3	3/3	3/3	3/3	3000
RV					
5-day	0/3	0/3	0/3	2/3	11.25
6-day	0/3	0/3	0/3	3/3	28.75
7-day	0/3	0/3	3/3	3/3	300

The results of a 7-day post incubation is the highest number for AdVF and RV infection with 3000 and 300 MPN/mL of infectious AdVF and RV, respectively. The 7-day incubation was selected for inactivation batch experiment and also in the pilot plant for infections virus detection.

3.3.3.2 Effect of temperature on the inactivation rate of rotavirus and enteric adenovirus

From the batch experiments, the results obtained show that removals of viruses were dominated by the adsorption mechanism during the early stage of the experiment. Therefore, in order to reduce the effect of adsorption, the first day was neglected, and the data of the 2nd day sample was set as the initial concentration (C_0). The ratios of virus infectivity to the initial concentration (C/C_0) were plotted based on Eq.3.3 as shown in Figures 3.5 and 3.6. Several studies reported that infectious viruses could survive in the environment, such as groundwater, for longer than 1000 days (Payment & Locas, 2011). The obtained results revealed that the infectivity of RV and AdVF greatly decreased during the initial stage followed by gradual decrease.

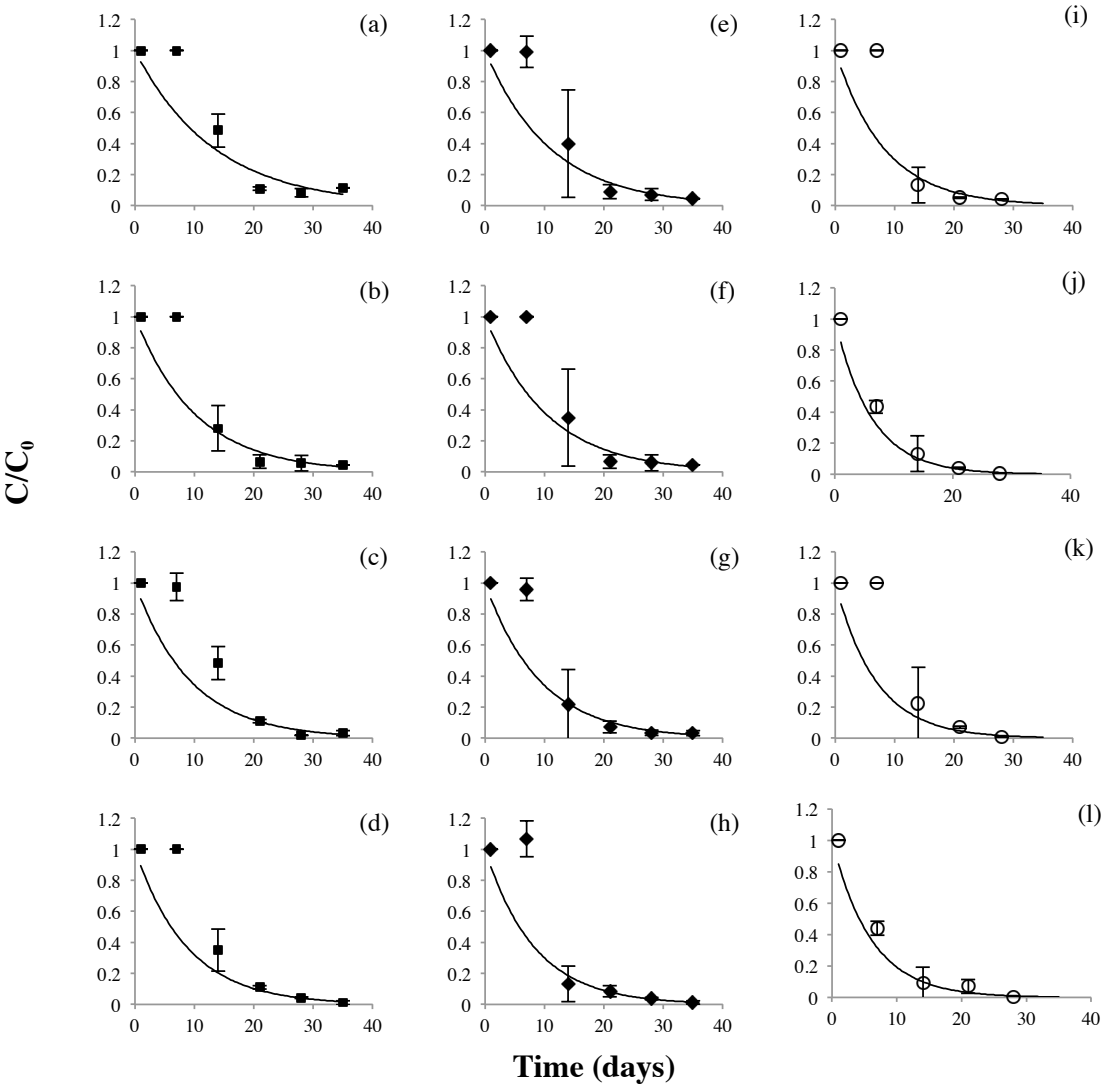

Figure 3.5: Inactivation of RV under batch conditions with sand (left column ■), with weathered granite soil (middle column ◆) and without sand or weathered granite soil (only A2O water) (right column ○) at variable temperatures of 4˚C (a, e, i), 15˚C (b, f, j), 25˚C (c, g, k) and 37˚C (d, h, l).

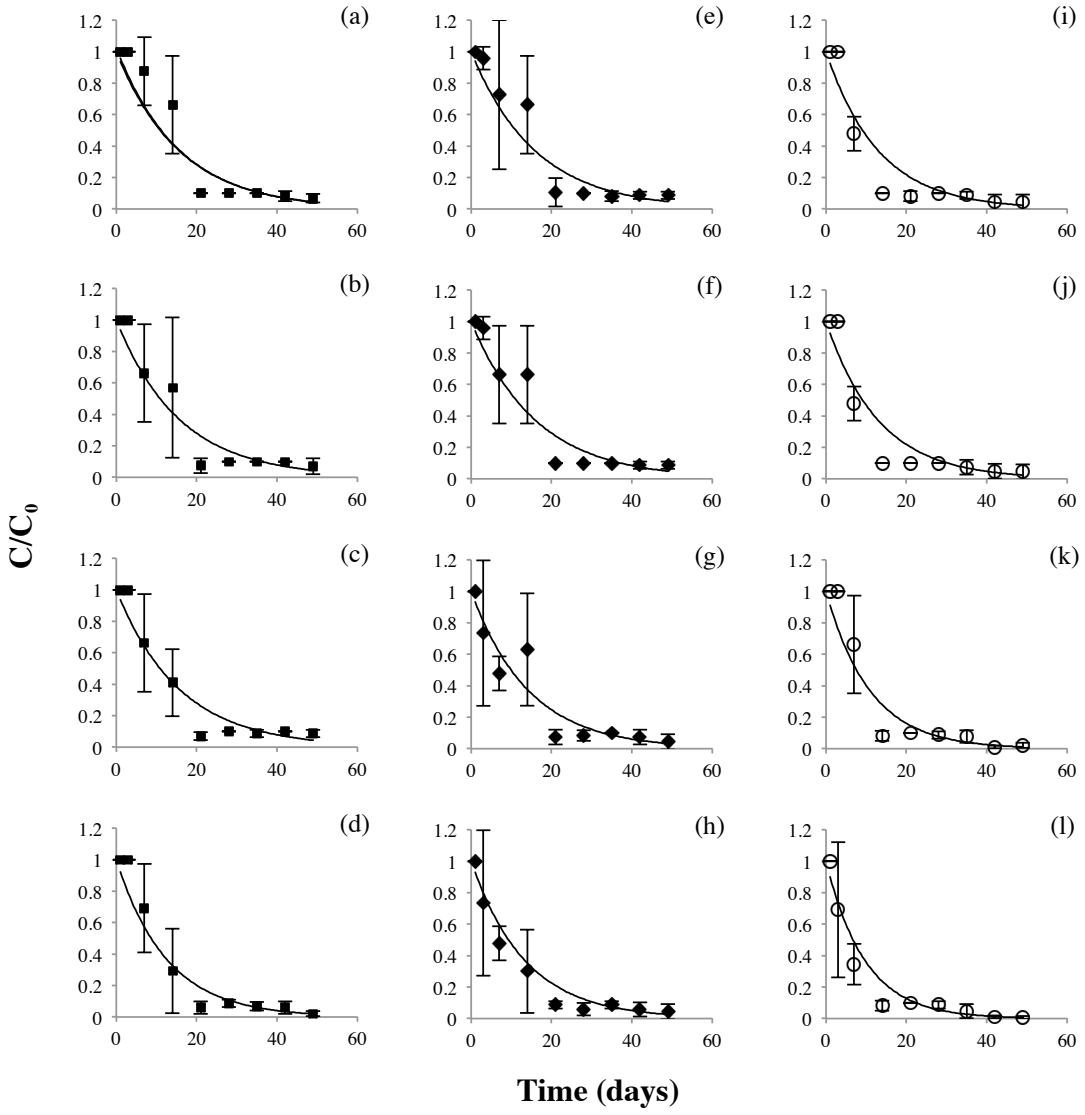

Figure 3.6: Inactivation of AdVF 40 in batch conditions with sand (left column ■), with weathered granite soil (middle column ◆) and without sand or weathered granite soil (only A2O water) (right column ○) at variable temperatures of 4˚C (a, e, i), 15˚C (b, f, j), 25˚C (c, g, k) and 37˚C (d, h, l).

The inactivation rate coefficient for free viruses in suspension with soils (μ_{eff}) and in liquid phase (μ_l) were evaluated from curve fitting and calculated from eq.3.3. All the inactivation rate coefficients were presented on Table 3.5. The results demonstrated that the inactivation rate coefficient for the both free viruses (RV and AdVF) in suspension with soils (μ_{eff}) and in liquid phase (μ_l) gradually increased with the increase of temperature. Nevertheless, the inactivation rate coefficients for the free RV and AdVF in liquid phase (μ_l) were frequently higher than in the suspension with

sand or weathered granite soil. These may suggest that the weathered granite soil and sand could protect the virus inactivation.

The RV and AdVF inactivation rate coefficients as 37˚C condition seem to be higher than with other temperatures. Even though this study observation agreed with the previous reports that high temperature enhanced virus inactivation (John and Rose, 2005), the significant correlation between temperatures (ranging from 4 °C to 37°C) and virus inactivation rates could run the statistical analysis with ANOVA two factor test at confidential level of 95% as shown in Appendix B. The analyses concludes that there is no significant difference in the yields of virus inactivation by the different temperature of 4-37˚C at $p>0.05$. The significant effect of virus inactivation is the time in the AdVF and RV batch experiment at $p<0.05$. Moreover, all inactivation results, clearly show that a large number of viruses can be inactivated during the first 21 days.

Table 3.5: the summary of virus adsorption and inactivation parameters

Parameters	**RV**				**AdVF**			
Temperature	4˚C	15˚C	25˚C	37˚C	4˚C	15˚C	25˚C	37˚C
Inactivation rate coefficient of Free virus in liquid phase $[\mu_l]$ (day^{-1}) (in A2O water)	0.122	0.162	0.146	0.165	0.076	0.076	0.091	0.103
Virus inactivation with sand								
Overall inactivation $[\mu_{eff}]$ (day^{-1})	0.075	0.098	0.107	0.114	0.064	0.064	0.064	0.080
Equilibrium constant $[k_{eq}]$ (mL/g)	16				16			
Virus inactivation with weathered granite soil								
Overall inactivation $[\mu_{eff}]$ (day^{-1})	0.091	0.096	0.108	0.120	0.063	0.062	0.070	0.075
Equilibrium constant $[k_{eq}]$ (mL/g)	40				125			

3.4 Discussions

The virus type is an important factor for virus adsorption and inactivation. This study found that the AdVF has a higher potential to be adsorbed onto sand and weathered granite soil than RV. It may be because of its isoelectric point of the viruses. Different viruses have different isoelectric points. The isoelectric point of AdVF is 6.8 (Seiradake and Cusak, 2005) but the isoelectric point of RV is 4.5 (Gutierrez et al., 2009), which makes RV to negatively charged in A2O water of pH 6.4. However, the soil and sand components usually are negatively charged in this pH range. Then negative charge of RV, in soil will push each other or RV can be adsorbed by the

minor but positively charged components. But for the AdVF this is nearly their isoelectric point, which means that the AdVF will become a no charge making the remove of AdVF easier than the RV. When we compare the soil materials for virus adsorption, the results show that the weathered granite soil has a higher capacity to adsorb the viruses. This is due to the fact that the soil characteristics, such as the specific surface, of weathered granite soil are better than sand. Also, the cation exchange capacity (CEC) is higher than in the sand, which contributes to the virus adsorption capacity.

The results of virus inactivation experiment showed that the inactivation rates of AdVF were in the range of 0.076-0.103 day^{-1} in treated A2O water (μ_1), 0.064-0.08 day^{-1} with sand ($\mu_{eff,sand}$) and 0.062-0.075 day^{-1} with weathered granite soil ($\mu_{eff,s\ oil}$). Sidhu and Toze (2012) studied the inactivation of several pathogens in groundwater at pH 7.24 and 22 ˚C. The study also tested Adenovirus 41 (AdV41) and the inactivation rate (μ_1) of AdV41 was 0.108 day^{-1} in their batch experiment. This inactivation rate is higher than that in the A2O water at 25 ˚C in this study.

Also inactivation rates of RV were in the ranged of 0.122-0.165 day^{-1} in A2O water (μ_1) to 0.075-0.114 day^{-1} with sand ($\mu_{eff,sand}$) and 0.091-0.120 day^{-1} with soil ($\mu_{eff,\ soil}$). Pancorbo et al. (1987) studied the RV with Wa strain inactivation in different water samples including groundwater at pH 6.7 and secondary wastewater at pH 6.6 at 20˚C. The RV inactivation rates were 0.36 and 0.33 day^{-1} in groundwater and secondary wastewater, respectively (Pancorbo et al., 1987). When compared with the RV inactivation rate in Pancorbo's study, the RV inactivation rate in the present study is lower. It may be because the quality of water was different. The difference in the virus inactivation rates can be attributed to differences in the chemical and biological properties of the water employed (Pancorbo et al., 1987).

The temperature condition between 4-37 ˚C showed no significant effect on AdVF and RV virus inactivation. Although, the highest inactivation in all virus inactivation experiment condition was found at 37˚C. The statistical analysis (p>0.05), this may suggest that the inactivation rate of AdVF and RV in sand and soil were not temperature-sensitive as same pathogenic viruses, such as Hepatitis A virus (HAV) (Schijven et al., 2000). It may be because these viruses are human enteric viruses that can endure in the human body temperature. Thus, the temperature up to 37˚C has no

significant effect on the viruses. Probably, the fast inactivation of those viruses mainly occurs at a temperature above 50 °C (Bertrand et al., 2012). This may demonstrate the importance of exploring the virus inactivation rate coefficient for target viruses based on the characteristics of a specific site. To the best of our knowledge, this is the first work that shows the inactivation rate coefficients of AdVF and RV, based on soils collected in Japan.

The inactivation rate coefficient of RV was slightly higher than those of AdVF under all conditions. At 4 ˚C, the lowest μ_{eff} of RV in the sand and weathered granite soil were 0.075 and 0.091 day^{-1}, respectively, whereas the lowest μ_{eff} of AdVF of those soil types were 0.064 and 0.063 day^{-1}, respectively. Obviously, the inactivation rate coefficient of AdVF in this study is higher than those of AdV2 reported by Ogorzaly et al. (2010), as 0.017 day^{-1} at 4˚C and 0.064 day^{-1} at 20˚C in groundwater. Because of the different water quality, the virus inactivation rate coefficient may be variable even in the same species of virus. This information indicated that the virus types influence the viral inactivation efficiencies.

Moreover, the soil and sand could protect the viruses from inactivation because the data shows that faster inactivation of the virus occurs in A2O water without sand or weathered granite soil. The obtained data of inactivation rate coefficients in this study can be applied to estimate the risk of AdVF and RV treated by SAT. However, the use of these data for estimating infection risks of the viruses should be limited because of the condition of this experiment, focused on the common soils (weathered granite soil and sand) in Japan. The adsorption and inactivation of the viruses in this study are the first step to estimate the efficiency of the SAT process to reduce virus in Japan.

3.5 Summary

In this chapter, the rotavirus and enteric adenovirus adsorption and inactivation efficiency were estimated. The adsorption and inactivation mechanisms depended on both soils and virus types. The results demonstrated that infectious AdV40 were more stable than the infectious RV at the same temperatures (4-37˚C). The AdV40 adsorption was higher than RV in sand and weathered granite soil. It is because AdV40 has higher isoelectric point than RV. The AdV40 adsorption was 0.6 to 3.2

$\log_{10}$ in sand and 1.5 to 3.9 $\log_{10}$ in weathered granite soil. The adsorption of RV was 0.2 to 1.5 $\log_{10}$ in sand and 0.8 to 2.4 $\log_{10}$ in weathered granite soil. For virus inactivation, RV was higher than AdV40 in sand, weathered granite soil and A2O water. Moreover, sand and weathered granite soil can protect AdV40 and RV inactivation.

This study provided useful information about human enteric viruses (RV and AdV40) adsorption and inactivation characteristics for the virus transportation model in sand and weathered granite soil, which is an essential part of viral risk assessment.

References

Anders R. & Chrysikopoulos C. V. 2005 Virus fate and transport during artificial recharge with recycled water. *Water Resources Research*, *41*(10).

Asano T., Burton F. L., Leverenz H., Tsuchihashi R. & Tchobanoglous G. 2007 *Water Reuse*. Metcalf&Eddy, New York.

Bertrand I., Schijven J. F., Sanchez G., Wyn-Jones P., Ottoson J., Morin T. & Gantzer C. 2012 The impact of temperature on the inactivation of enteric viruses in food and water: a review. *Journal of Applied Microbiology*, **112**(6), 1059-1074.

Blanc R. & Nasser A. 1996 Effect of effluent quality and temperature on the persistence of viruse in soil. *Water Science and Technology*, **33**(10), 237-242.

Burge W. D. & Enkiri N. K. 1978 Virus adsorption by five soils. *Journal of Environmental Quality*, **7**(1), 73-76.

Cruz J. R., Caceres P., Cano F., Flores J., Bartlett, A. & Torun B. 1990 Adenovirus types 40 and 41 and rotaviruses associated with diarrhea in children from Guatemala. *Journal of Clinical Microbiology*, **28**(8), 1780-1784.

Farkas K., Pang L., Lin S., Williamson W., Easingwood R., Fredericks R. & Varsani A. 2013 A gel filtration-based method for the purification of infectious rotavirus particles for environmental research applications. *Food and Environmental Virology*, **5**(4), 231-235.

Gerba C. P. & Lance J. C. 1978 Poliovirus removal from primary and secondary sewage effluent by soil filtration. *Applied and Environmental Microbiology*, **36**(2), 247-251.

Gerbo C. P., Goyal S. M., Cech I. & Bogdan, G. F. 1981 Quantitative assessment of the adsorptive behavior of viruses to soils. *Environmental Science & Technology*, **15**(8), 940-944.

Gutierrez L., Li X., Wang J., Nangmenyi G., Economy J., Kuhlenschmidt T. B.& Nguyen T. H. 2009 Adsorption of rotavirus and bacteriophage MS2 using glass fiber coated with hematite nanoparticles. *Water Research*, **43**(20), 5198-5208.

Haramoto E., Katayama H., Oguma K. & Ohgaki S. 2007 Quantitative analysis of human enteric adenoviruses in aquatic environments. *Journal of Applied Microbiology*, **103**(6), 2153-2159.

John D. E. & Rose J. B. 2005 Review of factors affecting microbial survival in groundwater. *Environmental Science & Technology*, **39**(19), 7345-7356.

Li D., Gu A. Z., Yang W., He M., Hu X. H. & Shi H. C. 2010 An integrated cell culture and reverse transcription quantitative PCR assay for detection of infectious rotaviruses in environmental waters. *Journal of Microbiological Methods*, **82**(1), 59-63.

Lion T., Baumgartinger R., Watzinger F., Matthes-Martin S., Suda M., Preuner S. & Gadner H. 2003 Molecular monitoring of adenovirus in peripheral blood after allogeneic bone marrow transplantation permits early diagnosis of disseminated disease. *Blood*, **102**(3), 1114-1120.

Matthess G., Pekdeger, A. & Schroeter J. 1988 Persistence and transport of bacteria and viruses in groundwater—a conceptual evaluation. *Journal of Contaminant Hydrology*, **2**(2), 171-188.

Moore R. S., Taylor D. H., Reddy M. M. & Sturman L. S. 1982 Adsorption of reovirus by minerals and soils. *Applied and Environmental Microbiology*, **44**(4), 852-859.

National Institute of Infectious Diseases (NIID) 2014 Rotavirus, 2010-2013. *IASR*, **35**(3), 63-64.

Ogorzaly L., Bertrand I., Paris M., Maul A. & Gantzer C. 2010 Occurrence, survival, and persistence of human adenoviruses and F-specific RNA phages in raw groundwater. *Applied and Environmental Microbiology*, **76**(24), 8019-8025.

Pancorbo O. C., Evanshen B. G., Campbell W. F., Lambert S., Curtis S. K. & Woolley T. W. 1987 Infectivity and antigenicity reduction rates of human rotavirus strain Wa in fresh waters. *Applied and Environmental Microbiology*, **53**(8), 1803-1811.

Payment P. & Locas A. 2011 Pathogens in water: value and limits of correlation with microbial indicators. *Groundwater*, **49**(1), 4-11.

Pedley S., Yates M., Schijven J. F., West J., Howard G., Barrett, M. & Chorus I. 2006 Pathogens: health relevance, transport and attenuation in *Protecting groundwater for health: managing the quality of drinking-water sources*. World Health Organization, IWA publishing, 49-80.

Pinto R. M., Diez J. M. & Bosch A. 1994 Use of the colonic carcinoma cell line CaCo-2 for in vivo amplification and detection of enteric viruses. *Journal of Medical Virology*, **44**(3), 310-315.

Powelson D. K., Simpson J. R. & Gerba C. P. 1990 Virus transport and survival in saturated and unsaturated flow through soil columns. *Journal of Environmental Quality*, **19**(3), 396-401.

Quanrud D. M., Carroll S. M., Gerba C. P. & Arnold R. G. 2003 Virus removal during simulated soil-aquifer treatment. *Water Research*, **37**(4), 753-762.

Schijven J. F. & Hassanizadeh S. M. 2000 Removal of viruses by soil passage: Overview of modeling, processes, and parameters. *Critical Reviews in Environmental Science and Technology*, **30**(1), 49-127.

Schijven J. F., Hassanizadeh S. M. & de Bruin R. H. 2002 Two-site kinetic modeling of bacteriophages transport through columns of saturated dune sand. *Journal of Contaminant Hydrology*, **57**(3), 259-279.

Seiradake E. & Cusack S. 2005 Crystal structure of enteric adenovirus serotype 41 short fiber head. *Journal of Virology*, **79**(22), 14088-14094.

Sidhu J. P. S. & Toze S. 2012 Assessment of pathogen survival potential during managed aquifer recharge with diffusion chambers. *Journal of Applied Microbiology*, **113**(3), 693-700.

Skraber S., Gassilloud B., Schwartzbrod L. & Gantzer C. 2004 Survival of infectious Poliovirus-1 in river water compared to the persistence of somatic coliphages, thermotolerant coliforms and Poliovirus-1 genome. *Water Research*, **38**(12), 2927-2933.

Sobsey M. D., Dean, C. H., Knuckles M. E. & Wagner R. A. 1980 Interactions and survival of enteric viruses in soil materials. *Applied and Environmental Microbiology*, **40**(1), 92-101.

Straub T., Bartholomew R., Valdez C., Valentine N., Dohnalkova A., Ozanich R. & Call D. 2011 Human norovirus infection of Caco-2 cells grown as a three-dimensional tissue structure. *Journal of Water and Health*, **9**(2), 225-240.

Yates M. V., Gerba C. P. & Kelley L. M. 1985 Virus persistence in groundwater. *Applied and Environmental Microbiology*, **49**(4), 778-781.

Zeng S. Q., Halkosalo A., Salminen M., Szakal E. D., Puustinen L. & Vesikari T. 2008 One-step quantitative RT-PCR for the detection of rotavirus in acute gastroenteritis. *Journal of Virological Methods*, **153**(2), 238-240.

Chapter 4

Reduction of enteric viruses in secondary wastewater effluent in soil aquifer treatment

4.1 Introduction

The fate of human enteric viruses in Soil Aquifer treatment (SAT) is the focus of this study. Since inactivation and adsorption are the main mechanisms of virus reduction in SAT (Yates et al., 1987), the adsorption and inactivation rate constants were estimated by batch experiments in Chapter 3. In the complicated system as in treated wastewater, the virus removal behavior may be different from batch experiment (Schijven and Hassanizadeh, 2000). Real viruses in the treated wastewater need to study. Many laboratory studies on the fate and transport of viruses in soil or porous media have usually been conducted with column experiments, and it is known that a column length less than one meter does not represent the virus reduction in the field (Pang, 2009). Therefore, a relatively long (i.e., 2.37 m) pilot-scale SAT column was used in this study. This chapter aims to quantify the enteric virus concentrations in the treated wastewater after A2O process and to determine the removal and inactivation capacity of the viruses in SAT.

4.2 Materials and methods

4.2.1 Sampling site and sample preparation

The pilot-scale column of SAT was operated at the Toba Wastewater Environment Conservation Center, Kyoto City, Japan. The treated wastewater from A2O process has been pumped continuously into the column as the SAT influent. The influent and effluent samples were collected twice a month between July 2013 and March 2015. The SAT column had an unsaturated zone 0.17 m from the top layer and the hydraulic retention time was approximately 28 days. The schematic of SAT is illustrated in Figure 4.1. The characteristics of packing material (i.e., sand) are mentioned in Chapter 3.

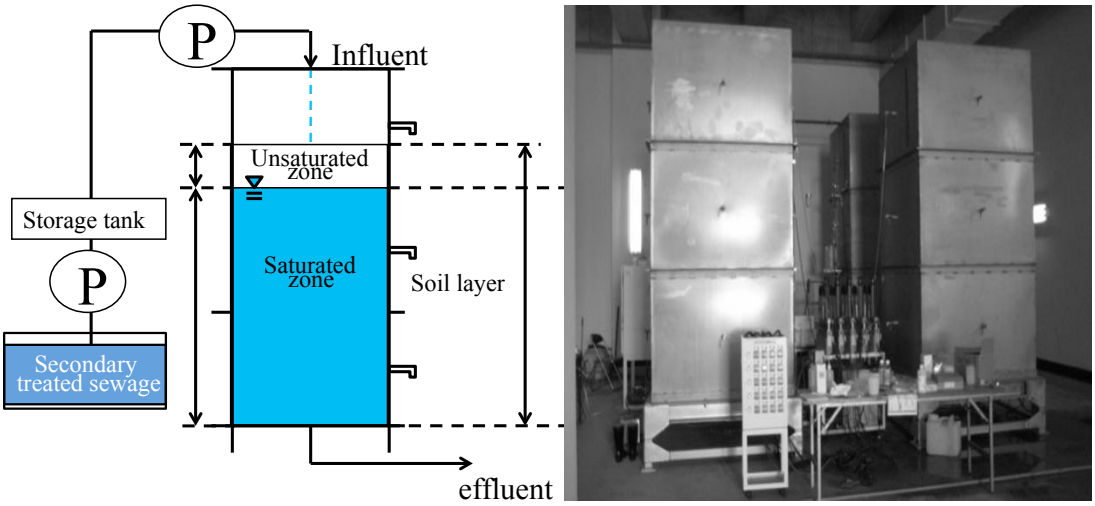

Figure 4.1: The schematic of the pilot-scale SAT reactor

Table 4.1: The specific conditions of the SAT column

Soil type	Sand
Influent flow rate	46 mL/min
Effluent flow rate	46 mL/min
Reactor construction	W 1.5 mx D1.5 mx H 3.0 m
Soil Height	2.37 m
Water level	2.20 m
Sampling site	1.50 m

4.2.2 Sample concentration

The virus concentration in the SAT effluent was very low and sample concentration was required. For this purpose, ultrafiltration (UF) was applied for primary concentration. Subsequently, Polyethylene glycol (PEG) precipitation method was used as a secondary concentration as shown in Figure 4.2. Before use, the UF (Pellicon 2, Millipore with 50 kDa MWCO of membrane filter) was rinse with MilliQ water several times, followed by 0.1 N H_3PO_4 and 250 mg/L NaOCl solution to remove the contaminants, such as organic matter and other viruses. During UF process, 50 L of raw samples were concentrated down to 1 L. In the case of the SAT influent samples, PEG precipitation was applied to these samples.

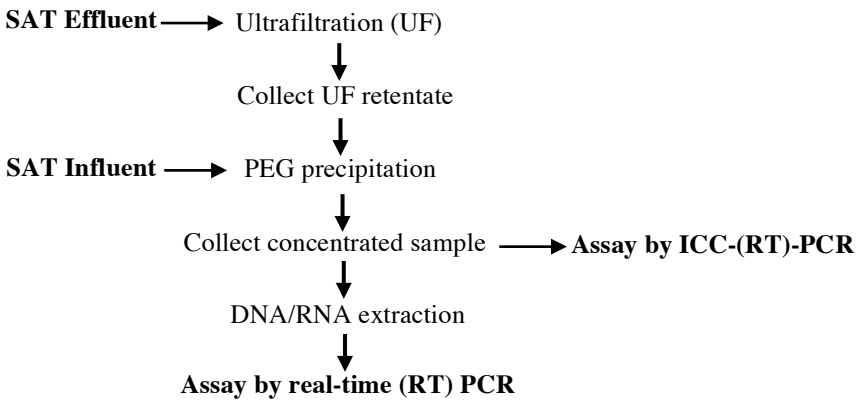

Figure 4.2: The diagram of virus concentration method.

The protocol of PEG precipitation method is shown in Figure 4.3. This method was modified from procedure reported by Hewitt et al. (2011). The pH of samples was adjusted to the range of 7.0 and 7.2. Then 2% NaCl and 8% polyethylene glycol (PEG) 6000 molecular biology grade (SERVA Electrophoresis) were completely dissolved in the samples. These samples were stored at 4 ˚C over night. On the following day, the samples were centrifuged at 10,000 × g at 4 ˚C for 45 min. The supernatant was discarded and the obtained pellet was resuspended in 2 mL of sterilized phosphate buffered saline (PBS) at pH 7.2. After the pH of the samples reached the range of 7.0 and 8.0, the samples were dispersed by ultra-sonication for 2 min. Subsequently, samples were shaken at room temperature for 1 h with every 15 min of vortexing to elute the virus from the pellet._After that, the samples were sonicated again for another 2 min and centrifuged at 10,000 × g for 20 min. Two milliliters chloroform was added and mixed vigorously for 15 min, then centrifuged at 1200 × g for 10 min. The chloroform phase was discarded by aspiration. This chloroform extraction was repeated twice. Antibiotic solution (GIBCO™) containing pennicilin-streptomycin-amphotericin was added to the samples at the final concentration of 1% in order to reduce any chances of microbial contamination. After that, the concentrated samples were stored at -80 ˚C until use.

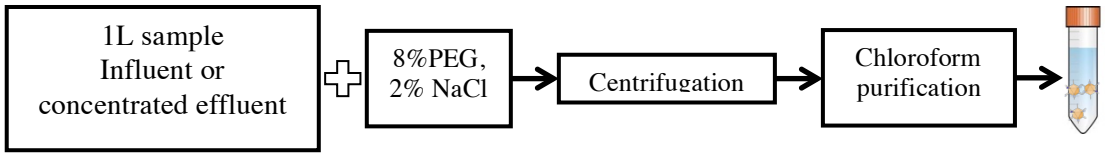

Figure 4.3: PEG precipitation diagram and virus purification

4.2.3 Viruses detection

a) Determination of virus concentration by qPCR

Before analyzing the samples by qPCR, DNA/RNA extraction is required as was mentioned in Chapter 3 in 3.2.3. Although the PCR assay provides rapid virus detection, the presence of PCR inhibitors in water samples resulting from the concentration method was the major drawback of this method (Lewis et al., 1988). The presence of endogenous inhibitors in the concentrated samples can be detected by spiking a known amplifiable target and its respective primers. In this study, the primer-sharing controls (PSCs) were selected as an endogenous inhibitor control (internal inhibitor control for virus detection) (Hata et al., 2011) for both of AdVF and RV because they can make the specific sequences for the virus types. The PSC sequences and qPCR mixture used in this study were shown in Table 4.2 and 4.3 (Kunimoto, 2015).

Table 4.2: Primers and probes sequences used for qPCR

Virus	Primer/Probe	Sequence	Target	Reference
AdV-F	Forward primer (AdVF-F)	5'-GCA GGA CGC CTC GGA GTA-3'	Hexon gene (128bp)	Heim et al (2003)
	Reverse primer (AdVF-R	5'-TGT CTG TGG TTA CAT CGT GGG T-3'		
	Probe (AdVF-P)	FAM-TAC TTC AGC CTG GGG AAC AAG TTC AGA AA-NFQ-MGB		
	PSC-Probe (FAdvP-PSC)	VIC-TGG TTC TCT CCG AAA TAG ATT TAG GGC TA-NFG-MGB		
	PSC-DNA	**GCAGGACGCCTCGGAGTA**TCTGAG CCCGGGCCTGGTGCAATTTGCCCG CGCCACCGATACG*TGGTTCTCTCCGA AATAGATTTAGGGCTA*TCCCACTG TGGCTCCG**ACCCACGATGTAACCA CAGACA**		Kunimoto (2015)
RV	Forward primer (Rota-NSP3-F)	5'-ACC ATC TAC ACA TGA CCC TCT ATG AG-3'	NSP3 (87bp)	Zeng (2008)
	Reverse primer (Rota-NSP3-R	5' GGT CAC ATA ACG CCC CTA TAG C-3'		
	Probe(NSP3-P)	FAM-AGT TAA AAG CTA ACA CTG TCA AA-MGB		
	PSC-Probe (NSP3-PSC)	VIC-TGG TTC TCT CCG AAA TAG ATT TAG GGC TA-NFG-MGB		
	PSC-RNA	**ACCATCTACACATGACCCTCTATG AG**CACAA*TGGTTCTCTCCGAAATAGA TTTAGGGCTA*AAATG**GCTATAGGGG CGGTTTGTGACC**		Kunimoto (2015)

A: Bold is primer annealing site, Italic probe hybridization site
Reference gene GenBank accession number DQ315364.2
Reference gene GenBank accession number EU984100.1

Table 4.3: The mixture chemical for qPCR detection of RV and AdVF

Duplex qRT-PCR of RV detection mixture	
Chemicals	**Volume (μL)**
2xBuffer	10
Forward Primer (10μL)	1.8
Reverse Primer (10μL)	1.8
RV-Probe (10μL)	0.5
PSC-Probe (10μL)	0.5
Nuclease-free water	0.5
40x Enzyme mix	0.5
PSC-RNA (100 copies)	2
RNA Template	2
Total	20

Duplex qPCR of AdVF detection mixture	
Chemicals	**Volume (μL)**
Nuclease-free water	2
Environmental Master Mix2.0	10
Forward Primer (10μL)	1.6
Reverse Primer (10μL)	1.6
Probe (5μM)	0.4
PSC-DNA Probe (5μL)	0.4
PSC-DNA (100 copies)	2
DNA Template	2
Total	20

To evaluate the magnitude of the inhibition effect on PCR detection according to the concentration method, PSCs were performed as mentioned previously. AdVF and RV detected by qPCR was carried out in duplex-(RT)-PCR using the PSC-DNA and PSC-RNA, respectively. For the evaluation of the PCR inhibitory effect, the PSCs were synthesized by the Hokkaido System Science and were measured at the same time as an internal control. PSCs have been spiked 100 copies/well. If the PSCs concentrations were below 10 (PCR inhibition), the samples needed to be diluted and analyzed again until the concentration of PSCs is under 10 copies/μL.

b) Determination of infectious viruses by ICC-(RT)-PCR

The concentrated samples, which had been purified with chloroform, were directly detected by ICC-(RT)-PCR, without DNA/RNA extraction. The procedure of this method had been described in 3.2.3.

c) DOC measurement

Dissolve organic carbon (DOC) in the SAT influent and effluent samples were measured by a TOC-L analyzer (Shimadzu, Japan). The samples were filtered through a glass fiber filter with a 0.45 μm pore size and subsequently measured by the TOC-L analyzer.

4.3 Results

4.3.1 DOC removal during SAT and one-year temperature profile in the SAT effluents

DOC data were collected from September 2012 to November 2014. The efficiency of the DOC removal has been calculated by pairing 1-month data between the SAT influent and the SAT effluent to account for the retention time of the SAT system. After pairing the data, the DOC removal was 69.6-89.3% (mean 80.1% or 0.63 $\log_{10}$) and the DOC concentrations in the SAT effluent were really stable (0.4-1.0 mgC/L). In short, SAT could be an effective treatment to remove DOC (Figure 4.4).

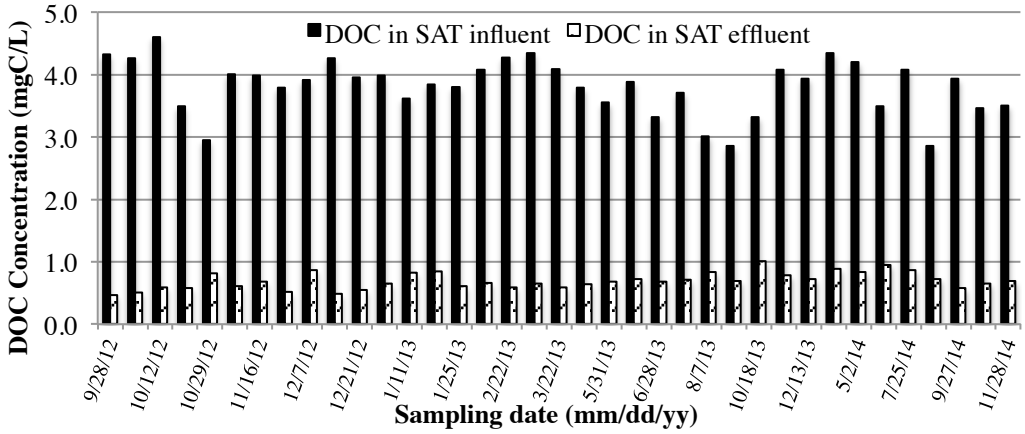

Figure 4.4: DOC concentration with 1-month pairing data of SAT influent and effluent sample for estimating the its removal

The SAT system could reduce the DOC concentration in SAT effluent down to 1 mgC/L or lower. Moreover, the DOC removal rate can be estimated with the first order reduction rate equation as in eq. 3.3. The DOC reduction rate was approximately 0.056 day^{-1}.

Water temperature is a significant parameter for virus inactivation in soil as mentioned in Chapter 2. Temperature data in the SAT effluent was collected from October 2012 to March 2014 (Figure 4.5).

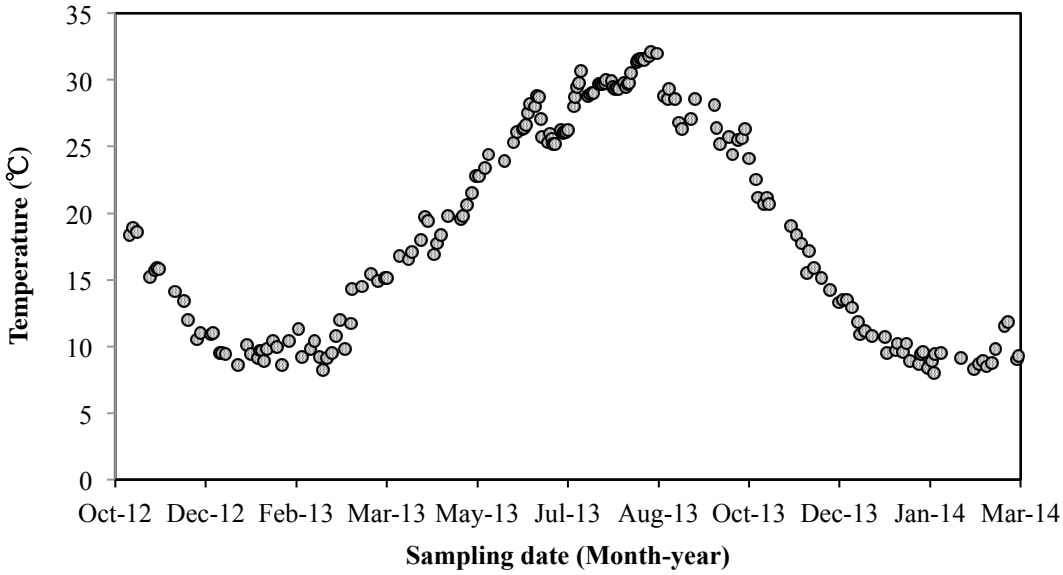

Figure 4.5: Temperature profile in SAT effluent from October 2012 to March 2014

The temperature increased up to 32 ˚C in the summer season from June to September, and it also decreased to 8 ˚C in the winter (January). From the stable DOC removal during the SAT, it can be said that the temperature has no major effect for DOC removal in the SAT system.

4.3.2 The effect of PCR inhibition on the SAT samples

PSCs data are shown in Figure 4.6. As previously mentioned, PSCs of 100 copies/μL were added to the q(RT)PCR reaction mixture in order to assess the PCR inhibition. From previous researches, the inhibition occurs when the PSC concentration is less than 10 copies/μL. The PSCs level in concentrated SAT influent and effluent samples were acceptable (10 copies/μL < level <1000 copies/μL). It indicated that the PCR inhibitor had little effect on these target virus detection by q(RT)PCR.

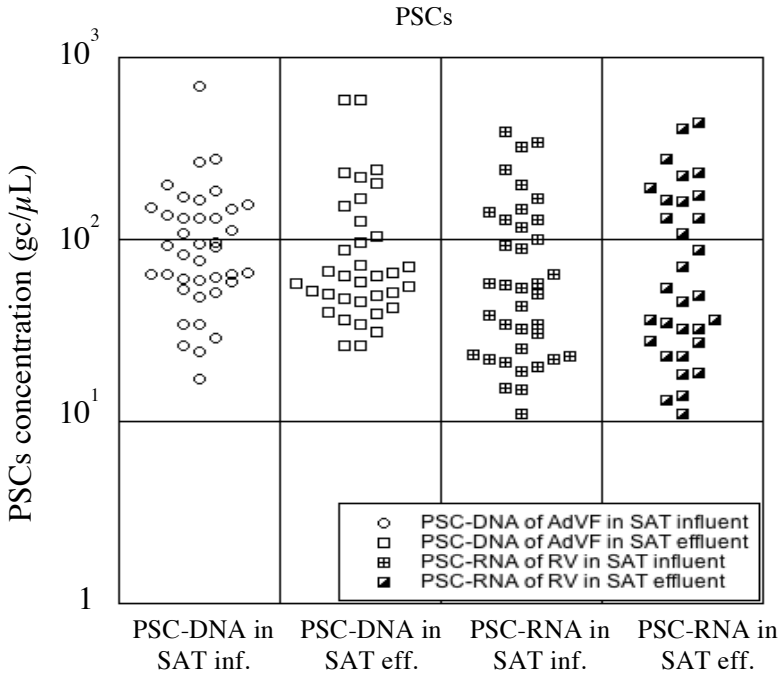

Figure 4.6 PSCs concentration detection (All sample spike PSCs with 100 copies/μL)

4.3.3 The virus concentrations in the SAT influent and SAT effluent samples

The infectious virus in the SAT influent was detected by using ICC-PCR. The example of infectious AdVF detection is shown in Figure 4.7. Infectious RV was also detected by using ICC-RT-PCR and the example of infectious RV detection is shown in Figure 4.8. Infectious AdVF can still detected in SAT influent but it is difficult to detect the infectious AdVF in SAT effluent. For RV, it could not be detected infectious RV in most of SAT influent and effluent samples.

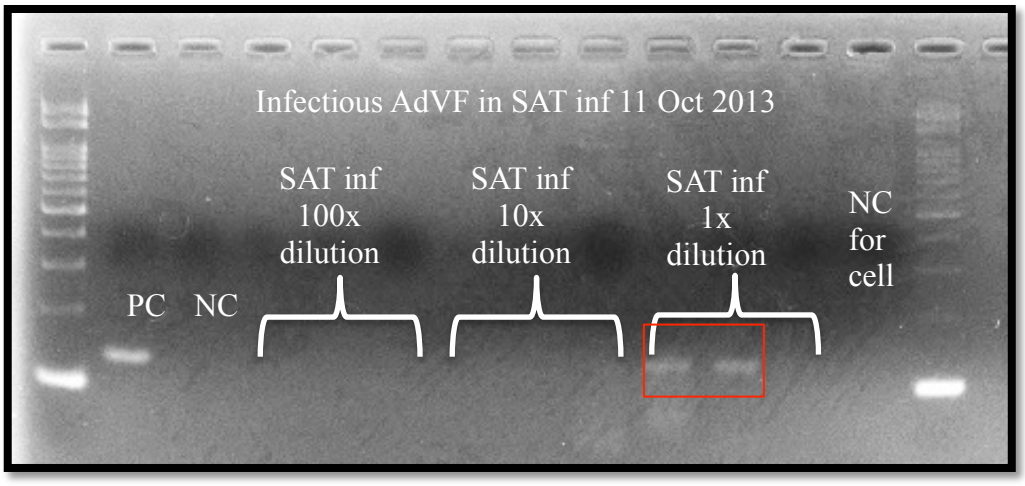

Figure 4.7 infections AdVF detection by ICC-PCR in SAT influent (detected sample)

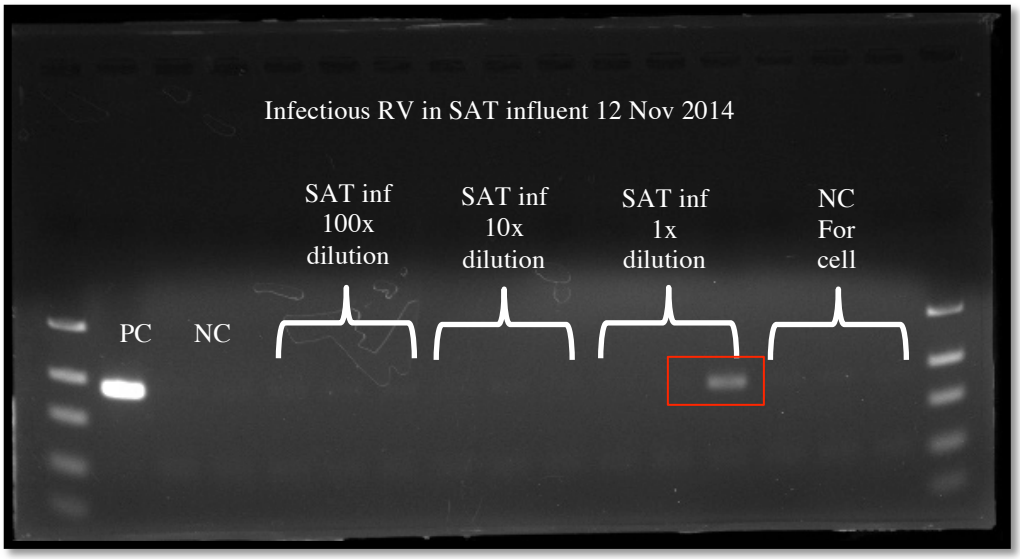

Figure 4.8 infections RV detection by ICC-PCR in SAT influent (detected sample)

The recovery rates of the concentration methods are shown in Table 4.4. The concentrations of AdVF and RV in SAT influent and effluent were calculated using the recovery rates in the same period of time.

Table 4.4: Recovery of adenovirus and rotavirus in SAT influent and effluent samples

Sampling date	%Recovery of AdVF		%Recovery of RV	
	SAT influent (PEG)	SAT effluent (UF+PEG)	SAT influent (PEG)	SAT effluent (UF+PEG)
25 Jul 2013-30 Oct 2013	24	0.073	8.6	0.075
15 Nov 2013-28 Nov 2013	32	0.073	12	0.075
6 Dec 2013-25 Feb 2014	32	24	12	0.37
23 Apr 2014-22 Aug 2014	32	1.8	12	0.5
12 Sep 2014- 10 Oct 2014	2	1.3	7.5	2.1
22 Oct 2014- 28 Nov 2014	2	0.4	7.5	2.5
10 Dec 2014 – 19 Dec 2014	6.1	0.4	34	2.5
7 Jan 2015-18 March 2015	2.2	0.6	7.3	1.1

a) AdVF concentration in SAT influent and effluent samples

AdVF data were collected from July 2013 to March 2015. By qPCR, 32 of 39 influent samples (82%) AdVF were detected. The concentration of AdVF ranged from $8x10^3$ to $2x10^6$ copies/L (mean $2x10^5$ copies/L) in the SAT influent, as shown as the white columns in Figure 4.9. The infectious AdVF data were collected at the same time. By ICC-PCR, 22 of 36 samples (61%) were positive for infectious AdVF. The concentration of infectious AdVF ranged from 10 to $4x10^3$ MPNIU/L (mean $8x10^2$ MPNIU/L) as shown in the brick columns in Figure 4.9. These data show that the AdVF is abundant in SAT influent (treated A2O water). In addition, the ratio of the

infectious AdVF to the genome based AdVF was estimated to be in the range of 0.00004 and 0.145 (mean 0.02).

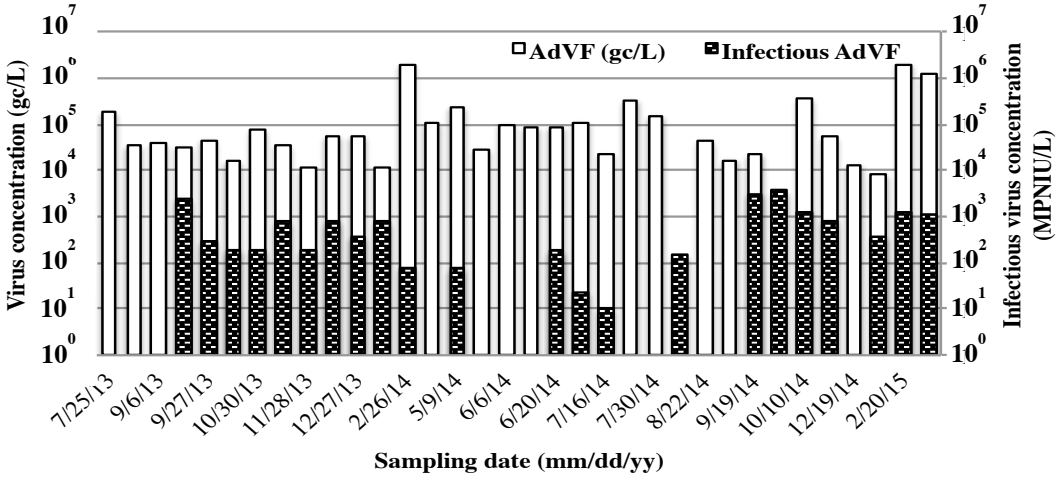

Figure 4.9 AdVF and infectious AdVF in SAT influent samples

For AdVF in SAT effluent, the data were collected in the same period for AdVF in the SAT influent. For 26 of 36 samples (72%), AdVF was detected by qPCR. The concentration of AdVF ranged from $6x10^2$ copies/L to $8x10^4$ copies/L (mean $9x10^3$ copies/L) in the SAT effluent samples as shown in Figure 4.10. By ICC-PCR 5 of 31 samples (16%) were positive for AdVF. The infectious AdVF concentration ranged from 5 to 100 MPNIU/L (mean 40 MPNIU/L). The ratio of infectious AdVF to the genome-based concentration was estimated to be in the range of 0.0005 and 0.0015 (mean 0.001).

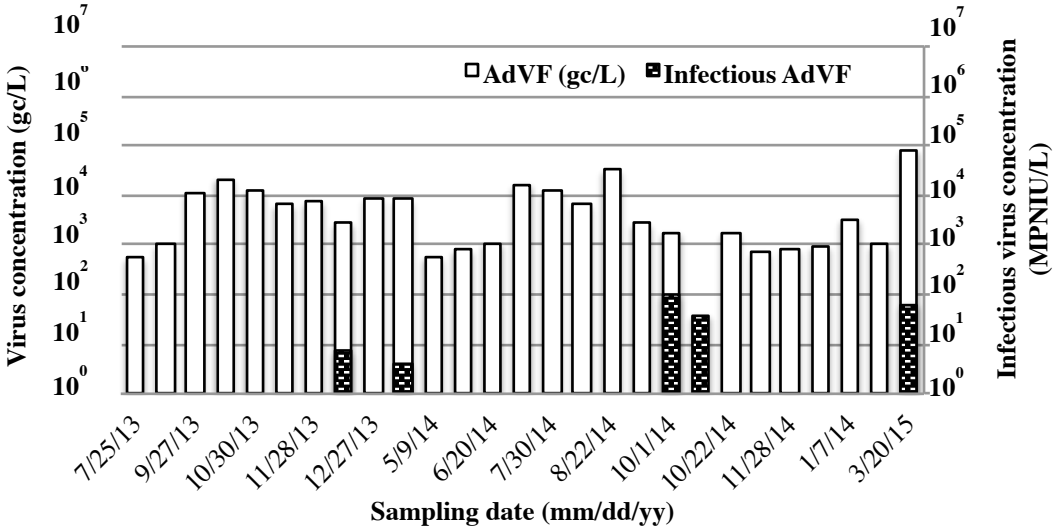

Figure 4.10 AdVF and infectious AdVF in SAT effluent samples

b) RV concentration in SAT influent and effluent samples

RV data in SAT influent was collected from July 2013 to March 2015. The qRT-PCR analysis found that 35 of 39 samples (89%) were positive for RV. The concentration of RV ranged from $2x10^3$ to $6x10^5$ copies/L (mean $1x10^5$ copies/L) in the SAT influent (the white columns in Figure 4.11). Moreover, the infectious RV data collected from April 2014 to March 2015. By ICC-RT-PCR, 3 of 37 samples (8%) were positive for infectious RV. The concentration of infectious RV ranged from 22 to 73 MPNIU/L (mean 51 MPNIU/L) (the brick columns in Figure 4.11). These data show that the genomes of RV are abundant in SAT influent (treated A2O water), but RV lost their infectivity during wastewater treatment processes. In addition, the ratio of the infectious RV to the total RV (genome based concentration) was estimated to be in the range of 0.001 to 0.005 (mean 0.003). Infectious RV was detected only in October, November and December in SAT influent samples. This period marks the beginning of winter in Japan.

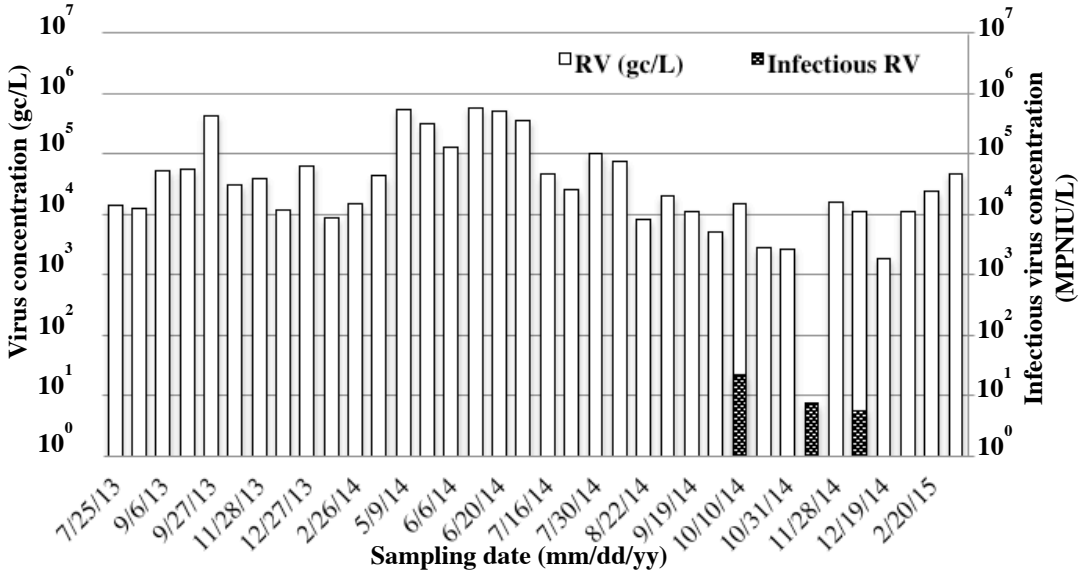

Figure 4.11 RV and infectious RV in SAT influent samples

For RV in SAT effluent, the data was collected at the same time as RV in SAT influent. The qPCR analysis found that 36 of 39 samples (92%) were positive for RV. The concentration of RV ranged from $7x10^2$ copies/L to $2x10^5$ copies/L (mean $3x10^4$ copies/L) in the SAT effluent samples as shown in Figure 4.12. In addition, infectious RV was collected in the same period as the SAT influent samples. By ICC-RT-PCR, 2 of 25 samples (8%) were positive for RV. The infectious RV concentrations were 8

MPNIU/L in both samples. The ratio of infectious RV to total RV ranged from 0.0004 to 0.004 (mean 0.0024).

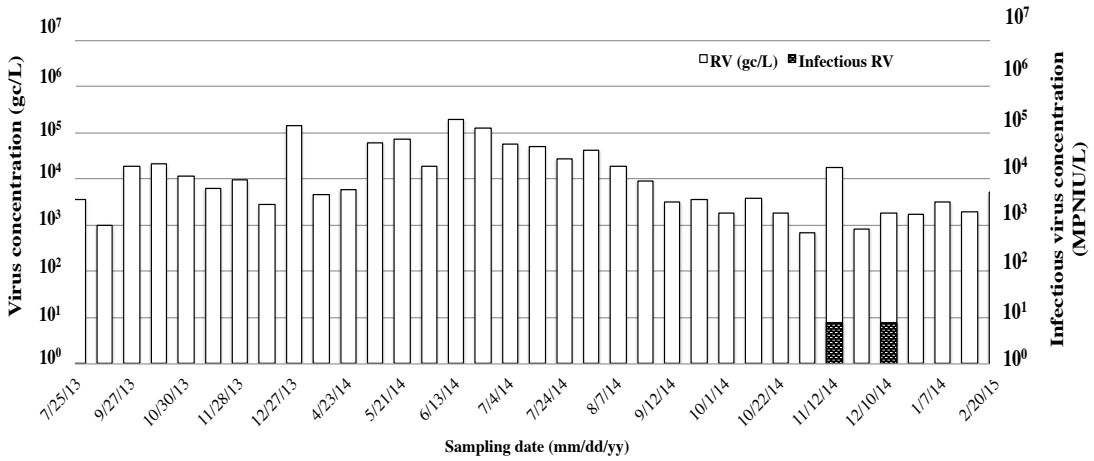

Figure 4.12 RV and infectious RV in SAT effluent samples

4.3.4 Virus removal in the SAT

To estimate the removal efficiency of the SAT, each qPCR concentration data (genome base) of influent and effluent were paired with an interval of 28 days (i.e., HRT obtained from the bromide tracer test). Eighteen paring data of AdVF of SAT influent and effluent samples were plotted in a column char as shown in Figure 4.13, and the removal of AdVF was calculated. The results showed that the highest and lowest removal capacity of the SAT was 2.24 and 0.09 $\log_{10}$, respectively. The average removal of AdVF was 0.72 $\log_{10}$.

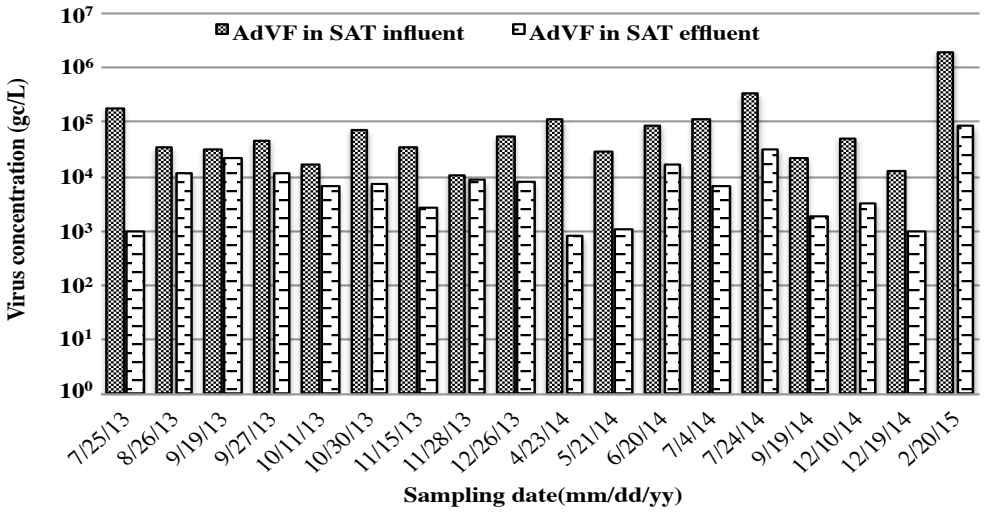

Figure 4.13 AdVF influent and effluent with 1-month pairing data of influent and effluent sample for estimating the its removal

The removal efficiency of RV in SAT during the period of May-July 2014 was paired with an interval of 28 days (i.e., HRT of the system). Sixteen pairing data of RV were plotted in the column chart as shown in Figure 4.13. The highest RV virus removal capacity of ranged from -0.55 $\log_{10}$ to 1.45 $\log_{10}$ (mean 0.15 log). However, few pairing data showed the negative removal. This indicated that the SAT sand column has low potential to adsorb RV. The seasonal pattern of regarding the presence of RV concentration may not conclude in this observation by genome data.

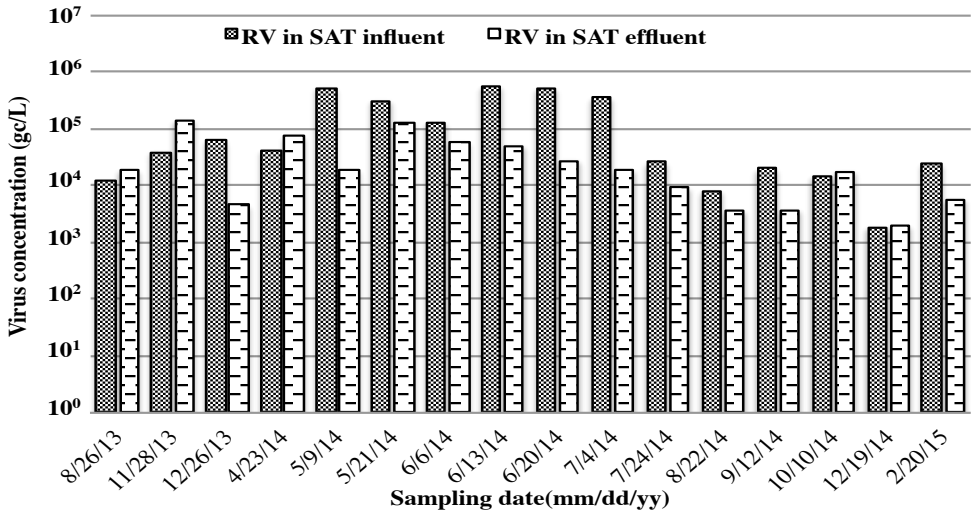

Figure 4.14: RV influent and effluent with 1-month pairing data of influent and effluent sample for estimating its removal

4.3.5 The relationship between the virus removal and other parameters (DOC removal and water temperature

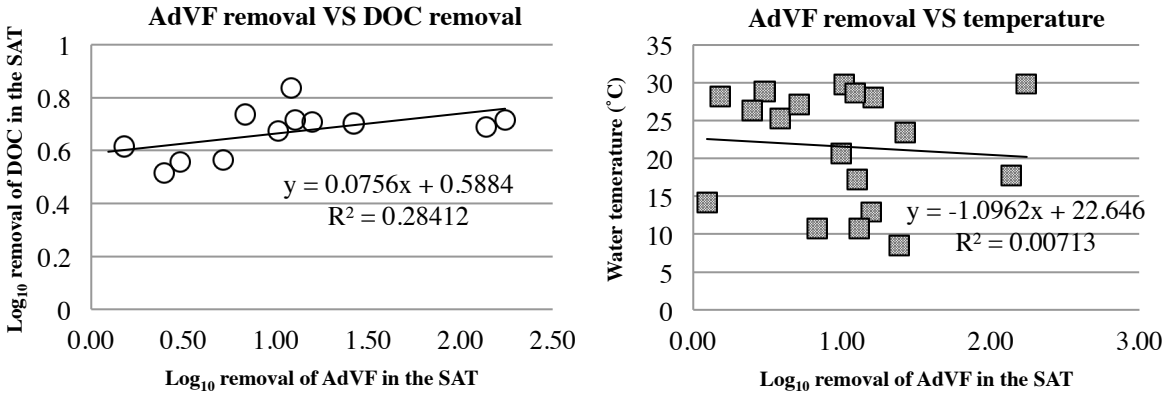

Figure 4.15: Correlation between the $\log_{10}$ AdVF removal and $\log_{10}$ DOC removal (left) and $\log_{10}$ AdVF removal and temperature (right) in the SAT column

The $\log_{10}$ DOC removal and the $\log_{10}$ AdVF removal at the same period are plotted in Figure 4.15. There is weak positive linear association between the $\log_{10}$ removal of AdVF in the SAT and $\log_{10}$ removal of DOC in the SAT. The value of R^2 is 0.28.

The water temperature and the $\log_{10}$ AdVF removal at the same period are plotted in the Figure 4.15. There is no linear association (the value of the R^2 is 0.007).

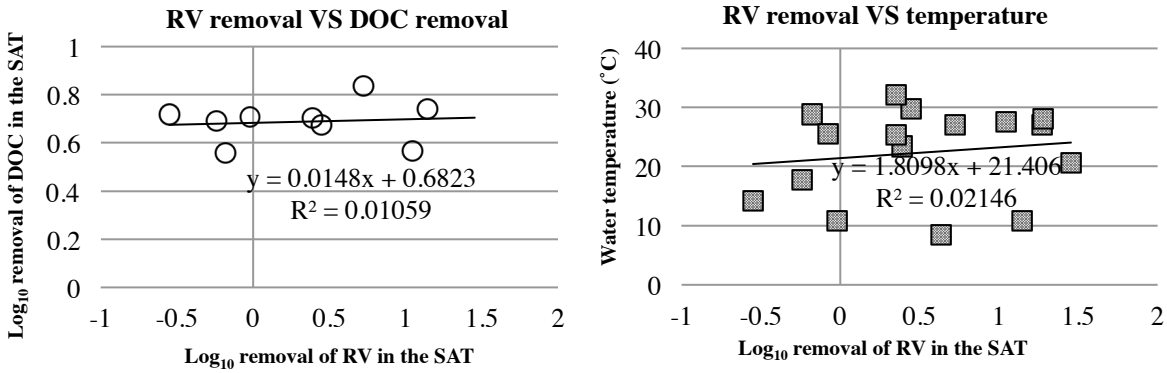

Figure 4.16: Correlation between the $\log_{10}$ RV removal and $\log_{10}$ DOC removal (left) and $\log_{10}$ RV removal and temperature (right) in the SAT column

Neither temperature nor DOC removal were found to affect RV removal during SAT as shown in Figure 4.16. Thr R^2 values showed that the relation between virus

removal and temperature is not significant (0.01) as same as the virus removal and DOC removal (0.02).

4.3.6 Virus inactivation in the SAT

The reduction (removal and inactivation) capacity of AdVF and RV can be estimated by the ICC-(RT)-PCR. However, the data of infectious viruses are limited. After pairing between influent and effluent samples, with an interval of 28 days (i.e., retention time), Only 4 data for AdVF and 2 data for RV are available (Figure 4.15), and the reduction capacity of AdVF ranged from 1.28 $\log_{10}$ to 2.03 $\log_{10}$ (mean 1.88 $\log_{10}$ reduction). In addition, RV reductions were 0.43 and 0.96 $\log_{10}$. The inactivations of viruses in SAT are shown in the Figure 4.17.

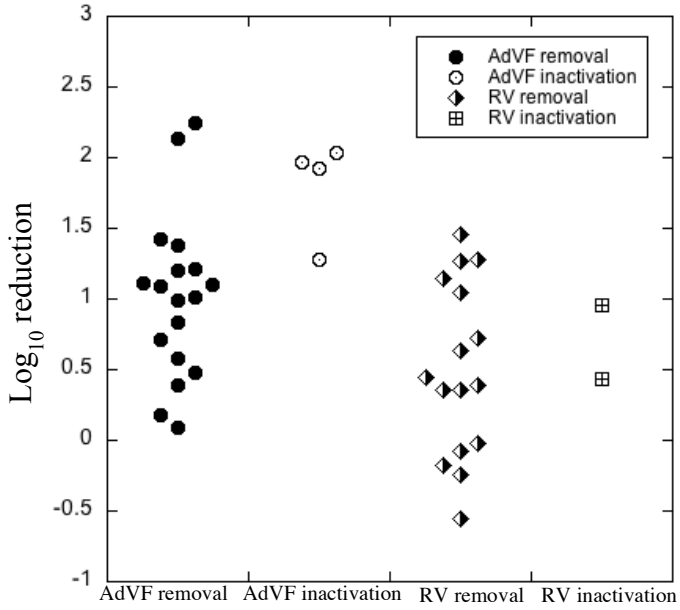

Figure 4.17 Infectious viruses with 1-month paring data of influent and effluent samples for estimating the inactivation capacity

The ICC-(RT)-PCR showed the whole reduction of the viruses (removal and inactivation). To estimate only inactivation rates, the data of qPCR gathered on the same date was used for calculation, as shown in Table 4.5. The calculation of all rate coefficients follow the first order decay rate as showed in the Eq. 3.6 in Chapter 3. Then the inactivation rate coefficient can be estimated from all reduction rate and removal rate coefficients.

Table 4.5: Estimation of virus inactivation rates in SAT

Virus	date (mm/dd/yy)	SAT inf. (MPN/L)	SAT eff. (MPN/L)	Over-all reduction rate (day^{-1})	SAT inf. (copies/L)	SAT eff. (copies/L)	Removal rate (day^{-1})	Inactivation rate (day^{-1})
AdVF	11/15/13	7.7×10^2	7.0	0.17	3.5×10^4	2.8×10^3	0.09	0.09
	12/26/13	3.7×10^2	4.0	0.16	5.5×10^4	8.1×10^3	0.07	0.09
	9/19/14	3.2×10^3	4.0×10^1	0.16	2.2×10^4	1.8×10^3	0.09	0.07
	2/20/15	1.2×10^2	6.0×10^1	0.11	2.0×10^4	8.3×10^4	0.11	0.00
RV	10/10/14	2.2×10^2	8.0	0.04	2.0×10^4	2.0×10^4	0.00	0.04

The average AdVF inactivation rate (μ_{AdVF}) was 0.06 day^{-1} and the RV inactivation rate (μ_{RV}) was 0.04 day^{-1}.

The AdVF inactivation rate coefficient obtained from the pilot experiment with sand column was nearly close to the inactivation rate coefficient obtained from the batch experiments (0.064 day^{-1}at 15°C) in Chapter 3.

In the case of RV, there is only one data for RV virus inactivation rate coefficient that can be estimated in the same sampling date and time. Moreover, most SAT influent and effluent samples cannot detect infectious RV. Furthermore, the inactivation rate coefficient of the RV obtained from the pilot experiment (0.04 day^{-1} was totally different from batch experiment (0.098 day^{-1} at 15°C).

4.4 Discussions

The concentration of AdVF ranged from 8×10^3 to 2×10^6 copies/L and RV ranged from 2×10^3 to 6×10^5 copies/L in the secondary treated wastewater in this study. The concentrations of AdVF and RV were higher than in any other study. It might be because of the different area that leads to different water condition and virus inactivation. Katayama et al. (2008) investigated AdVF in several types of water including raw sewage, secondary treated sewage, and river water. The Katayama study of secondary sewage in Japan found that the concentration range of AdVF was 1.03×10^4-2.48×10^5 PCR units/L. Haramoto (2007) reported that the AdVF in secondary treated sewage before chlorination was $6. \times 10^{-1}$-4.1×10^3 PDU (PCR-detection unit)/L. Moreover, Fong (2010) reported that AdVF concentration ranged between 1.05×10^3 and 4.42×10^4 viruses/L in the secondary effluent. A seasonal trend was not observed for the concentration of adenovirus DNA in wastewater samples.

This pattern was also observed in this study, in the way the adenovirus DNA was constant in the entire year of the SAT influent samples.

RV is most frequently detected in the winter and rarely detected in the summer months in the temperate zone by etiology studies (Cook et al., 1990). There is no data available for RV concentration in the sewage and secondary sewage in Japan. However, RV in secondary sewage was reported to be $4.0x10^{2}$-$5.0x10^{4}$ copies/L and $1x10^{0}$-$3x10^{1}$ PFU/L in secondary treated sewage in China (Li et al., 2010). The seasonal trend was observed in the RV concentration. Especially in winter, it is relatively high (Li et al., 2010). In this study, infectious RV can be detected only from October to December, the beginning of winter in Japan. It seems to be the same seasonal pattern as in Li's study. Furthermore, the infectious RV was rarely detected in SAT influent samples. It has possibility of high removal and inactivation of RV during the wastewater treatment plant.

In the present study, SAT sand column longer than 1 meter was used to achieve more reliable virus removal. The results of virus removal in this column experiment were totally different from the batch experiment in Chapter 3. The removal efficiencies of both viruses were lower than the batch experiment. Page et al. (2010) reported that the RV removal in the Tula Valley aquifer with RV was 0-0.8 $\log_{10}$ removal (most likely 0.2 $\log_{10}$ removal). The same trend of RV virus removal was found in this study, RV removal ranged from -0.55 $\log_{10}$ to 1.45 $\log_{10}$ (mean 0.15 $\log_{10}$ removal).

The removal of AdVF was 0.09-2.24 $\log_{10}$ (mean 0.73 $\log_{10}$ removal). Another research of adenovirus removal by soil aquifer treatment usually could not detect the adenovirus in the effluent in aquifer systems (Beleke et al., 2011). Moreover, the previous studies mostly use the bacteriophage as the model virus or surrogate enteric virus. The removal of bacteriophage also fluctuated depending on the environmental conditions and virus types. Thus, it is difficult to compare the AdVF removal data with previous study.

The AdVF showed a higher removal than the RV in the SAT column. It might have been because of the isoelectric point of the viruses (6.8 IEP of AdVF, 4.5 IEP of RV, (Seiradake and Cusak, 2005; Gutierrez et al., 2009). The results also show the same trend, described in the previous part of the batch experiment in 3.4 of Chapter 3.

The effect of DOC and temperature on virus removal was evaluated in this study. There was no relationship between DOC and virus removal in the SAT. Also, it is found that the removal of the virus (genome based results) and the DOC did not depend on temperature.

In addition, inactivation rate coefficient of AdVF in the column experiment is the same rate in the batch experiment. Due to the same conditions of A2O water and sand, the inactivation of AdVF just depended on time. Therefore, the inactivation rate of AdVF is not quite different. However, the limited data for infectious RV were detected in SAT influent and effluent, only one inactivation rate could be calculated. The RV inactivation rate was really low comparing with the batch experiment result.

4.5 Summary

The concentrations and reductions of AdVF and RV were investigated with a pilot – scale SAT reactor. The infectious AdVF was 4-100 MPNIU/L but few infectious RV was detected in the SAT influent water. The virus reduction was described by removal (genome base detection) and inactivation (ICC-PCR detection). The AdVF overall reduction (removal and inactivation) ranged from 1.28-2.03 $\log_{10}$ and the RV reduction ranged from 0.43-0.96 $\log_{10}$. The reduction of the AdVF was higher than the RV. All infectious viruses data and the removal and inactivation of viruses in this study were used as an input to the model of virus transport in soil, addressed in the next chapter for predictive simulation of virus transport in the SAT in Japan.

References

Bekele E., Toze, S., Patterson B. & Higginson S. 2011 Managed aquifer recharge of treated wastewater: Water quality changes resulting from infiltration through the vadose zone. *Water Research*, **45**(17), 5764-5772.

Cook S. M., Glass R. I., LeBaron C. W. & Ho M. S. 1990 Global seasonality of rotavirus infections. *Bulletin of the World Health Organization*, **68**(2), 171.

Cook N., de Ridder G. A., D'Agostino M. & Taylor M. B. 2013 Internal amplification controls in real-time polymerase chain reaction-based methods for pathogen detection. *Real-Time PCR in Food Science: Current Technology and Applications, ed. by Rodríguez-Lázaro D. Caister Academic Press, Poole, UK*, 35-42.

Fong T. T., Phanikumar M. S., Xagoraraki I. & Rose J. B. 2010 Quantitative detection of human adenoviruses in wastewater and combined sewer overflows influencing a Michigan river. *Applied and Environmental Microbiology*, **76**(3), 715-723.

Gutierrez L., Li X., Wang J., Nangmenyi G., Economy J., Kuhlenschmidt T. B. & Nguyen, T. H. 2009 Adsorption of rotavirus and bacteriophage MS2 using glass fiber coated with hematite nanoparticles. *Water Research*, **43**(20), 5198-5208.

Haramoto E., Katayama H., Oguma K. & Ohgaki S. 2007 Quantitative analysis of human enteric adenoviruses in aquatic environments. *Journal of Applied Microbiology*, **103**(6), 2153-2159.

Hata A., Katayama H., Kitajima M., Visvanathan C., Nol, C. & Furumai H. 2011 Validation of internal controls for extraction and amplification of nucleic acids from enteric viruses in water samples. *Applied and Environmental Microbiology*, **77**(13), 4336-4343.

Heim A., Ebnet C., Harste, G. & Pring-Åkerblom P. 2003 Rapid and quantitative detection of human adenovirus DNA by real-time PCR. *Journal of Medical Virology*, **70**(2), 228-239.

Hewitt J., Leonard M., Greening G. E. & Lewis G. D. 2011 Influence of wastewater treatment process and the population size on human virus profiles in wastewater. *Water Research*, **45**(18), 6267-6276.

Hijnen W. A. M., Beerendonk E. F. & Medema G. J. 2006 Inactivation credit of UV radiation for viruses, bacteria and protozoan (oo) cysts in water: a review. *Water* Research, **40**(1), 3-22.

Hoorfar J., Cook N., Malorny B., Wagner M., De Medici D., Abdulmawjood A. & Fach P. 2003 Making internal amplification control mandatory for diagnostic PCR. *Journal of Clinical Microbiology,* **41**(12), 5835-5835.

Hoorfar J., Malorny B., Abdulmawjood A., Cook, N., Wagner M. & Fach P. 2004 Practical considerations in design of internal amplification controls for diagnostic PCR assays. *Journal of Clinical Microbiology*, **42**(5), 1863-1868.

Ikner L. A., Gerba C. P. & Bright K. R. 2012 Concentration and recovery of viruses from water: a comprehensive review. *Food and Environmental Virology*, **4**(2), 41-67.

Katayama H., Haramoto E., Oguma K., Yamashita H., Tajima A., Nakajima H. & Ohgaki S. 2008 One-year monthly quantitative survey of noroviruses, enteroviruses, and adenoviruses in wastewater collected from six plants in Japan. *Water Research*, **42**(6), 1441-1448.

Kunimoto K. 2015 *Reduction efficiencies of viral infections risks by soil aquifer treatment in water reclamation system* (Unpublished Master's thesis). Kyoto University, Kyoto, Japan. [In Japanese].

Lewis G. D. & Metcalf T. G. 1988 Polyethylene glycol precipitation for recovery of pathogenic viruses, including hepatitis A virus and human rotavirus, from oyster, water, and sediment samples. *Applied and Environmental Microbiology*, **54**(8), 1983-1988.

Li D., Gu A. Z., Yang W., He M., Hu X. H. & Shi H. C. 2010 An integrated cell culture and reverse transcription quantitative PCR assay for detection of infectious rotaviruses in environmental waters. *Journal of Microbiological Methods*, **82**(1), 59-63.

Lodder W. J. & de Roda Husman A. M. 2005 Presence of noroviruses and other enteric viruses in sewage and surface waters in The Netherlands. *Applied and Environmental Microbiology*, **71**(3), 1453-1461.

Page D., Dillon P., Toze S., Bixio D., Genthe B., Cisneros B. E. J. & Wintgens T. 2010 Valuing the subsurface pathogen treatment barrier in water recycling via aquifers for drinking supplies. *Water Research*, **44**(6), 1841-1852.

Pang L. 2009 Microbial removal rates in subsurface media estimated from published studies of field experiments and large intact soil cores. *Journal of Environmental Quality*, **38**(4), 1531-1559.

Pinto R. M., Diez J. M. & Bosch A. 1994 Use of the colonic carcinoma cell line CaCo-2 for in vivo amplification and detection of enteric viruses. *Journal of Medical Virology*, **44**(3), 310-315.

Schijven J.F. & Hassanizadeh S.M. 2000 Removal of Viruses by Soil Passage: Overview of Modeling, Processes, and Parameters. *Critical Reviews in Environmental Science and Technology* **30**(1), 49-127.

Schijven J. F., Hoogenboezem W., Hassanizadeh M. & Peters J. H. 1999 Modeling removal of bacteriophages MS2 and PRD1 by dune recharge at Castricum, Netherlands. *Water Resources Research*, **35**(4), 1101-1111.

Seiradake E. & Cusack S. 2005 Crystal structure of enteric adenovirus serotype 41 short fiber head. *Journal of Virology*, **79**(22), 14088-14094.

Yates M. V., Yates S. R., Wagner J. & Gerba C. P. 1987 Modeling virus survival and transport in the subsurface. *Journal of Contaminant Hydrology*, **1**(3), 329-345.

Chapter 5

Prediction of virus transport in soil aquifer treatment by numerical simulation

5.1 Introduction

The virus reduction in soil passage is becoming a worldwide interest, because it is applicable not only for the protection of groundwater but also for the treatment of reclaimed water that may be contaminated with pathogenic viruses from fecal sources (Yates, 1985; Havelaar et al., 1993). The spreading or movement of virus in soil porous is typically governed by the advection and dispersion processes, whereas the virus reduction in soil passage involves more complex interaction of several process, including virus adsorption and inactivation (Yates et al., 1987). Moreover, the irreversible removal (trapping and filtration) also affect to the virus reduction in soil passage (Jin et al., 1997). Therefore, many studies have been carried out for determination the factors contributing to virus removal in soil treatment both of laboratory and field scales (Schijven and Hassanizadeh, 2000).

Virus removal and transport in soil aquifer is generally described by a differential equation and solved by numerical methods. One-dimensional transport equation with constant and steady state water flow is widely used for studying the fate and transport of virus in laboratory scale (Bales et al., 1997; DeBorde et al., 1999). However, under field conditions the temporal and spatial variations in water flow velocities often affect to transverse dispersion and advection, resulting in more complex behavior. Thus, a two-dimensional, or even a three-dimensional transport model may be more adequately described in field case.

In the present study, the 2-D virus transport model was used as a predictive tool for simulating the virus reduction in Soil Aquifer Treatment (SAT) from treated municipal wastewater in Katsura River Basin, Kyoto, Japan. The conditions (injection flow rate, distance between pumping and abstraction, and water recovery) of SAT were varied for virus reduction simulation. The goal of this chapter is to simulate virus reduction profile in SAT and determine the suitable case (appropriate condition) for water reclamation. The model required the specific input data (specific condition

of virus, water and soil type and groundwater velocities) to make an accurate prediction of the virus reduction in SAT. The virus inactivation coefficient was obtained from batch experiment, whereas the virus irreversible removal coefficient was estimated by one-dimensional transport model, which calibrated from the data of the column experiment. Subsequently, these parameters, including, simulated groundwater velocity in the target area, virus concentration, virus inactivation and removal coefficients were incorporated to perform predictive simulation by 2-D model.

5.2 Theory of virus transport model in soil passage

5.2.1 One-dimensional of virus transport model in the porous media theory

Virus transport equation was developed from the solute transport model in the porous media equation with including the dispersion and advection and assumption of one-dimensional, homogenous, steady-state water flow, saturated porous medium and constant velocity (Gerke and Genuchten, 1993). The equation was written as

$$R\frac{\partial C}{\partial t} = D\frac{\partial^2 C}{\partial x^2} - v\frac{\partial C}{\partial x} \tag{5.1}$$

where C is the concentration of contaminants (virus concentration (virus/L)) in the suspension; D (cm^2/day) is the coefficient of longitudinal dispersion; t (day) is time; v (cm/day) is Darcy velocity; x (cm) is the distance along the vertical axis, R is the retardation factor. Here R is defined by the following equation:

$$R = 1 + \frac{\rho_B}{\varepsilon} k_{eq} \tag{5.2}$$

where the ρ_B is the dry bulk density of the soil, ε is the soil porosity, and k_{eq} is the partition coefficient. For virus transprot in the porous media, the retardation factor (R) refers to the equilibrium adsorption of virus. In most experiments conducting on virus movement into soil, little or no retardation was found (Schijven and Hassanizadeh, 2000) especially in the filed scale studies the estimation of retardation factor was one (Pieper et al., 1997; Schijven et al., 1999). Jin et al., (1997) also estimate the retardation of ϕX174 virus and found no retardation (R=1) in any of the column experiments. Therefore, the retardation in this study was assumed to be 1 and irreversible removal process should be considered. Due to the fact that viruses is typically not removed by reversible adsorption, previous studies suggested that virus

reduction was highly removed by a first-order irreversible removal process, such as trapping and filtration (Jin et al., 1997). Form such major mechanisms, the fate and transport of virus in soil passage could be illustrated as shown in Figure 5.1

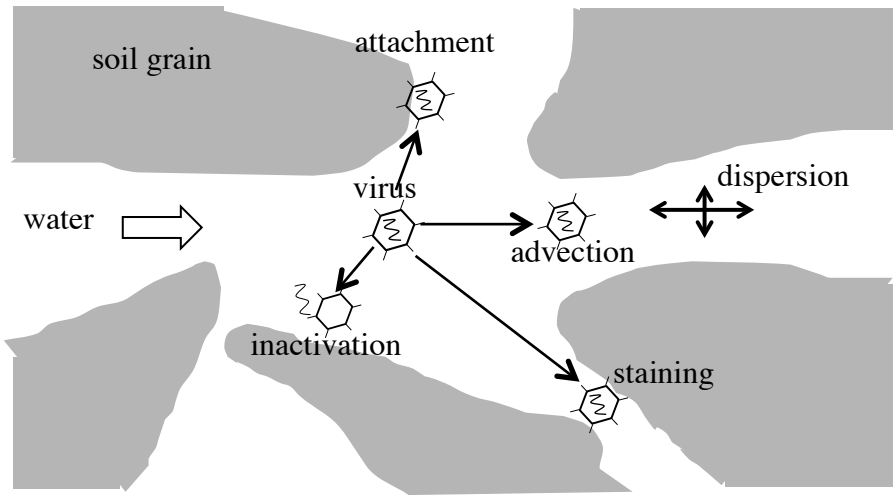

Figure 5.1: Fate and transport of virus in soil passage (Bradford et al., 2013)

Even though some research attempted to develop a model by integrating the first order inactivation rate constants of free and attached viruses into such model (Chrysikopoulos and Sim, 1996; Sim and Chrysikopoulos, 1998), the several studies did not distinguish between inactivation of free and attached viruses (Yates and Yates, 1987; Tim and Mostaghimi, 1991; Yates and Ouyang, 1992; Gitis et al., 2011; Chrysikopoulos and Aravantinou, 2012), as the differentiation between free and attached virus inactivation process obviously require more sensitive and effective methods for analysis the inactivation occurred in soil. Therefore, in the present study, the inactivation rate from both free and attached viruses were combined into only one inactivation rate constant. According to these mechanisms (inactivation and irreversible removal) without retardation, the 1-D virus transport equation becomes

$$\frac{\partial C}{\partial t} = D\frac{\partial^2 C}{\partial x^2} - v\frac{\partial C}{\partial x} - k_{irr}C - \mu C \tag{5.3}$$

when, k_{irr} (day^{-1}) is the irreversible removal coefficient denoting as extra sink term (Jin et al., 1997; Matthess et al., 1988). μ (day^{-1}) is first-order inactivation rate constant of virus.

5.2.2 Two-dimensional of virus transport model in the porous media theory

The equation of virus transport in the porous media with 2-D model can be described as below:

$$\frac{\partial C}{\partial t}+u\frac{\partial C}{\partial x}+v\frac{\partial C}{\partial y}=\frac{\partial}{\partial x}\left(D_x\frac{\partial C}{\partial x}+D_{xy}\frac{\partial C}{\partial y}\right)+\frac{\partial}{\partial y}\left(D_{xy}\frac{\partial C}{\partial x}+D_y\frac{\partial C}{\partial y}\right)-k_{irr}C-\mu C \quad (5.4)$$

where u and v are the water velocity in the x- and y-direction, respectively. When x and y and axises are aligned with the direction of the velocity reactor in a uniform flow. D_x, $D_{y,}$ D_{xy} are the component of a dispersive coefficient in the x-, y- and xy-coordinate directions. These components of diffusive transport can be calculated by following equations.

$$D_x=\frac{\alpha_L u^2+\alpha_{Th}v^2}{\sqrt{u^2+v^2}}+D_M$$

$$D_y=\frac{\alpha_L v^2+\alpha_{Th}u^2}{\sqrt{u^2+v^2}}+D_M$$

$$D_{xy}=D_{yx}=(\alpha_L-\alpha_{Th})\frac{u\cdot v}{\sqrt{u^2+v^2}} \quad (5.5)$$

where α_L and α_{Th} are a longitudinal dispersivity and a horizontal transverse dispersivity, respectively. D_m is termed the effective molecular diffusion coefficient, which it may be so small and negligible when the velocity of groundwater is high. At that case, D_m is assured to be 0. However, α_L and α_{Th} can be calculated as eq.5.6 regarding to the study of Neuman (1987, 1990):

$$\alpha_L=0.0175L^{1.46}$$
$$\alpha_{Th}=0.01L \quad (5.6)$$

α_L is the longitudinal dispersivity: α_{Th} is the horizontal transverse dispersivity, L is the distance between the treated sewage injection points to a particular position. The irreversible removal rate and the inactivation rate are grouped because both terms depend only on virus concentration. Thus, the equation becomes.

$$\frac{\partial C}{\partial t}+u\frac{\partial C}{\partial x}+v\frac{\partial C}{\partial y}=\frac{\partial}{\partial x}\left(D_x\frac{\partial C}{\partial x}+D_{xy}\frac{\partial C}{\partial y}\right)+\frac{\partial}{\partial y}\left(D_{xy}\frac{\partial C}{\partial x}+D_y\frac{\partial C}{\partial y}\right)-(k_{irr}+\mu)C \quad (5.7)$$

5.3 Methods

The study aimed to simulate the fate and transport of two significant viruses, consisting of Adenovirus-F (AdVF) and Rotavirus (RV), in soil aquifer treatment at

target site by using 2-D transport model. Current study was divided into 3 parts, as shown in Figure 5.2. In the first part, the irreversible removal coefficient (k_{irr}) as input parameter of 2-D model, was investigated according to the information from pilot-scale SAT in Chapter 4. To estimate the k_{irr}, a manual calibration process with trial-and-error approach, called inverse modeling, was carried out in 1-D virus transport model. The numerical equation was derived by finite difference method on a python grogram. The calculated concentration of viruses from 1-D Model were repeatedly compared with the observed concentration at the outlet point until the best-fit value was obtained. The commonly used statistical analysis including root mean square error (RMSE), correlation coefficient (r), and model efficiency (EF) are determined as a goodness of fit criteria.

The other significant input parameter for 2-D model is the inactivation rate coefficient (μ). Unlikely to k_{irr}, these coefficients of both viruses, AdVF and RV, were obtained from Batch experiment under controlled conditions in Chapter 3. Due to the fact that the infection viruses based on ICC-PCR were rarely observed from treated wastewater and SAT effluent in present study; therefore, it was particularly difficult to estimate the actual inactivation rate coefficients from a few data of column experiment. Then, the inactivation rate coefficients from batch experiment were applied into 2-D model.

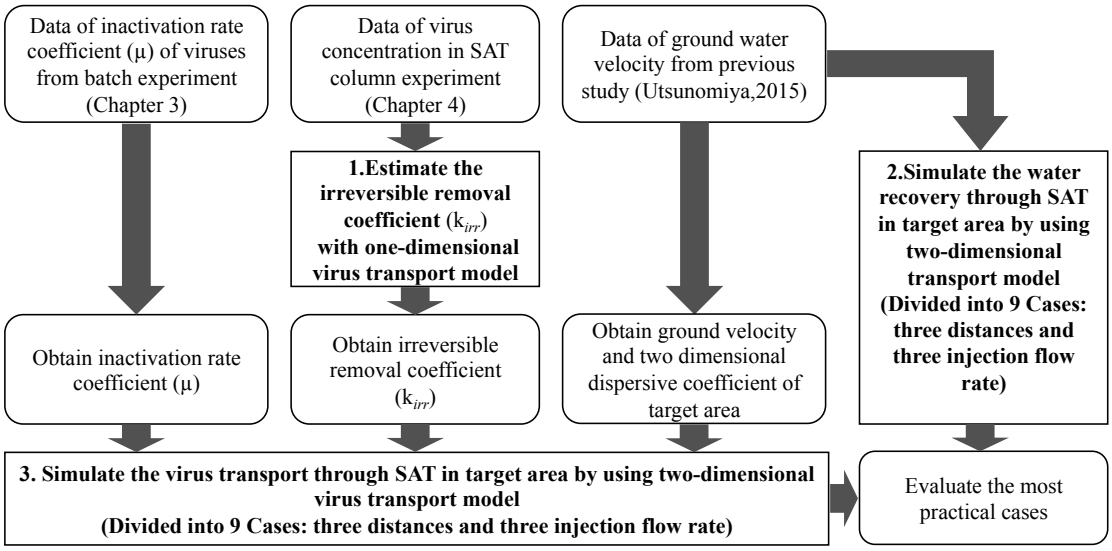

Figure 5.2: Diagram of approaches for simulating the virus transport in SAT

In the second and the third parts, the water recovery and virus removal were simulated based for 9-case scenarios. Water recovery was predicted for their scenarios by using a 2-D transport model (eq. 5.5) without inactivation and irreversible removal. At the same hydrological conditions, the virus concentration profiles in soil aquifer were simulated in the 2-D model by applying the inactivation coefficient and the irreversible removal coefficient obtained in the first part.

5.3.1 One-dimensional model approach and data analysis

a) One-dimensional model approach

The virus transport in soil model was simulated with eq. 5.3, and the irreversible removal coefficient (k_{irr}) was estimated from the experimental data in the SAT pilot plant column (1 month HRT) detected by qPCR (inactivation was not included i.e., μ=0). Therefore, the μ is equal to 0. The input parameters are shown in Table 5.1.

Table 5.1: Parameters used in the one-dimensional virus transport model

Parameters	Values	Unit
Flow rate (Q)	46	mL/min
Area (A)	150x150	cm^2
Dispersion coefficient (D)	51.84	cm^2/day
Porosity (ϕ)	0.37	
Soil density (ρ_s)	1400	kg/m^3

Assuming one-dimensional transport in a homogenous sand column with constant velocity, finite-difference approach is widely used for solving this equation. When the inactivation term is absent, the equation was discretized with Forward-in-time and Central-in-space (FTCS) scheme for solving this partial difference equation. Then, the equation becomes:

$$C_i^{n+1} = C_i^n + \Delta t\left(D\frac{C_{i+1}^n - 2C_i^n + C_{i-1}^n}{\Delta x} - v\frac{C_{i+1}^n - C_{i-1}^n}{\Delta x} - k_{irr}C_i^n \right) \tag{5.8}$$

where C^n and C^{n+1}represent the virus concentration at the old (n) and new (n+1) time level C_{i-1}, C_i and C_{i+1} are the concentration at nodes i-1, i and i+1
The Eq. 5.8 could be rearranged as

$$C_i^{n+1} = \underbrace{\left(\frac{\Delta t \cdot D}{\Delta x^2} + \frac{v}{2\Delta x}\right)}_{\text{constant = h}} C_{i-1}^n + \underbrace{\left(1 - \frac{2\Delta t \cdot D}{\Delta x^2}\right)}_{\text{constant = f}} C_i^n + \underbrace{\left(\frac{\Delta t \cdot d}{\Delta x^2} - \frac{v}{2\Delta x}\right)}_{\text{constant = g}} C_{i+1}^n \tag{5.9}$$

Also, the following boundary conditions were used:

$$C(0,t) = C_0$$
$$\left.\frac{\partial C(x,t)}{\partial x}\right|_{x=\infty} = 0 \tag{5.10}$$

There are three important criteria for the stability and accuracy of standard finite different methods (Holzbecher, 1998). These represented by conditions of the Peclet number, Courant number and Neuman boundary condition on the x direction as following equations:

Plecet number: $$\frac{u\Delta x}{D} < 1 \tag{5.11}$$

Courant number: $$\frac{u\Delta t}{\Delta x} < 1 \tag{5.12}$$

Neuman condition: $$\frac{D\Delta t}{\Delta x^2} < \frac{1}{2} \tag{5.13}$$

Where u is the velocity of water that passes through the SAT column, D is the dispersion coefficient. Grid size dx or Δx of 0.1 cm and time step dt or Δt of 0.1 day were selected in this simulation. The model was run on Python to simulate the virus concentration in the SAT effluent and to compare it with the observed data of the SAT effluent that has been collected for 2 years.

b) Statistical fitness criteria

The match between the model response and observations could be examined qualitatively in the preliminary stages of the calibration process. Some statistical measure of goodness of fit should be used for more quantitative comparison assessment. Several basic statistical measures of goodness of fit (Loague and Green, 1991; Zheng and Bennett, 2002; Moriasi et al., 2007) are introduced including maximum error (ME), root mean square error (RMSE), correlation coefficient (r), modeling efficiency (EF) and coefficient of residual mass (CRM).

The RMS, r and EF were selected to indicate good fitting of virus adsorption coefficient in this study. In the case of good fitting, the values of RMS, r and EF are close to 0.0, 1.0 and 1.0, respectively. The mathematical expressions of these statistical indexes are given as followings.

Root mean square error (RMSE):

$$RMSE = \left[\sum_{i=1}^{n} \frac{(P_i - O_i)^2}{n}\right]^{0.5} \times \frac{100}{\overline{O}} \tag{5.14}$$

Correlation coefficient (r):

$$r = \sum_{i=1}^{n}(P_i - \overline{P})(O_i - \overline{O}) / \sqrt{\sum_{i=1}^{n}(P_i - \overline{P})^2} \sqrt{\sum_{i=1}^{n}(O_i - \overline{O})^2} \quad (5.15)$$

Modeling efficiency (EF):

$$EF = (\sum_{i=1}^{n}(O_i - \overline{O})^2 - \sum_{i=1}^{n}(P_i - O_i)^2) / \sum_{i=1}^{n}(O_i - \overline{O})^2 \quad (5.16)$$

where P_i and O_i are the modeled and observed values of the ith model dependent variables (virus concentration); n is the number of samples; and $\bar{O}$ is the mean of the observed data. The lower limit of the RMSE is zero. RMSE is a measure of the imperfection of the calculated values to the observed data. A small value of RMSE indicates a close fit to the observation. However, using only RMSE may lead to misinterpretation. The r value is a measure of the proportion of the total variance of observed data compared to the predicted data. The r value is ranged from -1 to 1, which more closing to 1 indicates a strong correlation between two variables. Unlike to r, the maximum value of EF is one. EF ranged between 0.0 to 1.0 are acceptable. Yet, EF is less than zero the model-predicted values are worse than simply using the observed mean. (Loague and Green, 1991; Zheng and Bennett, 2002)

5.3.2 Implemented of 2-dimensional transport model to Katsura River Basin

a) The selected area

The target area of SAT project is Katsura River Basin, which is located at longitude of E 135˚39’00” and latitude of N 34˚48’00”. The study area covered the distance of 500 m to the North and 500 m to the East.

The data of groundwater flow and velocity of this area was obtained from the simulation by using MODFLOW 2000 in the previous study of Utsunomiya (2015).
The simulation covered approximately 90 km^2 as shown in Figure 5.2 (a). In MODFLOW analysis, when the mesh of 5 m x 5 m was employed, the ground water level (meter) was obtained as shown in Figure 5.3 (b). Subsequently, with the injection flow rates at the injection point with 500, 1000, and 2000 m^3/day flow rate vector field was calculated (Utsunomiya, 2015). By using this information, three groups of velocity profile information depending on the injection flow rate were integrated into the 2-D transport model in this chapter.

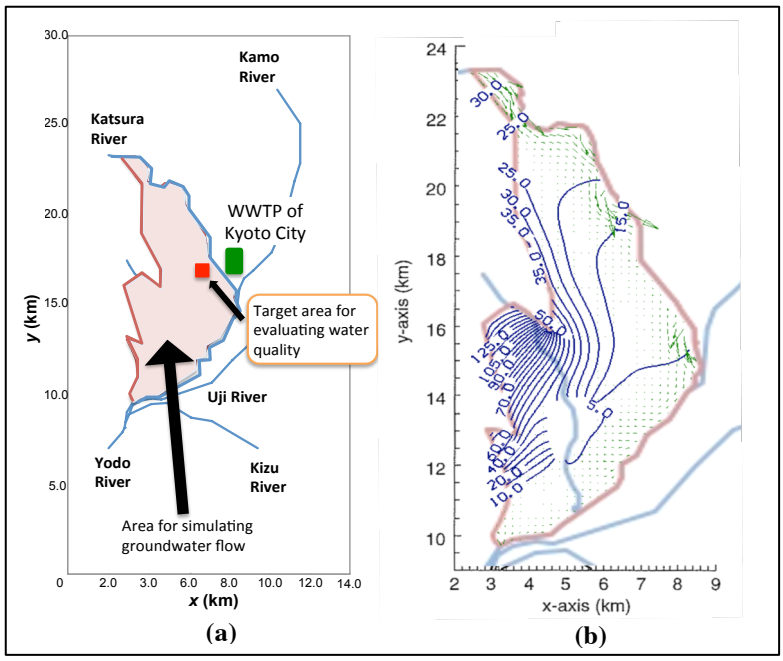

Figure 5.3: a schematic view of the analysis region and the contour line of groundwater level profile in Katsura River Basin (Utsunomiya, 2015)

b) Two-dimensional of the water recovery simulation in the target area

Direct injection well was selected for SAT implementation among SAT types because the capacity of the injection well is higher, and longer estimated life cycle is expected than vadose zone well and infiltration basin (USEPA, 2004; Aharoni et al., 2011). The direct injection well performed by injecting reclaimed water directly into deep aquifer. Thus, 2-D transport model was suitable for simulation.

Water recovery rate is one of the most important criteria for project consideration, which refers to the percentage of reclaimed water that can be recovered after injection. The water recovery should be appropriate, whereas the quality of reclaimed water is still satisfied. Based on the study of Utsunomiya (2015), at the same site, because of influence of groundwater level, it was suggested that the withdrawal point should be located at the south direction of the injection point in order to obtain a suitable recovery rate.

The water recovery refers to the percentage of reclaimed water that could be withdrawn. Typically, around 35% of reclaimed water was allowed or recommended for mixing with other water resource for potable purpose in order to ensure its quality (Lazarova et al., 2013). The recovery rate is related to the amount of water injected or

injection flow rate and the site characteristics. Therefore, to investigate the water recovery of each scenario, the different injection flow rates varied at 500, 1000 and 2000 m^3/day were applied into the 2-D model. In terms of virus reduction, the reduction capability is normally relied on the retention time or travel time of virus in SAT. This travel time is influenced by the groundwater flow and the distance between the injection point and abstraction point. Previous study indicated that the distance as great as 50 to 100 m and perhaps 6-month retention time would be sufficient for virus removal by soil (Asano and Cotruvo, 2004). Even though a very long retention of SAT can ensure water quality in terms of virus reduction, it may be not practical in a limited space as in Japan. Therefore, the effect of shorter retention time of SAT (up to 2 months) should be investigated in this study. Under these conditions, the models were set up with the varied of the distance between injection point and withdrawal point (50, 100 and 200 m). From the three distances and the three injection flow rates, 9-case scenarios were created.

The advection-dispersion transport model was selected to estimate the water recovery. The equation is written as:

$$\frac{\partial C}{\partial t} + u\frac{\partial C}{\partial x} + v\frac{\partial C}{\partial y} = \frac{\partial}{\partial x}\left(D_x\frac{\partial C}{\partial x} + D_{xy}\frac{\partial C}{\partial y}\right) + \frac{\partial}{\partial y}\left(D_{xy}\frac{\partial C}{\partial x} + D_y\frac{\partial C}{\partial y}\right) \tag{5.17}$$

In this part, the 2-D virus transport model is also numerically solved using a finite-difference method with FTCS. The numerical solution of the 2-D virus transport model is generated by the discretization of the model equation with a finite difference approach, then the partial differential equation (Eq. 5.17) becomes:

$$C_{i,j}^{n+1} = \Delta t\left(D_x\frac{C_{i+1}^n - 2C_i^n + C_{i-1}^n}{\Delta x^2} - u\frac{C_{i+1}^n - C_{i-1}^n}{2\Delta x} + D_y\frac{C_{j+1}^n - 2C_j^n + C_{j-1}^n}{\Delta y^2} - v\frac{C_{j+1}^n - C_{j-1}^n}{2\Delta y} + D_{xy}\frac{C_{i+1,j+1}^n - C_{i+1,j-1}^n - C_{i-1,j+1}^n + C_{i-1,j-1}^n}{2\Delta x\Delta y}\right) + C_{i,j}^n \tag{5.18}$$

where $C_{i,j}^{n+1}$ is the virus concentration for cell (i,j) as shown in Figure 5.4 at new time level n+1, $C_{i,j}^n$ is the virus concentration for cell (i,j) at time level n, other parameters were defined in the eqs. 5.4 to 5.6. Moreover, the positions of cell i-1, i, i+1, j-1, j, j+1 are shown in Figure 5.4.

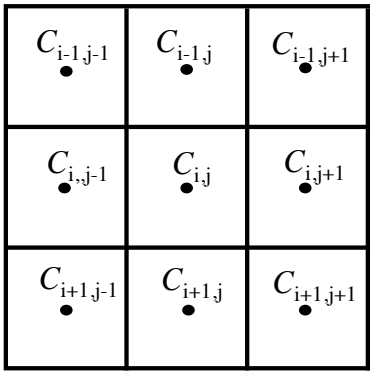

Figure 5.4: The center finite-difference grid for 2-D model

The space and time steps were chosen to satisfy the numerical stability and convergence conditions of the Plecet, Courant numbers and Neuman boundary conditions as given below

Plecet number

$$P_e = \frac{u\Delta x}{D_x} < 1$$
$$P_e = \frac{v\Delta y}{D_y} < 1 \tag{5.19}$$

Courant number

$$Co_x = \left|\frac{u\Delta t}{\Delta x}\right| \le 1$$
$$Co_y = \left|\frac{v\Delta t}{\Delta y}\right| \le 1 \tag{5.20}$$

Neumann boundary conditions

$$\frac{D_x\Delta t}{\Delta x^2} + \frac{D_y\Delta t}{\Delta y^2} \le 0.5 \tag{5.21}$$

The state transition matrix determines the numerical solution. Eq.5.18 can be rewritten in the following form:

$$C_{t+\Delta t} = AC_t \tag{5.22}$$

where $C_{t+\Delta t}$ and C_t refer to the state variables described as vectors of virus concentrations at all nodes in the problem domain at time t and t+Δt, respectively, and A refer to the state transition matrix which gives a finite difference scheme or driving operator to advance at time step state to the next time step.

The initial concentration of each point was set as zero: *C(x,y,0)=0*, while the boundary conditions, were given below.

C(Rx,Ry,t) = Cin; Cin =100 for water recovery estimation,
R_x, R_y are the coordinates of the recharge point position

The model grid was defined on a 2-D plane domain. The nested grid was used by Local-uniform-grid refinement (LUGR) method (Trompert, 1993) because this method can decrease the computing time with high-resolution. Four regions were identified the intrinsic interval as shown in Figure 5.5. The first region (region I) has 100 x 100 grid points with the grid interval 5 x 5 m^2. Then the mesh sizes are 2.5 x 2.5, 0.5 x 0.5, and 0.1 x 0.1 m^2 of region II, III and IV, respectively. The grid ratio between region I and region II was 1:2, the others were 1:5. The smallest grid meshes in the region IV was assumed to be the same concentrations in all meshes due to the calculation from region III.

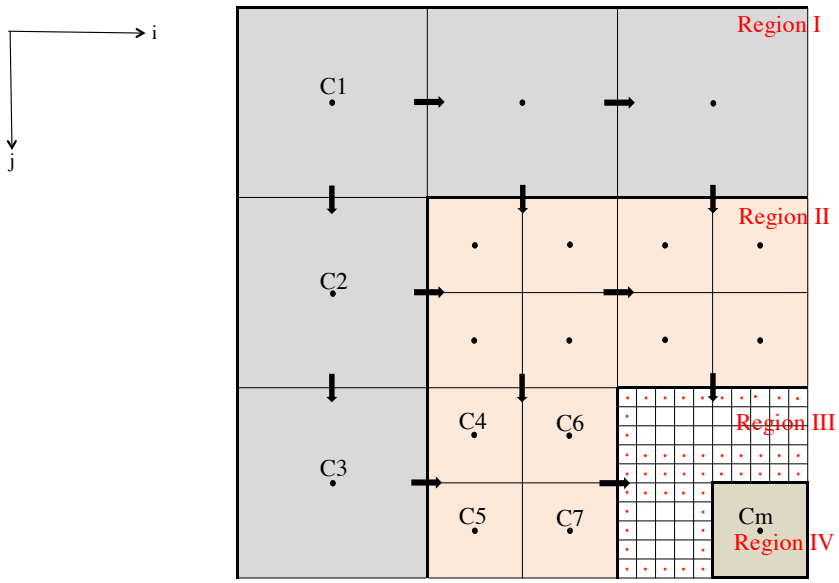

Figure 5.5: The relative position of nested grid from coarse to fine grid for clarity the boundary condition in 2-D plane

The D_x, D_y and D_{xy} in each point were calculated from eqs. 5.5 and 5.6. In the numerical scheme, the time interval per each time step was control by the stability criteria of Courant number and Neuman boundary. The time interval time always control by the region III because of small interval distance. Thus, each simulation case had different interval time step such as 1/200 day of Case 1 but the total time step was 50 days. Then a Mathematica program was used to simulate the virus concentration profile.

5.3.3 Two-dimensional virus transport approach

The method has been mentioned in 5.3.2 with the reaction term (overall reduction rate, $(k_{irr}+\mu)$). This governing equation could be discretized as below:

$$C_{i,j}^{n+1} = \Delta t(D_x \frac{C_{i+1}^n - 2C_i^n + C_{i-1}^n}{\Delta x^2} - u\frac{C_{i+1}^n - C_{i-1}^n}{2\Delta x} + D_y \frac{C_{j+1}^n - 2C_j^n + C_{j-1}^n}{\Delta y^2} - v\frac{C_{j+1}^n - C_{j-1}^n}{2\Delta y} +$$
$$D_{xy}\frac{C_{i+1,j+1}^n - C_{i+1,j-1}^n - C_{i-1,j+1}^n + C_{i-1,j-1}^n}{2\Delta x \Delta y} - (k_{irr} + \mu)C_{i,j}^n) + C_{i,j}^n \quad (5.18)$$

The initial and boundary conditions were set as same as the water recovery simulation but the initial concentration (C_{in}) is the mean infectious virus concentration that was detected in the secondary treated sewage as shown in Table 5.2.

Table 5.2: Parameters used in the two-dimensional virus transport model

Parameters	Value
Flow rate (Q) m^3/day (Case 1 and Case 7)	500
Flow rate (Q) m^3/day (Case 3)	2000
Velocity (v) cm/day (Utsunomiya, 2015)	MODFLOW simulation
Overall reduction rate coefficient ($k_{irr}+\mu$) day^{-1}	0.164 (0.1+0.064) of AdVF, 0.168 (0.07+0.098) of RV
C_{in} AdVF (mean) SAT influent samples	828 MPNIU/L
C_{in} RV (mean)* SAT influent samples	103 MPNIU/L

* The mean value of infectious RV was calculated by the lowest infectious and genome copy ratio with 0.001 because it is nearly the infectious RV that was detected in the SAT influent (22-73 MPN/L)

The examples of Python code for 1-D and mathematica code for 2-D of virus transport in SAT are shown in Appendix C.

5.4 Results

5.4.1 Estimation of the irreversible rate constants of virus in SAT by one-dimensional virus transport model

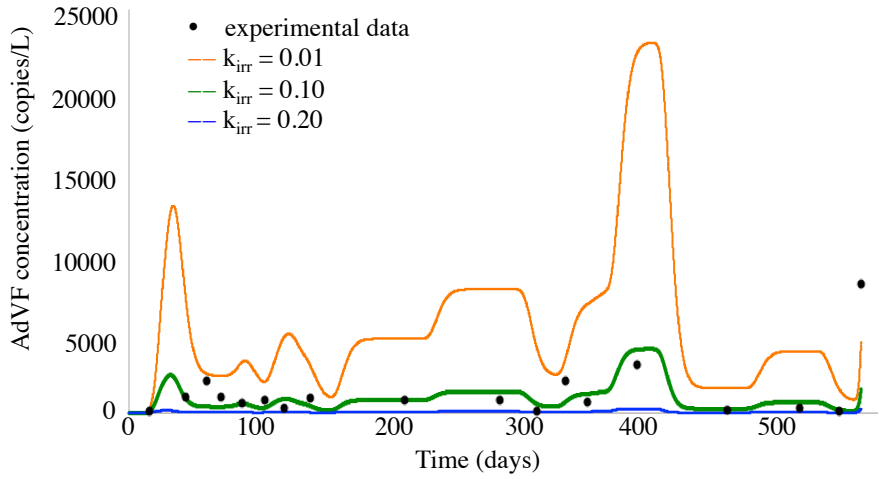

Figure 5.6: Comparison of model estimation with SAT experimental data (genome data) of AdVF with different irreversible removal coefficients

Figure 5.6 illustrated the comparison between the virus concentration of AdVF estimated by the model calculation (line) and the observed values (dot) in SAT effluent. It was found that there was fluctuation in both predicted and measured concentrations. The fluctuation of calculated values mainly caused by the concentration of virus in SAT influent, which was major input parameters. Moreover, level of fluctuation (the range between the highest and lowest values) seems to be increased when a low coefficient (μ) was used for simulation. This may indicate that the virus concentration of influent SAT highly affect to the concentration at the outlet when the removal coefficient of system was fairly low.

From inverse modeling approach, it was found that an irreversible removal coefficient (k_{irr}) of AdVF in the range of 0.06 to 0.10 day^{-1} was the suitable estimated values because it could provide the calculated virus concentration closed to the experimental data. Among this range, 0.10 day^{-1} of k_{irr} for AdVF probably was the best-estimated coefficient because all results of statistical indicators were acceptable and consistent with the standard criteria (e.g. EF > 0, low RMSE and r ≥ 0.5) as shown in Table 5.3. Therefore, the k_{irr} was set to 0.1 in the 2-D virus transport model of AdVF.

For inactivation coefficient of AdVF, it is not different 0 to 0.09 (mean 0.06) day^{-1} in the column experiment and 0.064 day^{-1} in batch experiment at 15°C. The batch inactivation experiment was selected to apply in the virus transport model because the temperature of groundwater is approximately 15°C.

Table 5.3: Model performance statistic for AdVF 1-D prediction with different irreversible removal coefficients

AdVF	Statistic analysis		
μ_a	RMSE(%)	r	EF
0.12	148	0.57	-0.08
0.10	139	0.51	0.05
0.09	135	0.48	0.12
0.08	131	0.45	0.14
0.07	132	0.42	0.13

If predicted and observed values were equal, then the statistical analysis would yield: RMSE =0.0; r =1.0 and EF =1.0

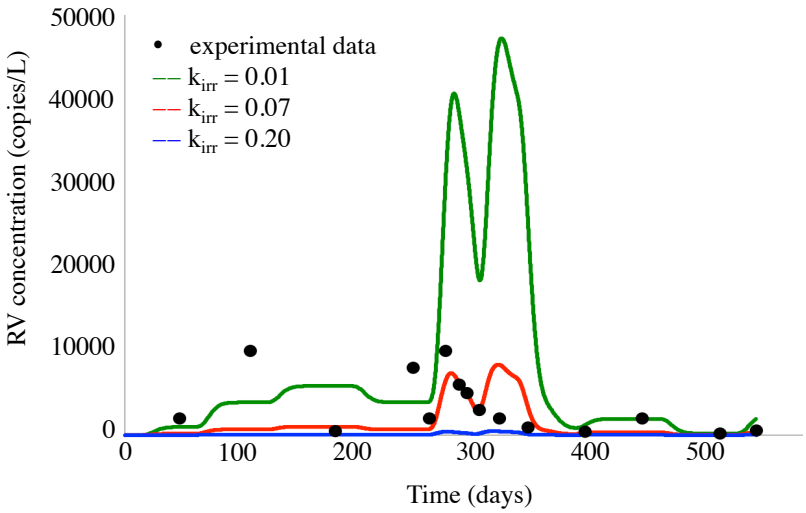

Figure 5.7; Comparison of model estimation with SAT experimental data (genome data) of RV with different adsorption coefficients

Similarly, the approximated k_{irr} of RV was examined by manual trial-and-error method and identified with three statistical tests. As shown in Figure 5.7, there was highly fluctuation of calculated concentration during the date of 300. This probably be due to the dramatically increase of concentration in the influent. Nevertheless, results showed that the good correlation between the calculated concentrations and the experimental data was obtained when the estimated k_{irr} of RV was in the range of 0.07 to 0.09 day^{-1}. From the statistical analyses, k_{irr} of 0.07 day^{-1} of RV probably was the best-estimated value, resulting in the good statistical results (e.g. low RMSE, $r \geq 0.5$ and $EF > 0$) as shown in Table 5.4. Thus, k_{irr} of 0.07 day^{-1} of RV was selected as input value for the simulation of 2-D virus transport model. For inactivation coefficient of RV, there were limited data of infectious RV detected in the column experiment. The inactivation of AdVF in batch and column experiment was not different; therefore, RV virus inactivation might be the same trend as AdVF. The batch inactivation experiment of RV with 0.094 day^{-1} at 15°C was selected to apply into the 2-D virus transport model because the temperature of groundwater is approximately 15°C.

Table 5.4: Model performance statistic for RV 1-D prediction with different irreversible removal coefficients

RV	Statistic analysis		
μ_a	RMSE(%)	r	EF
0.03	246	0.45	-5.38
0.05	134	0.47	-0.90
0.07	93	0.50	0.08
0.09	94	0.50	0.07
0.12	110	0.52	-0.27

*If predicted and observed values were equal, then the statistical analysis would yield: RMSE =0.0; r =1.0 and EF =1.0

5.4.2 Water recovery by 2-D simulation

The water recovery at the Katsura River Basin was simulated into 9 cases as shown in the Table 5.5. Water recovery refer to the amount (in percentage) of reclaimed water or recycle water from SAT, while the $\log_{10}$ reduction represents to the reduction that was caused by dispersion and advection (or dilution effect). The results revealed that the increase of water injection directly resulted in the increase of water recovery rate (good correlation; r = 0.72). Even though most cases provided the water recovery above 40%, the calculated hydraulic retention times (HRT) were highly different. The two longest HRT (above 100 day) were found in the cases of 7 and 8, which the withdrawal point was located at 200 m from injection point. However, it was found that very low recovery (20.5 %) also occurred in Case 7 in other words most volume of extraction consisted of groundwater. Probably, this case may be not practicle for project establishment. Interestingly, even though most cases showed a higher recovery rate than the value of 35% suggested by other study (Lazarova et al., 2013), the HRT of some cases were still longer than 60 days, which it might be sufficient for virus removal. However, in the limited space, the practical case is in Case 1 because the HRT of around 23 days was found at distance of 50 m and at injection flow rate of 500 m^3/day and the water recovery is 40.7%. In comparison among the similar injection flow rate (equal water production), at highest flow rate of 2000 m^3/day from 3 locations (Case 3, 6, and 9), the water recoveries were too high, and HRT were short. Thus, flow rate of 1000 or 500 m^3/day seem to be more reasonable and practical, in terms of a suitable recovery rate and a sufficient HRT.

Table 5.5 Simulation of water recovery in the Katsura River Basin with different infection flow rates and distance between injection and withdrawal points

Case	The distance between injection and withdrawal points	Injection flow rate	Water recovery (%)	Apparent $\log_{10}$ reduction by dilution	HRT (days)
1	50	500	40.7	0.39	23
2	50	1000	55.5	0.26	15
3	50	2000	57.9	0.24	10
4	100	500	42.6	0.37	69
5	100	1000	59.0	0.23	40
6	100	2000	65.0	0.19	24
7	200	500	20.5	0.69	183
8	200	1000	47.5	0.32	104
9	200	2000	53.7	0.27	62

The effect of dispersion and advection can be calculated and the $\log_{10}$ reduction of viruses due to the dispersion and advection were in the range of 0.19 to 0.39 $\log_{10}$ except Case 7. The water recovery simulations are shown in Figure 5.8.

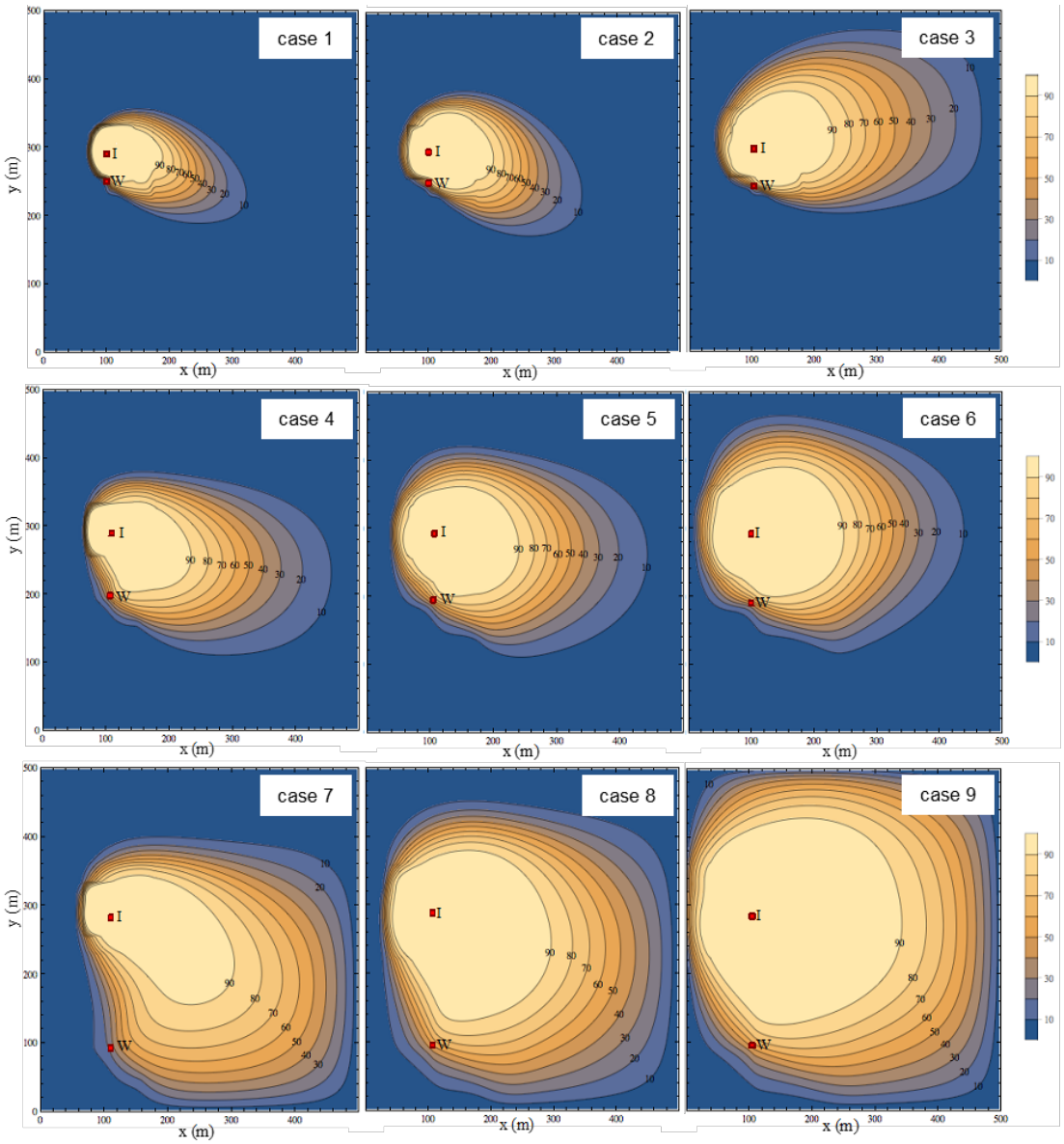

Figure 5.8: The water recovery (%) of all nine cases simulation
*** ■I; injection point, ■W; withdrawal point
The water recovery simulation results

5.4.3 Two-dimensional virus concentration profile simulation

According to the estimated values of k_{irr} of AdVF and RV by 1-D model and the inactivation coefficients of AdVF and RV obtained from batch experiment, the overall reduction coefficients ($k_{irr} + \mu$) were 0.164 day^{-1}(0.1+0.064) and 0.168 day^{-1} (0.07+0.098) of AdVF and RV, respectively. Then the virus reduction profiles were

simulated by 2-D model with these values for SAT implementation in the Katsura River Basin. All nine simulated cases of virus output concentrations and their reduction are shown in Table 5.6.

Table 5.6: Simulated virus concentration at the withdrawal point by 2-D model

Cases	meters	Injection flow rate (m^3/day)	Water recovery (%)	HRT (day)	AdVF prediction MPNIU/L	RV prediction MPNIU/L	AdVF reduction log_{10}	RV reduction log_{10}
1	50	500	41	23	$2.5x10^{1}$	3.0	1.52	1.54
2		1000	56	15	$1.0x10^{2}$	$1.3x10^{1}$	0.90	0.91
3		2000	58	10	$1.9x10^{2}$	$2.3x10^{1}$	0.64	0.64
4	100	500	43	69	$4.9x10^{-1}$	$5.6x10^{-2}$	3.23	3.26
5		1000	59	40	9.6	1.1	1.94	2.00
6		2000	65	24	$5.3x10^{1}$	6.3	1.20	1.22
7	200	500	20	183	$6.2x10^{-5}$	$6.1x10^{-6}$	7.12	7.23
8		1000	48	104	$3.1x10^{-2}$	$3.3x10^{-3}$	4.43	4.49
9		2000	54	62	1.2	$1.3x10^{-1}$	2.84	2.89

All nine cases were calculated the virus concentration at the withdrawal point with the same AdVF and RV concentration input. The highest virus concentration at the withdrawal point was observed in Case 3 with 190 and 23 MPNIU/L of AdVF and RV, respectively. The reduction efficiencies are 0.64-log_{10} reduction of AdVF and RV. The lowest virus concentration is in Case 7 with 0.000062 and 0.000006 MPNIU/L of AdVF and RV, respectively at the withdrawal point. The reduction efficiencies are 7.12 and 7.23-log_{10} reduction of AdVF and RV, respectively. The virus concentration is 25 and 3 MPNIU/L of AdVF and RV, respectively at the withdrawal point in the practical case (Case 1). The reduction efficiencies are 1.52 and 1.54-log_{10} reduction of AdVF and RV, respectively. The retention time is the key difference on the virus concentration profile. For example, 10 and 183 days are the retention time of Case 3 and Case 7, respectively, and the HRT caused the large different virus concentration at the withdrawal point. The longer HRT contributes to the higher reduction of virus. The simulated virus concentration profiles at Katsura River Basin of Case 1, Case 3 and Case 7 were shown in Figures 5.9-5.14. The other cases also were simulated and shown in Appendix D.

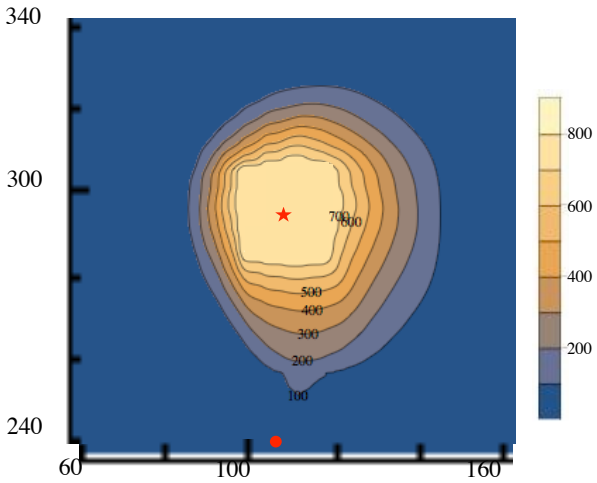

Figure 5.9: Case 1 of AdVF simulation profile after 2D transport model in Katsura River Basin with 0.164 day^{-1} reduction rate coefficient; ★ denotes the injection point, • denotes the withdrawal point; x-and y-axes show the distance values in meters

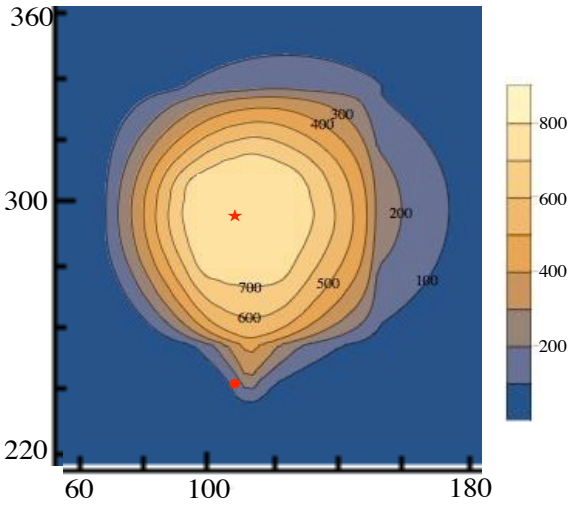

Figure 5.10: Case 3 of AdVF simulation profile after 2D transport model in Katsura River Basin with 0.164 day^{-1} reduction rate coefficient; ★ denotes the injection point, • denotes the withdrawal point; x-and y-axes show the distance values in meters

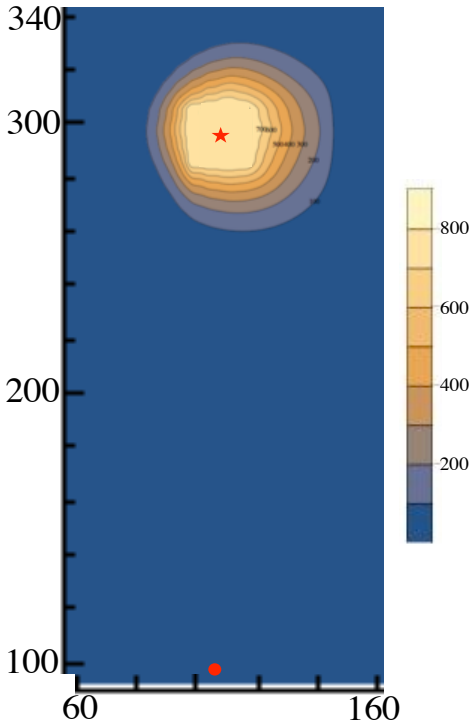

Figure 5.11: Case 7 of AdVF simulation profile after 2D transport model in Katsura River Basin with 0.164 day^{-1} reduction rate coefficient; ★ denotes the injection point, • denotes the withdrawal point; x-and y-axes show the distance values in meters

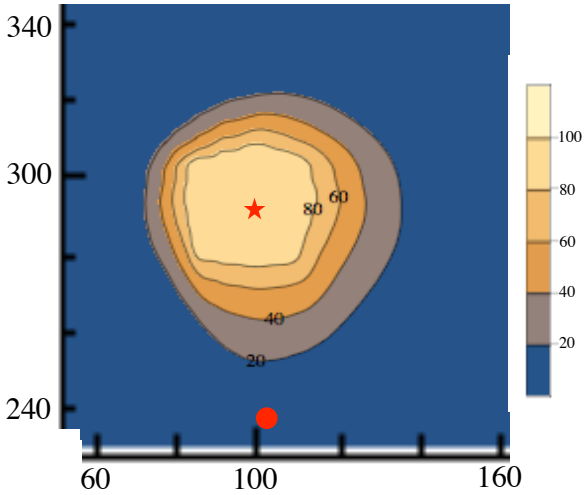

Figure 5.12: Case 1 of RV simulation profile after 2D transport model in Katsura River Basin with 0.168 day^{-1} reduction rate coefficient; ★ denotes the injection point, • denotes the withdrawal point; x-and y-axes show the distance values in meters

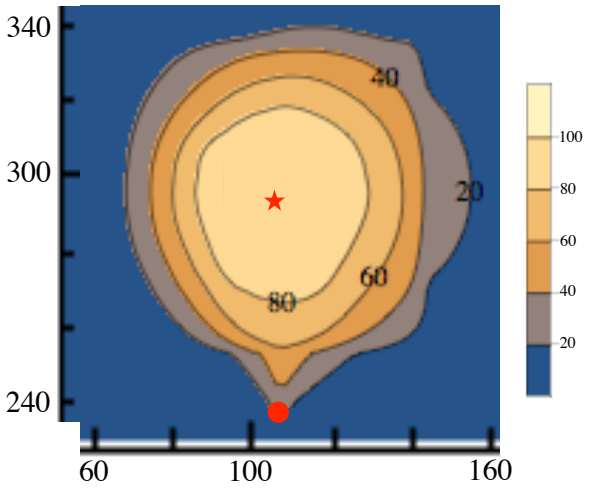

Figure 5.13: Case 3 of RV simulation profile after 2D transport model in Katsura River Basin with 0.168 day^{-1} reduction rate coefficient; ★ denotes the injection point, • denotes the withdrawal point; x-and y-axes show the distance values in meters

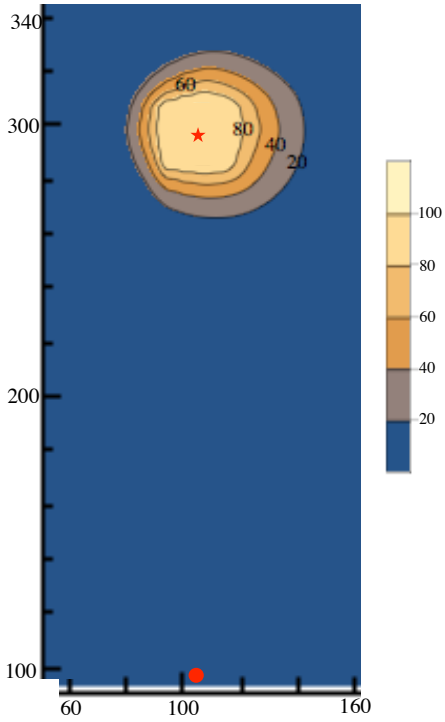

Figure 5.14: Case 7 of RV simulation profile after 2-D transport model in Katsura River Basin with 0.168 day^{-1} reduction rate coefficient; ★ denotes the injection point, • denotes the withdrawal point; x-and y-axes show the distance values in meters

5.4 Discussions

The key input parameters for virus transport model in porous media are the virus inactivation and removal coefficients. According to the estimation of irreversible removal rates by one-dimensional model, AdVF showed higher removal during SAT

than RV (i.e., the irreversible removal rates are 0.10 and 0.07 day^{-1} for AdVF and RV, respectively). It strongly agrees with the fact that AdVF is larger than RV is the primary reason for this result.

In prior works, the virus transport model in soil have been often estimated by using the bacteriophage data, but its behavior on environment is considerably different from human enteric viruses, such as the concentration of bacteriophage is higher and its multiplication do not reflect to human infectivity. Therefore, development of virus transport model should be rather based on human enteric virus because it could provide a more accuracy in terms of applications. Only a few studies was conducted on human enteric viruses, such as Tim and Mostaghimi (1991) investigated polovirus I transport in the column experiment with an advection-dispersion model. However, that study did not reveal the inactivation effect.

The key input parameters for virus transport model in porous media are the coefficients of virus inactivation and irreversible removal. According to the estimation of irreversible removal rates by one-dimensional model, AdVF showed slightly higher removal during SAT than RV (i.e., the irreversible removal rates are 0.10 and 0.07 day^{-1} for AdVF and RV, respectively). The irreversible removal may be due to the geometrical blocking effect. Possibly, a larger size of AdVF could contribute to a higher removal. Nevertheless, at longer operation period of SAT (over 2 years), the irreversible removal efficiency may be reduced from limited porous area. Further investigations on the effect of long-term operation are required.

Based on this study, it suggested that the most practical case for applying to Katsura river basin is the condition of 500 m^3/d injection flow rate at distance of 500 meters to withdrawer point. Moreover, it is revealed that HRT is an important parameter for the removal of virus. Moreover, HRT shows a positive correlation with virus reduction (r=0.997) in both AdVF and RV. Similarly, the distance between the injection and withdrawal points has a good correlation with the virus reduction (r=0.81) for both viruses. Nonetheless, the correlation between the injection flow rate and virus reduction is not clear (r=-0.47). This may be due to the effect of water flow rate, resulting in different virus reduction. According to study of Teustsch et al., (1991), it

reported that prediction of one-dimensional model based on MS2 phage had a high accuracy only under high-flow rate experiment. Because current study was carried out the pilot-scale SAT under low flow rate condition (46 ml/min or 0.1 m/d), which is closed to normal ground velocity of target area, ranged between 0.1 to 1.4 m/d. Applying the input model parameters obtained from those conditions may be limited for a high-injection flow rate simulation case. To expand the capability of prediction, the effect of water flow rate in a wider range need to be studied. Moreover, HRT plays an important role on virus reduction. As in the case of shortest HRT and high injection flow rate, it suggests that dilution and dispersion are the main mechanism involving to virus reduction. In such case, even though the virus reduction of 0.64-$\log_{10}$ could be observed, the infectivity of those viruses probably exist, resulting in high risk to consumer's health.

5.5 Summary

In this chapter, the virus reduction simulation by a mathematical model to predict virus transport in SAT was conducted. The model input required the specific virus inactivation and removal rate coefficients. The irreversible removal rate was estimated and validated with the estimation data against the experiment data in the SAT pilot plant by the one-dimensional transport model. The results of the modeled data of the irreversible removal rate compare well to the measured virus in the SAT effluent. This succeeds to the prediction of the virus concentration in a more realistic scenario with two-dimensional model. The best simulation result is in Case 7 with the 200 m distance between the injection and withdrawal point and 500-m^3/day injection flow rate and approximately 6 months of HRT. In this case, the model gave a large virus reduction at the withdrawal point. However, in terms of application to a limited space like Japan, it seems to show that Case 1 at distance of 50 m and 500-m^3/day injection flow rate achieve more appropriate HRT (25 days) with its acceptable water recovery. In addition, the worst-case was in Case 3 because of the lowest virus reduction due to the shortest HRT. The virus reduction by the three cases were:

- Case 1 (practical case): the virus reduction during SAT was 1.52 $\log_{10}$ and 1.54 $\log_{10}$ of AdVF and RV, respectively.

- Case 3 (the worst case): the virus reduction during SAT was 0.64 $\log_{10}$ both of AdVF and RV, respectively.

- Case 7 (the best case): the virus reduction during SAT was 7.12 $\log_{10}$ and 7.23 $\log_{10}$ of AdVF and RV, respectively.

The results of present study could reveal the possible virus concentration profile at target area by using two-dimensional virus transport model, the maximum allowable virus concentration in drinking water is still required in the next chapter by quantitative risk assessment (QMRA) in order to achieve the safe drinking water.

References

Aharoni A., Guttman J., Cikurel H. & Sharma S. 2011 Guidelines for design, operation and maintenance of SAT (and hybrid SAT) systems. *Mekorot and UNESCO-IHE, 18530*.

Asano T. & Cotruvo J. A. 2004 Groundwater recharge with reclaimed municipal wastewater: health and regulatory considerations. *Water Research*, **38**(8), 1941-1951.

Asano T., Burton F.L., Leverenz H.L., Tsuchihashi R. & Tchobanoglous G. 2007 Water Reuse Issues, Technologies, and Applications. Metcalf & Eddy, McGraw-Hill, New York.

Bales R. C., Li S., Yeh T. C. J., Lenczewski M. E. & Gerba C. P. 1997 Bacteriophage and microsphere transport in saturated porous media: Forced□gradient experiment at Borden, Ontario. *Water Resources Research*, **33**(4), 639-648.

Bradford S. A., Morales V. L., Zhang W., Harvey R. W., Packman A. I., Mohanram A. & Welty, C. 2013 Transport and fate of microbial pathogens in agricultural settings. *Critical Reviews in Environmental Science and Technology*, **43**(8), 775-893.

Chrysikopoulos C. V. & Aravantinou A. F. 2012 Virus inactivation in the presence of quartz sand under static and dynamic batch conditions at different temperatures. *Journal of Hazardous Materials*, **233**, 148-157.

Chrysikopoulos C. V. & Sim Y. 1996 One-dimensional virus transport in homogeneous porous media with time-dependent distribution coefficient. *Journal of Hydrology*, **185**(1), 199-219.

Deborde D. C., Woessner W. W., Kiley Q. T. & Ball P. 1999 Rapid transport of viruses in a floodplain aquifer. *Water Research*, **33**(10), 2229-2238.

Dowd S. E., Pillai S. D., Wang S. & Corapcioglu M. Y. 1998 Delineating the specific influence of virus isoelectric point and size on virus adsorption and transport through sandy soils. *Applied and Environmental Microbiology*, **64**(2), 405-410.

Echigo S., Nakatsuji M., Takabe Y. & Itoh S. 2015 Effect of preozonation on wastewater reclamation by the combination of ozonation and soil aquifer treatment. *Water Science & Technology: Water Supply*, **15**(1), 101-106.

Gerke H. H. & Genuchten M. V. 1993 A dual-porosity model for simulating the preferential movement of water and solutes in structured porous media. *Water Resources Research*, **29**(2), 305-319.

Gitis V., Dlugy C., Gun J. & Lev O. 2011 Studies of inactivation, retardation and accumulation of viruses in porous media by a combination of dye labeled and native bacteriophage probes. *Journal of Contaminant Hydrology*, **124**(1), 43-49.

Havelaar A. H., Van Olphen M. & Drost Y. C. 1993 F-specific RNA bacteriophages are adequate model organisms for enteric viruses in fresh water. *Applied and Environmental Microbiology*, **59**(9), 2956-2962.

Holzbecher E. O. 1998 *Modeling density-driven flow in porous media: principles, numerics, software* (Vol. 1). Springer Science & Business Media.

Jin Y., Yates M. V., Thompson S. S. & Jury W. A. 1997 Sorption of viruses during flow through saturated sand columns. *Environmental Science & Technology*, **31**(2), 548-555.

Lazarova V., Asano T., Bahri A. & Anderson J. 2013 Milestones in water reuse: the best success stories. *Water Intelligence Online*, **12**, 9781780400716.

Loague K. & Green R. E. 1991 Statistical and graphical methods for evaluating solute transport models: overview and application. *Journal of contaminant hydrology*, **7**(1), 51-73.

Matthess G., Pekdeger A. & Schroeter J. 1988 Persistence and transport of bacteria and viruses in groundwater—a conceptual evaluation. *Journal of Contaminant Hydrology*, **2**(2), 171-188.

Microrisk 2006 Microbiological risk assessment: a scientific basis for managing drinking water safety from source to tap. EU project under 5FP. (http://www.microrisk.com/publish/cat_index_11.shtml)(visited 08.08.15)

Moriasi D. N., Arnold J. G., Van Liew M. W., Bingner R. L., Harmel R. D. & Veith T. L. 2007 Model evaluation guidelines for systematic quantification of accuracy in watershed simulations. *Transactions of the ASABE*, **50**(3), 885-900.

Neuman S. P., Winter C. L. & Newman C. M. 1987 Stochastic theory of field-scale Fickian dispersion in anisotropic porous media. *Water Resources Research*, **23**(3), 453-466.

Neuman S. P. 1990 Universal scaling of hydraulic conductivities and dispersivities in geologic media. *Water Resources Research*, **26**(8), 1749-1758.

Pieper A. P., Ryan J. N., Harvey R. W., Amy G. L., Illangasekare T. H. & Metge, D. W. 1997 Transport and recovery of bacteriophage PRD1 in a sand and gravel aquifer: Effect of sewage-derived organic matter. *Environmental Science & Technology*, **31**(4), 1163-1170.

Ray, C. (Ed.). 2012 *Riverbank filtration: understanding contaminant biogeochemistry and pathogen removal* (Vol. 14). Springer Science & Business Media.

Schijven J. F., Hoogenboezem W., Hassanizadeh M. & Peters J. H. 1999 Modeling removal of bacteriophages MS2 and PRD1 by dune recharge at Castricum, Netherlands. *Water Resources Research*, **35**(4), 1101-1111.

Schijven J.F. & Hassanizadeh S.M. 2000 Removal of Viruses by Soil Passage: Overview of Modeling, Processes, and Parameters. *Critical Reviews in Environmental Science and Technology* **30**(1), 49-127.

Sim Y. & Chrysikopoulos C. V. 1998 Three-dimensional analytical models for virus transport in saturated porous media. *Transport in Porous Media*, **30**(1), 87-112.

Takabe Y., Kameda I., Suzuki R., Nishimura F. & Itoh S. 2014 Changes of microbial substrate metabolic patterns through a wastewater reuse process, including WWTP and SAT concerning depth. *Water Research*, **60**, 105-117.

Teutsch G., Herbold-Paschke K., Tougianidou D., Hahn, T. & Botzenhart K. 1991 Transport of microorganisms in the underground—processes, experiments and simulation models. *Water Science & Technology*, **24**(2), 309-314.

Tim U. S. & Mostaghimi S. 1991 Model for predicting virus movement through soils. *Groundwater*, **29**(2), 251-259.

USEPA 2004 *Guidelines for Water Reuse*. EPA/625/R-04/108. US Environmental Protection Agency, Washington, DC.

Utsunomiy Y. 2015 *Modeling of probabilistic water quality assessment for implementation of soil aquifer treatment in water reclaimed system* (Unpublished Master's thesis). Kyoto University, Kyoto, Japan. (In Japanese).

Yates M. V., Gerba C. P. & Kelley L. M. 1985 Virus persistence in groundwater. *Applied and Environmental Microbiology*, **49**(4), 778-781.

Yates M. V. & Ouyang Y. 1992 VIRTUS, a model of virus transport in unsaturated soils. *Applied and environmental microbiology*, **58**(5), 1609-1616.

Yates M. V., Yates S. R., Wagner J. & Gerba C. P. 1987 Modeling virus survival and transport in the subsurface. *Journal of Contaminant Hydrology*, **1**(3), 329-345.

Zheng C. & Bennett G. D. 2002 *Applied contaminant transport modeling* (Vol. 2). New York: Wiley-Interscience.

Chapter 6

Viral risk assessment in the reclaimed water treated by SAT implemented in Katsura River Basin

6.1 Introduction

The protection of public health is a key requirement when evaluating water reuse and reclamation especially from treated wastewater. Quantitative microbial risk assessment (QMRA) is being increasingly applied to estimate the potential of microbial risk to human health (Haas et al., 1999; Medema et al., 2009). Also, it is used for evaluating the risk of enteric viruses in reclaimed water (Toze et al., 2010; Olivieri et al., 2014). Therefore, risk assessment approach by QMRA was performed to evaluate the viral risk in reclaimed water treated by SAT in this study in order to answer the questions: how much will public health be safe or how many additional water treatment will need for human safety.

In the previous chapter, infectious virus concentration was estimated with a numerical transport model of SAT. Then the estimated output data of virus concentration (SAT effluent at the withdrawal point) were applied for evaluating the viral risk by QMRA. The aim of this chapter is to estimate the potential risk of human enteric viruses in the reclaimed water treated by SAT and the level of treatment requirements using QMRA. This chapter consists of viral risk assessment of reclaimed water by QMRA, yearly infection risk of viruses in the reclaimed water, uncertainty analysis according to the unit of dose harmonization and the additional water treatment requirements for human safety.

6.2 Virus assessment of reclaimed water by QMRA

6.2.1 QMRA procedure

The steps of QMRA have been mentioned in Chapter 2. The estimated data of virus concentration in Chapter 5 were applied to viral risk assessment by QMRA. The procedure of QMRA is summarized in Figure 6.1. The output data of infectious virus were estimated by the 2-dimensional transport model in Katsura River Basin with the infectious virus data detected after the A2O process. Case 1, Case 3 and Case 7 were

used as the practical, lowest virus reduction and highest virus reduction scenarios, respectively.

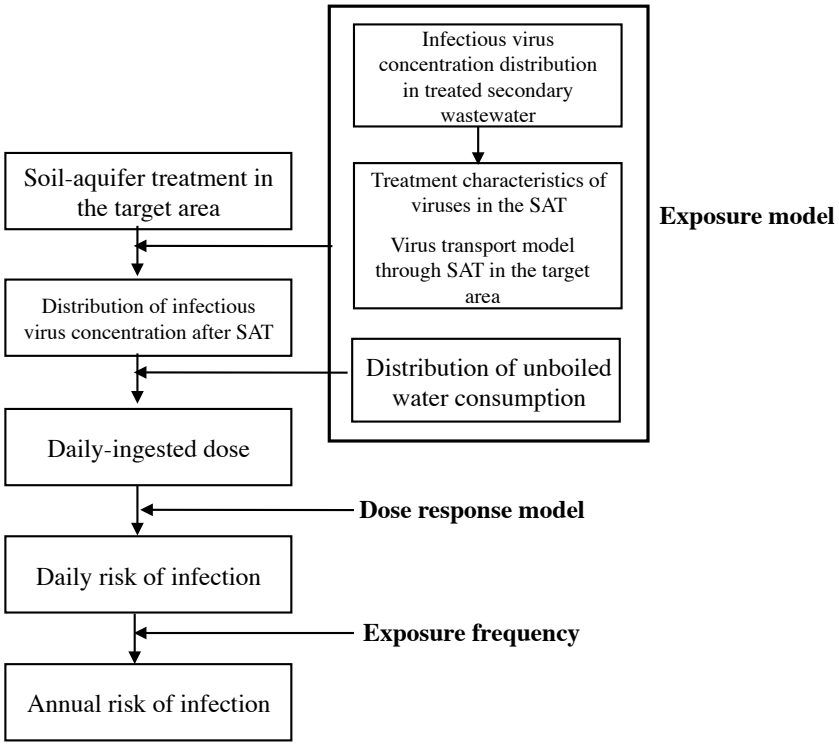

Figure 6.1: The procedure to estimate the expected annual infection risk from consumption of effluent-treated secondary sewage by SAT

The Monte Carlo simulation was used (Crystal ball®7, Decisinoering); this method gives statistical distributions and evaluated outcomes by the repeated random samplings of input data. Up to 100,000 iterations were run to make a proper statistical distribution.

6.2.2 Required data for viral risk assessment

a) Virus concentration

The virus concentration at the withdrawal point of SAT was obtained from the numerical simulation in the Katsura River Basin as described in Chapter 5. The distribution data were generated from the output of infectious AdVF and RV concentrations after SAT with practical case (Case 1), the best case (Case 7) and the worst case (Case 3) by Crystal ball as shown in Figures 6.2 and 6.3.

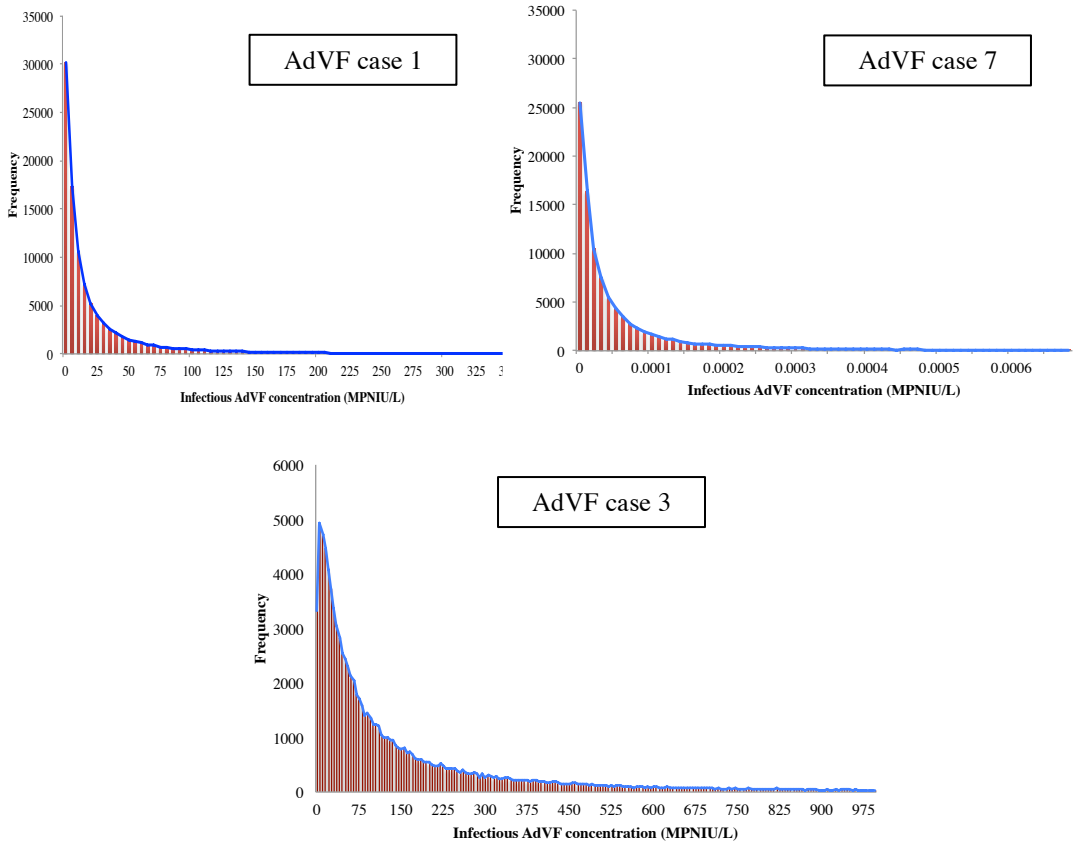

Figure 6.2: The distribution of infectious AdVF concentrations in Case 1, Case 7 and Case 3 after implementation at Katsura River Basin

All the distributions of infectious AdVF concentration output were well fitted with a lognormal distribution. The mean and standard deviation are 34.64 and 104.05 MPNIU/L, respectively in Case 1. The mean and standard deviation are 0.00009 and 0.00026 MPNIU/L, respectively in Case 7, and the mean and standard deviation are 261.71 and 786.04 MPNIU/L, respectively in Case 3.

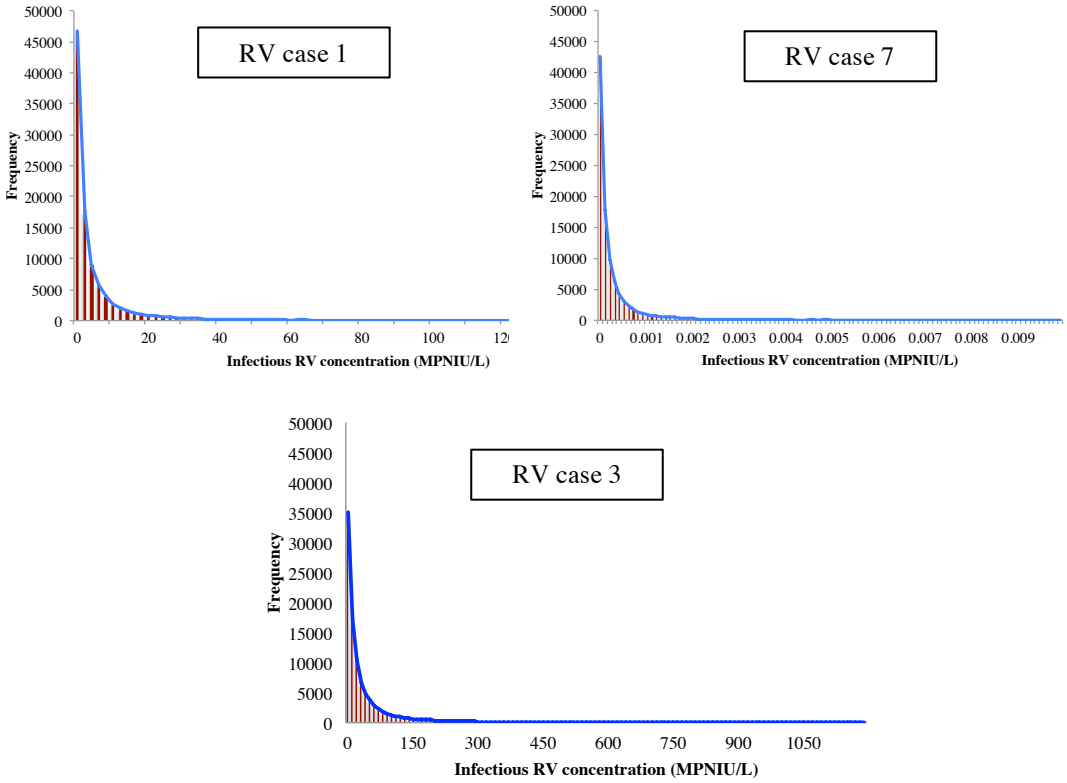

Figure 6.3: The distribution of infectious RV concentrations in Case 1, Case 7 and Case 3 after implementation at Katsura River Basin

RV concentrations in SAT influent and effluent samples also have been measured for 2 years, but the infectious RV was rarely detected. Therefore, the concentrations of infectious RV were calculated by the infectious RV to genome-based RV ratio as mentioned in Chapter 4. In this study, the minimum ratio was used as infectious RV estimation (mean 103 MPNIU/L) because the estimation data was close to the real detected infectious RV in SAT influent sample (22-73 MPNIU/L). Then the distributions of RV were generated as shown in Figure 6.3.

Similarly to AdVF, all the distributions of infectious RV concentration well fitted to a lognormal distribution. The mean and standard deviation are 3.16 and 10.11 MPNIU/L, respectively in Case 1. The mean and standard deviation are 0.000006 and 0.000027 MPNIU/L in Case 7 and The mean and standard deviation are 24.51 and 78.34 MPN/L in Case 3.

6.2.3 Water consumption

To account for the variability in water consumption within population, the water consumption data was obtained from the Osaka City Waterworks Bureau in 2009

(Komatsu et al., 2013), and exponential distribution was applied to the data for assessing the daily exposure in QMRA.

Then the probability of exposure in each case was calculated by Crystal ball (Table 6.1).

Table 6.1: Probability density function of the virus concentrations at the withdrawal point and water consumption

Element		PDF type	Estimation parameters
Estimated concentration of AdVF	Case 1	Lognormal	$\mu = 34.64$; $\sigma = 104.05$
	Case 3	Lognormal	$\mu = 261.71$; $\sigma = 786.04$
	Case 7	Lognormal	$\mu = 0.00009$; $\sigma = 0.00026$
Estimated concentration of RV	Case 1	Lognormal	$\mu = 3.16$; $\sigma = 10.11$
	Case 3	Lognormal	$\mu = 24.51$; $\sigma = 78.34$
	Case 7	Lognormal	$\mu = 6.49 \times 10^{-6}$; $\sigma = 2.07 \times 10^{-5}$
Water consumption		Exponential	$\lambda = 3.06 \times 10^{-3}$

After that, the dose-response models of the target viruses (adenovirus and rotavirus) are needed to estimate the daily and yearly risk infection.

6.2.4 Dose-response model

Dose-response models are the relationship between the rate of exposure (virus dose) and the rate of effect on human consumption. Commonly, dose-response models use animal behavior or data obtained from controlled experiments in which healthy adults consume pathogens. The dose-response models of AdVF and RV are shown below.

The studies on dose-response models of adenovirus and rotavirus are summarized in Table 6.2

Table 6.2: Dose-Response Models for AdV and RV

Organism	Measure of Exposure	Model	Endpoint	Parameter	Reference
AdV-4	Dose	Exponential	Human infection	$r = 0.4172$	Crabtree et al. (1997), Haas et al. (1999)
RV	Dose	Beta-Poisson	Human	$\alpha = 0.26$, $\beta = 0.42$	Gerba et al., 1996
RV	Dose	Beta-Poisson	Human	$\alpha = 0.2531$, $\beta = 0.4265$	Hass et al., 1999 Regli et al., 1991 Rose and Sobsey, 1993
RV	Dose	Beta-Poisson	Human	$\alpha = 0.232$, $\beta = 0.247$	Rose and Gerba, 1991
RV	Dose	Hypergeometric beta-Poisson	Human infection	$\alpha = 0.167$, $\beta = 0.191$	Teunis and Havelaar (2000)

The β-Poisson model is the dominant dose-response model for rotaviruses. The β-Poisson model was the first used for drinking water and food technology, and is an

appropriate model to assess virus ingestion and the probability of infection (Rose and Gerba 1991; Tanaka et al. 1998).

$$P_d = 1-(1-D_i/\beta)^{-\alpha} \quad (6.1)$$

where P_d is daily probability of infection through ingestion of pathogens; D_i is the daily consumed dose of contaminant (in FFU/days); β is the β-Poisson distribution coefficient; and α is a model parameter. There are several dose response parameters for RV, but the values of α and β are approximately 0.26 and 0.42, respectively. Therefore, this study used α=0.26 and β =0.42 (Gerba et al., 1996) for RV virus dose-response model.

The only dose-response data set available for adenoviruses is the one for the respiratory adenovirus, Ad4 (Crabtree et al., 1997). Haas et al. (1999) used this data set, and determined that the dose-response data was best described by the following exponential model:

$$P_d = 1-\exp(-r\, D_i) \quad (6.2)$$

where, P_d represents the probability of infection, D is the number of adenovirus ($TCID_{50}$) inhaled or ingested, and r is the constant describing the dose-response, and the analysis showed that r = 0.4172 (Crabtree et al., 1997).

Then the daily infection risk P_d (infection person^{-1} day^{-1}) was calculated by using the Monte Carlo simulation with the equations below:

$$P_d(Rotavirus) = 1-(1+\frac{D}{0.42})^{-0.26} \quad (6.3)$$

$$P_d(Adenovirus) = 1-e^{(-0.4172xD)} \quad (6.4)$$

Annual risk can be assessed from daily riskas follows:

$$P_a = 1-(1-P_d)^{365} \quad (6.5)$$

where P_a (infection person^{-1} year^{-1}) is the annual probability of infection through ingestion of pathogens.

6.2.5. Uncertainty Analysis

The uncertainty analysis of dose units and inactivation rate were performed.

a) Impact on inactivation rate of AdVF

The inactivation rate of AdVF in column experiment was up to 0.1 day^{-1} (mean 0.06). However, the inactivation rate of RV is limited in this study because few infectious RV were detected in the SAT column experiment. Therefore, uncertainty analysis was performed with different inactivation rates of AdVF by the Monte Carlo method as mentioned in 6.2.3.

b) The unit of AdV and RV dose-response model

Table 6.3: Dose harmonized unit for AdV and RV

Pathogen	Method in this study	Quantification method	Harmonization factor	Rational/Comment
Adenovirus	ICC-PCR (MPNIU)	$TCID_{50}$ viral particulates for AdV4 inhaled; Couch et al. (1969)	1 $TCID_{50}$ ≈ 3600 ICC-qPCR unit	1 $TCID_{50}$ ≈0.7 PFU McBride et al., (2013) Fongaro et al., (2013) 1 PFU ≈ 2512 ICC-qPCR unit in lagoon water
Rotavirus	ICC-RT-PCR (MPNIU)	Focus Forming Units (FFU), Ward et al. (1986)	1 FFU ≈ 1500 ICC-RT-qPCR unit	Payne et al. (2006), McBride et al., (2013) 1 PFU≈ 3FFU Li et al., (2010) 1 PFU ≈ 500 ICC-RT-qPCR log-log equation of y = 0.8624x+2.9338

Dose harmonized unit (Conversion unit from ICC-(RT)-PCR to $TCID_{50}$ and FFU for AdV and RV, respectively) is crucial for viral risk assessment because early studies established dose-response models by using the different unit from those used in recently studies and this study. There are several ratios that previous researchers attempted to harmonize the unit of the virus to the original unit of dose-response model.

For example, McBride et al. (2013) estimated the virus risk from genome-based concentration detected by qPCR, and the study converted the genome unit to the original unit of dose response model. However, Kundu (2011) evaluated no good correlation between genome base concentration (qPCR data) and infectious virus ($TCID_{50}$) due to the variation of the infectious-to-genome ratio for different type of

water. Therefore, it is better to convert the infectious unit to original infectious unit (ICC-PCR to $TCID_{50}$ or FFU) of the virus dose-response model. The literature information for the unit conversion of infectious AdVF and RV conversion unit is summarized in Table 6.3.

Adenovirus

Equivalences should be maintained between the dose obtained in clinical trials and dose measured in the environmental samples. A clinical trial of adenovirus used median tissue culture infective dose ($TCID_{50}$); that of amount of pathogenic agent that will produce pathological change in 50% of cell culture inoculated (Couch et al., 1966), whereas adenovirus in several previous studies were reported as genomes per unit volume. The relationship between $TCID_{50}$ and plaque forming unit (PFU) was shown in Wuertz et al. (2011) as 1 $TCID_{50}$ being equal to 0.7 PFU. He and Jiang (2005) reported a ratio of genome to PFU of 0.001 in primary treated effluent.

Fongaro et al. (2013) analyzed the samples from various sites (lagoon water, spring source water and public supply system water) with PFU and genome copies by ICC-qPCR. The plaque assay value equivalence (PFU/mL) was compared to ICC-qPCR value (copies/mL). On average, one PFU unit was equivalent to ~2512 copies by ICC-qPCR.

Rotavirus

Li et al. (2010) detected the infectious RV by ICC-RT-qPCR in environmental water samples. The correlation between ICC-RT-qPCR results and those from the plaque assay was described as a linear relationship: $y = 0.8625x + 2.9388$ ($R^2 = 0.9575$) where y is $\log_{10}$ of infectious RV detected by ICC-RT-qPCR (copies/mL) and x is $\log_{10}$ RV concentration in PFU/mL.

Assumption about relationship between ICC-PCR and ICC-qPCR

The assumption of the equivalence of ICC-PCR and ICC-RT-PCR results will be discussed in this study. There are two assumptions of unit conversion from ICC-PCR to ICC-qPCR. The first assumption is the ICC-PCR result is equal to ICC-qPCR

result. The second assumption is to compare the experiment from ICC-PCR result and ICC-qPCR result and the ratios are 1:50 and 1:500 for AdVF and RV, respectively.

All the parameters (inactivation rate, dose unit conversion by literature data, and dose unit conversion of uncertainty analysis were shown in Table 6.4. Case 1 was used as a base case for uncertainly analysis in this study

Table: 6.4: Uncertainty analysis of unit conversion of AdVF and RV and the reduction constant rate of AdVF

Virus	Uncertainty issue	Value	Remarks
AdVF	Removal and inactivation rate constant	$\mu = 0 - 0.09$ day^{-1} $k_{irr} = 0.1$ day^{-1}	The inactivation constant rates of AdVF are up to 0.1 in Chapter 4. Therefore, overall reduction ($k_{irr}+\mu$) up to 0.19 should be considered
	Unit conversion	1 $TCID_{50} \approx 3600$ ICC-RT-PCR unit	Literature data for unit conversion
		1 $TCID_{50} \approx 72$ ICC-RT-PCR	The present study tested with the sensitivity between ICC-PCR and ICC-qPCR the ratio is 1:50 in Appendix E
RV	Unit conversion	1 FFU ≈ 1500 ICC-RT-PCR unit	Literature data for unit conversion
		1 FFU ≈ 3 ICC-RT-PCR unit	The sensitivity between ICC-RT-PCR and ICC-RY-qPCR was tested in this study and the ratio is 1:500 in Appendix E

6.3 Results and Discussions of AdVF and RV risk assessment by QMRA

6.3.1 Yearly infection risks of AdVF and RV in the reclaimed water

The viral risk assessment was calculated by the QMRA and the statistical estimation of AdVF and RV risk results of Cases 1, 3, and 7 are shown in Table 6.5.

According to the US.EPA guidline, the acceptable infection risk of pathogenic microorganism should be below 10^{-4} infection/person/year or less than one infection per 10,000 people per year from pathogen. The yearly infection risks of AdVF and RV associated with direct exposure of reclaimed water treated by SAT in Katsura River Basin exceeded the acceptable risk for any estimates (i.e., mean, median, upper and lower 95% CI bound) values. This means that the reclaimed water implemented in SAT has high potential risks of AdVF and RV. These results indicated that optimization of the SAT operating conditions or additional water treatment is necessary.

Table 6.5 Risk estimation of AdVF and RV by the QMRA

Case 1 (Practical case scenaraio)

	Lower 95% CI boundary	Median	Mean	Upper 95% CI bound
AdVF dose	$3.08x10^{-2}$	$2.20x10^{0}$	$1.14x10^{1}$	$7.73x10^{1}$
Daily risk of infection (infection/person/day)	$1.27x10^{-2}$	$6.01x10^{-1}$	$5.70x10^{-1}$	1.00
Yearly risk of infection (infection/person/year)	$9.91x10^{-1}$	1.00	$9.94x10^{-1}$	1.00
RV dose	$2.63x10^{-3}$	$1.89x10^{-1}$	$1.05x10^{0}$	$7.39x10^{0}$
Daily risk of infection (infection/person/day)	$1.62x10^{-3}$	$9.23x10^{-2}$	$1.46x10^{-1}$	$5.32x10^{-1}$
Yearly risk of infection (infection/person/year)	$4.47x10^{-1}$	1.00	$9.63x10^{-1}$	1.00

Case 3 (Worst case scenaraio)

	Lower 95% CI boundary	Median	Mean	Upper 95% CI bound
AdVF dose	$2.34x10^{-1}$	$1.65x10^{1}$	$8.46x10^{1}$	$5.92x10^{2}$
Daily risk of infection (infection/person/day)	$9.31x10^{-2}$	$9.99x10^{-1}$	$8.54x10^{-1}$	1.00
Yearly risk of infection (infection/person/year)	1.00	1.00	$9.99x10^{-1}$	1.00
RV dose	$1.93x10^{-2}$	$1.45x10^{-0}$	$7.92x10^{0}$	$5.49x10^{1}$
Daily risk of infection (infection/person/day)	$1.16x10^{-2}$	$3.22x10^{-1}$	$3.29x10^{-1}$	$7.19x10^{-1}$
Yearly risk of infection (infection/person/year)	$9.86x10^{-1}$	1.00	$9.94x10^{-1}$	1.00

Case 7 (Best case scenario)

	Lower 95% CI boundary	Median	Mean	Upper 95% CI bound
AdVF dose	$7.88x10^{-8}$	$5.47x10^{-6}$	$2.84x10^{-5}$	$1.98x10^{-4}$
Daily risk of infection (infection/person/day)	$3.29x10^{-8}$	$2.28x10^{-6}$	$1.18x10^{-5}$	$8.27x10^{-5}$
Yearly risk of infection (infection/person/year)	$1.20x10^{-5}$	$8.32x10^{-4}$	$4.18x10^{-3}$	$2.97x10^{-2}$
RV dose	$2.98x10^{-8}$	$6.29x10^{-7}$	$2.09x10^{-6}$	$1.33x10^{-5}$
Daily risk of infection (infection/person/day)	$1.85x10^{-8}$	$3.89x10^{-7}$	$1.29x10^{-6}$	$8.21x10^{-6}$
Yearly risk of infection (infection/person/year)	$6.74x10^{-6}$	$1.42x10^{-4}$	$4.70x10^{-4}$	$2.99x10^{-3}$

6.3.2 Expected Log_{10} reduction to achieve the viral risk acceptable level

Practical case scenario (Case1)

The requirements of additional virus reduction to achieve 10^{-4} infection/person/year after the SAT system were estimated. The results of Case 1 were shown in Figure 6.4. The additional required log-reductions of AdVF, which calculated by the Monte Carlo method, were greater than or equal to 8.07, 6.53, 7.24 and 4.68 for 97.5 percentile, median, mean, and 2.5 percentile, respectively in water treatment processes. The

additional treatment requirement for RV was calculated in the same procedure as the AdVF. The additional required log-reductions of RV were greater than or equal to 7.20, 5.63, 6.37 and 3.75 for 97.5 percentile, median, mean, and 2.5 percentile, respectively. In view of the safety for water consumer, the 97.5 percentile value was selected to be on the safe side to recommend the use of additional water treatment.

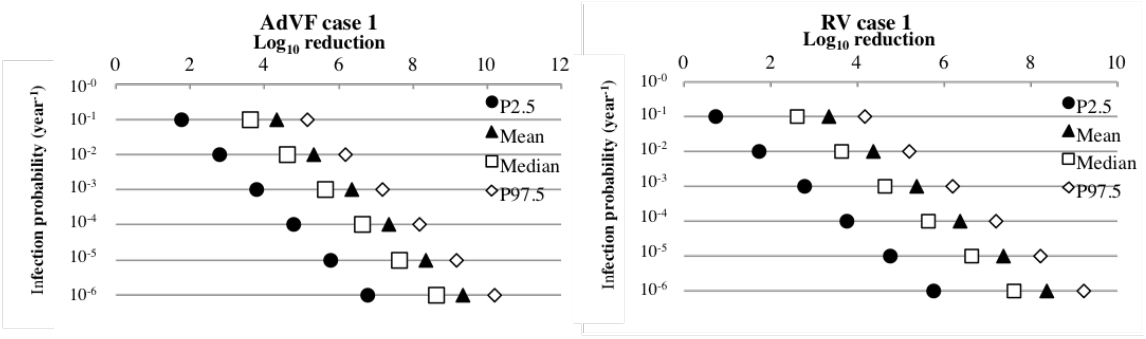

Figure 6.4:The requirement of AdVF and RV $\log_{10}$-reduction in additional water treatment in the practical case simulation

The worst-case scenario (Case 3)

The worst-case scenario has lower virus reductions due to the shorter retention time. The infection risks of AdVF and RV have been calculated in the same approach as Case 1 and were shown in the Figure 6.5. The results suggested that the additional log-reductions of AdVF required were greater than or equal to 8.89, 7.61, 8.11 and 6.32 for 97.5 percentile, median, mean, and 2.5 percentile, respectively. Moreover, the additional reductions of RV required were greater than or equal to 8.10, 6.52, 7.25 and 4.66 for 97.5 percentile, median, mean, 2.5 percentile, respectively.

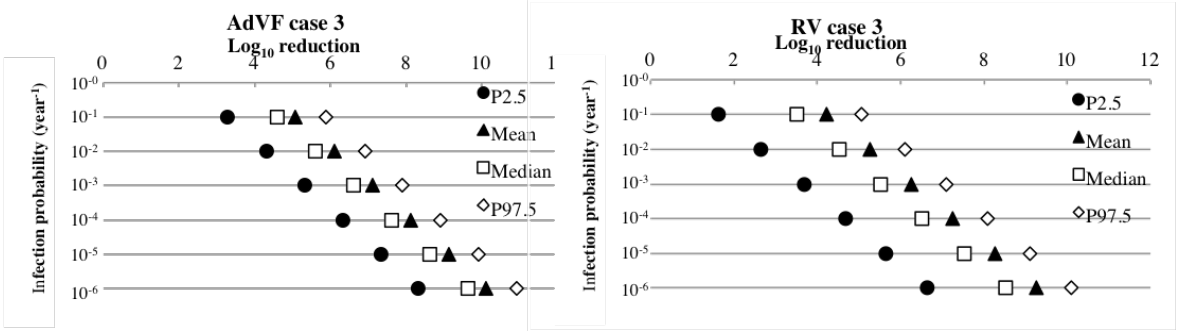

Figure 6.5: the requirement of AdVF and RV $\log_{10}$-reduction in additional water treatment in the worst-case simulation

The best-case scenario (Case7)

The best-case scenario has a higher removal rate of the virus because of a higher retention time. The AdVF and the RV also have been calculated in the same procedure as Case 1 and were shown in Figure 6.6. The results indicate that the addition log–reduction levels of AdVF required were greater than or equal to 2.47, 0.92, 1.63 for 97.5 percentile, median, and mean values, respectively. But the 2.5 percentile value was below the acceptable level (i.e., 10^{-4} infection/person/year). Moreover, the additional log-reduction levels of RV required were greater than or equal to 3.36, 1.78 and 2.52 for 97.5 percentile, median, and mean values, respectively, while 2.5 percentile achieved the acceptable risk.

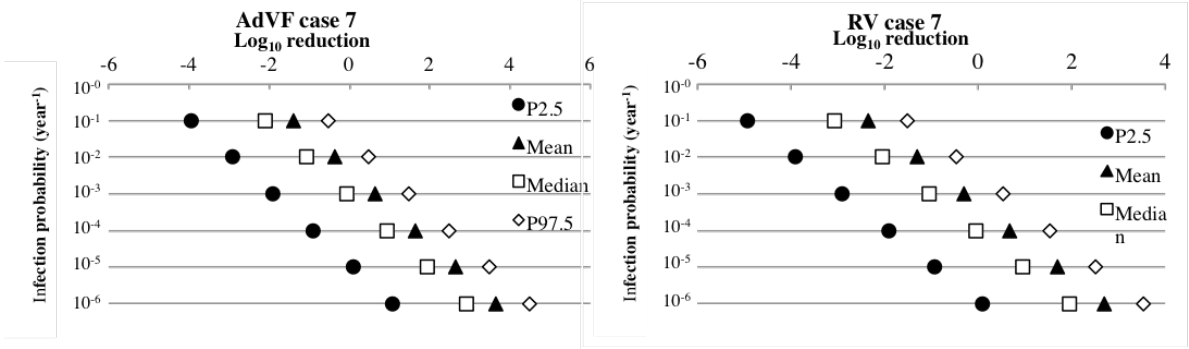

Figure 6.6: The requirement of AdVF and RV $\log_{10}$-reduction in additional water treatment in the best-case simulation

In this study, the virus removal and inactivation were used to simulate the virus concentration after SAT in the target area. The results showed that SAT with a short retention time is insufficient for the virus reduction. Hence, the additional water treatment is required after SAT system to ensure the reclaimed water safety.

Consequently, this study indicated that the numerical transport model and viral risk model are very useful tools to make a decision of implementation of SAT system and additional treatment requirement after SAT system.

6.3.3 Uncertainty analysis

The uncertainty analysis was done only for Case 1 (Table 6.6)

6.3.3.1 Uncertainty analysis on the risks associated with AdVF

The uncertainty of AdVF risk in the reclaimed water is divided in two issues. The first one is the uncertainty in the inactivation rate (i.e., discrepancy between batch

experiment and column experiment). The second is the uncertainty in the conversion of dose unit. The original unit of dose response model is categorized into 2 cases, the assumption of ICC-PCR is nearly equal to ICC-qPCR, and the assumption of ICC-PCR is conversed to the sensitivity of ICC-qPCR (1:50) as mentioned in Appendix E.

Table 6.6 Estimated of AdVF and RV yearly infection risk in the QMRA by different cases

	Yearly risk of infection (infection/person/year)			
AdVF	**Lower 95% CI boundary**	**Median**	**Mean**	**Upper 95% CI boundary**
Base case at case 1	$9.91x10^{-1}$	1.00	$9.94x10^{-1}$	1.00
Case A (0.19)	$9.70x10^{-1}$	1.00	$9.92x10^{-1}$	1.00
Case B (harmonized unit to $TCID_{50}$)	$7.19x10^{-4}$	$5.07x10^{-2}$	$1.42x10^{-1}$	$8.44x10^{-1}$
Case C (harmonized unit to $TCID_{50}$ with 1:50 ratio of ICC-PCR: ICC-qPCR	$1.04x10^{-1}$	1.00	$8.65x10^{-1}$	1.00
RV				
Base case at case 1	$4.47x10^{-1}$	1.00	$9.63x10^{-1}$	1.00
Case A (harmonized unit to FFU)	$1.39x10^{-3}$	$1.36x10^{-1}$	$2.85x10^{-1}$	1.00
Case B (harmonized unit to FFU with 1:500 ratio of ICC-RT-PCR: ICC-RT-qPCR	$5.18x10^{-1}$	1.00	$9.69x10^{-1}$	1.00

a) Impact on inactivation rate of AdVF

According to the model simulation of infectious AdVF with 0.164 day^{-1} (from the batch inactivation and column removal data), the inactivation coefficients of AdVF in the column were fluctuated from 0 to 0.1 day^{-1}. It leads to thencrease of overall reduction up to 0.19 day^{-1} (0.1 of adsorption + 0.09 of inactivation). The impact of the reduction rate (adsorption and inactivation rates) between 0.164 and 0.19 day^{-1} was examined by using the uncertainty analysis. The results of the yearly infection risk of were shown in Table 6.6. The mean value of the AdVF yearly infection risk is not very different from the base case (0.164 day^{-1}).

Also, the expected log-reduction was calculated to confirm the results as shown in Figure 6.7. The AdVF required additional log removals of 7.94, and 7.10, and 4.56 for 97.5 percentile, mean, and 2.5 percentile, respectively of the 0.19 day^{-1} reduction rate.

The expected log-reduction was lower than the base case approximately by $\log_{10}$. Hence, the reduction rate between 0.164 and 0.19 day^{-1} had a low impact on the yearly infection risk of AdVF.

b) Impact of unit of dose-response model

For the AdVF, after changing the unit of *D* from MPN to $TCID_{50}$ by using the ratio of ICC-qPCR (copies) to ICC-PCR (MPN) and 1 $TCID_{50}$ ~ 3600 ICC- qPCR (Fongaro et al., (2013) and McBride et al (2013)), the yearly infection risk was calculated and shown in Table 6.6. The 2 cases of unit conversion are assumed: (1) ICC-PCR nearly equal to ICC-RT-PCR and (2) the sensitivity of ICC-PCR: ICC-qPCR is 1:50.

- Impact of unit of dose response model (ICC-PCR is nearly equal to ICC-RT-qPCR)

The mean value of the AdVF yearly infection risk was $1.42x10^{-1}$ infection/person/year. Moreover, a large difference was found in 2.5 percentile and median values. Then, the additional log-reduction required was calculated to see the impact of the *D* value (Figure 6.10). This case needs additional log-reduction levels of 1.12, 3.68, and 4.52 for 2.5 percentile, mean, and 97.5 percentile, respectively. The requirements for additional water treatment are lower than the base case.

- Impact of unit of dose response model (ICC-PCR is* 50 *times more sensitive than ICC-qPCR)

For the unit conversion by assuming the ratio of 1:50 of ICC-PCR: ICC-qPCR, the mean value of the AdVF yearly infection risk was $8.81x10^{-1}$ infection/person/year. This yearly risk is slightly different from that in the base case (without unit conversion) for the 2.5 percentile value. Then the impact of the *D* value on AdVF and RV risk assessment was shown in Figure 6.7. The requirements of additional water treatment were calculated as 3.12, 5.68, and 6.52 for 2.5 percentile, mean, and 97.5 percentile, respectively, to achieve the safety guidance with 10^{-4} infection/person/year. The additional water treatment requirement is lower than the base case significantly.

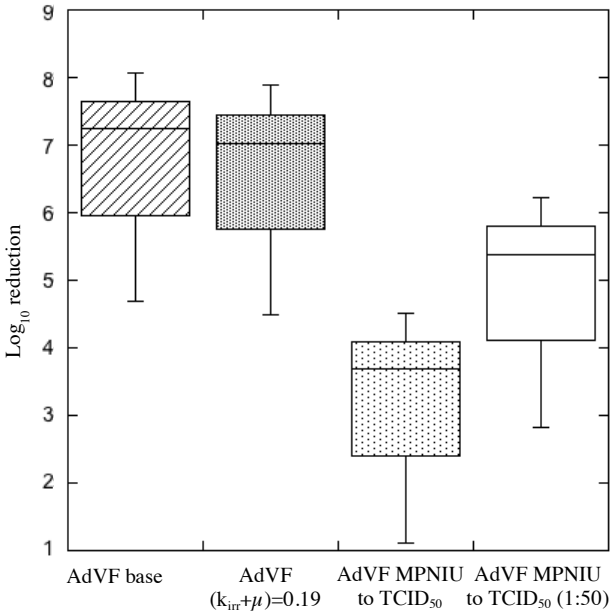

Figure 6.7: The additional water treatment needed to achieve 10^{-4} infection/person/year for AdVF

6.3.3.2 RV risk uncertainty analysis

The uncertainty of RV risk in the reclaimed water also needs to consider the conversion of dose unit. For RV, the dose unit was converted from ICC-RT-PCR to FFU because the FFU is the unit of dose-response model in 6.2.3. The unit conversion is divided into 2 cases, the assumption of ICC-PCR is nearly equal to ICC-qPCR and the assumption of ICC-PCR is converted with a sensitivity of ICC-qPCR (1:500) as shown in Appendix E.

- Impact on unit of dose response model (ICC-PCR is nearly equal to ICC-qPCR)

The mean value of the RV yearly infection risk was 2.85×10^{-1} infection/person/year. Moreover, the significant difference was found in the 2.5 and 97.5percentile mean and median values compared with those in the base case (without unit conversion of *D*). Then, the required additional log-reduction was calculated to see the impact of the *D* value (Figure 6.8). This case needs additional reduction greater than or equal to 1.15 $\log_{10}$ of P2.5, 4.09 $\log_{10}$ of mean and 4.93 log10 of P97.5. The additional water treatment requirements are lower than the base case.

- Impact on unit of dose response mode (ICC-PCR is 1000 times more sensitive than ICC-qPCR)

After using the ratio for the unit conversion, the mean yearly infection risk of RV was $9.93x10^{-1}$ infection/person/year. The significant difference was found for the 2.5 Percentile value. Then, the additional log-reductions required were calculated to see the impact of the *D* value to achieve the safety guidance with 10^{-4} infection/person/year of water consumers. This case needs 4.16 $\log_{10}$ of P2.5, 7.08 $\log_{10}$ of mean and 7.94 $\log_{10}$ of P97.5. The additional water treatment requirements are slightly higher than the base case.

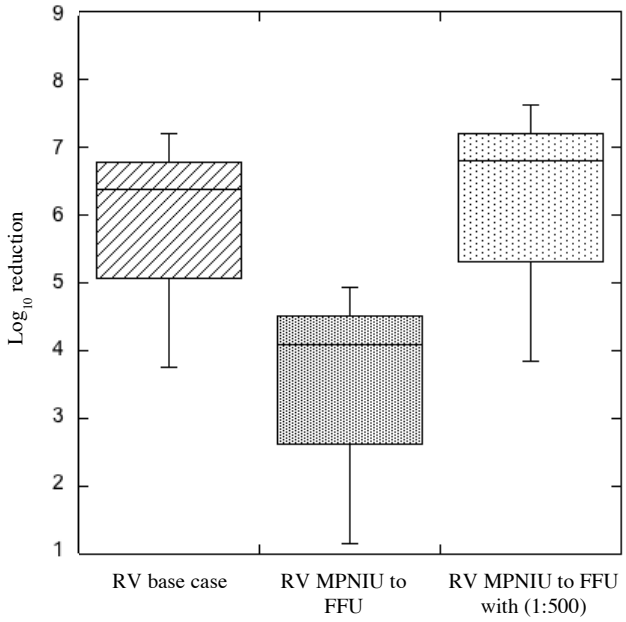

Figure 6.8: the additional water treatment needed to achieve 10^{-4} infection/person/year for RV

The uncertainty analysis demonstrated that the difference between the inactivation rates of AdVF 0.164 and 0.19 day^{-1} is not significant for the AdVF yearly risk assessment. However, an estimation of harmonized dose unit is needed to improve the accuracy of QMRA for AdVF and RV. In addition, the ratio of ICC-PCR to ICC-qPCR is highly important and needs further research efforts.

It is clear that the unit of *D* (Dose) affected the estimation of the yearly risk. However, the harmonized unit in this study obtained from the literature data, somehow, is different when it comes to the experimental condition. Accordingly, it can be pointed out that the comparison between the MPNIU by the ICC-PCR and

$TCID_{50}$ or FFU of AdVF and RV should be further studied to improve the accuracy of the risk calculation model.

6.4. Discussions about additional water treatment to achieve the viral acceptable risk

The simple and compact processes with low energy consumption would appropriate options. One of simple processes is a disinfection unit (i.e., UV and chlorination) and a physical treatment unit (i.e., MF). The disinfection processes are really effective to inactivate viruses. The review of the disinfection units and microfiltration to eliminate adenovirus and rotavirus are shown in Table 6.7. In Japan, ozonation, chlorination, and UV radiation are usually selected for the disinfection of sewage (Japan Sewage Works Association, 2009).

Table 6.7: Virus log_{10} reduction by UV, Chlorination, Ozonation and Microfiltration

UV	mJ/cm2					References
Log reduction	1	2	3	4		
AdVF	42	83	125	167		Hijnen (2009)
RV	10	20	29	39		
Cl_2	mg/L.min					
Log reduction	1	2	3	4	4.5	
AdVF	-	0.03(5˚C)	0.1	0.75 (5˚C)		Au (2004), Thurston-Enriquez et al.(2003),
RV	-	0.01~0.05 (5˚C)		0.05(˚C)	0.1 (5˚C)	
MF	Log reduction					
AdVF	<1					Sato et al., 2011
RV	<1					
Ozonation						
AdVF	3.3					Japan Sewage Works Associarion, 2009
RV	5					

UV treatment is not effective for adenovirus because adenovirus is UV resistant. The data of UV inactivation dose for a required log inactivation by viruses is shown in Table 6.8. Based on additional water treatment requirement, the simple processes for the potable use of SAT effluent combination are considered. Log-reduction levels of simple disinfection units or combination units were calculated from literature data. The results were shown in Figures 6.9 and 6.10.

Table 6.8: UV inactivation dose for a required log inactivation by viruses

Virus	MIC required (log)	1	2	3	4
	DNA/RNA type	Required UV dose ($mJ.cm^{-2}$)			
Adenovirus type 2,15,40,41	Double strand DNA	42	83	125	167
Adenovirus type 40	Double strand DNA	56	111	167	-
Adenovirus (not type 40)	Double strand DNA	25	50	-	-
Coxsackie virus B5	Single strand RNA	8	17	25	34
Hepatitis A	Single strand RNA	6	11	17	22
Rotavirus SA-11	Double strand RNA	10	20	29	39

MIC is mean inactivation capacity; the data obtained from Hijnen et al., 2006 and Microrisk (2006)

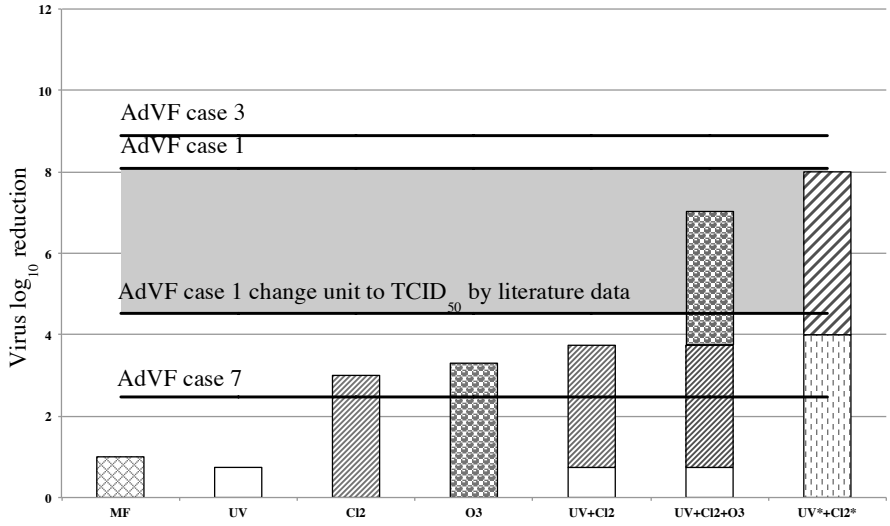

Figure 6.9: Expected log_{10} reduction of AdVF after SAT by additional water treatment processes

The practical case is in Case 1 with HRT 23 days still needed additional 8.07 log_{10} reduction by water treatment and the best case simulation in Case 7 with HRT 183 days required 2.47 log_{10} reduction for AdVF. However, the worst case (Case3) needed 8.89 log_{10} reduction in additional water treatment. In Case 1, the uncertainly analysis of the unit conversion of virus was estimated, and for the control of AdVF in Case 1 the additional water treatment level required was in the range of 4.52 to 8.07 log_{10} reduction as shown in the grey area. Any single processes of MF, UV and chlorination cannot achieve this range of additional reduction. The combination of $UV+O_3+Cl_2$ or the $UV^*+Cl_2^*$ (high dose of UV ~ 167 mJ/cm^2) can achieve the expected log_{10}-reduction. From the literature data, the additional water treatments are not sufficient to inactivate AdVF in Case 3. However, the combination process of $UV^*+Cl_2^*$ have a high possibility to achieve the required log-reduction for AdVF.

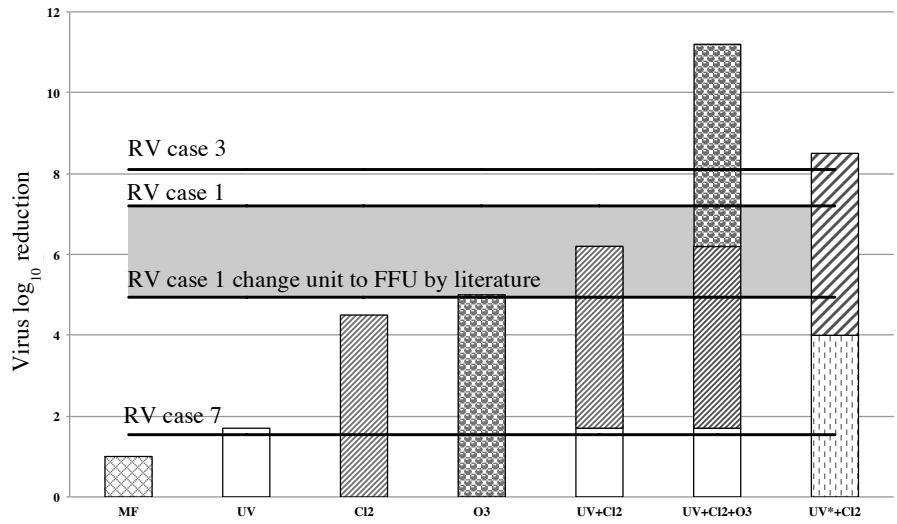

Figure 6.10: Expected log_{10} reduction of RV after SAT by additional water treatment processes

RV required additional water treatment of 7.20 log_{10} in Case 1, 8.10 log_{10} in Case 3, and 1.53 log_{10} in Case 7. The uncertainly analysis of the dose conversion unit was estimated as in AdVF in Case 1. The additional water treatment required was in the range of 4.93 to 7.20 log_{10} to achieve the viral safety guideline in Case1. As shown in Figure 6.9, only the combination processes of UV+Cl_2, UV+Cl_2+O_3 and UV*+Cl_2* can achieve the expected log-reduction of Case 1 range. The combination processes of UV+Cl_2+O_3 and UV*+Cl_2* can achieve the expected log_{10} reduction in Case 3.

The simple disinfection units such as UV treatment, chlorination and ozonation are suitable to apply after SAT system because they are simple and required small space. Recently, ozonation is widely used for drinking water and it is very effective to inactivate virus. However, ozonation costs are generally high in comparison with other disinfection techniques.

Itoh et al. (2015) mentioned that the combination of SAT, UV treatment, and chlorination are suitable for virus inactivation. Chlorination can produce residual effect in distribution system that contributes to a higher level of microbial safety. This is a quite simple process, compared with conventional water treatment processes in Japan or advance oxidation processes (AOPs). In addition, for pathogen inactivation, virus, bacteria and protozoa should be inactivated by UV and chlorination. Recently, *Cryptosporidium* and *Giadia* polluted groundwater especially in Japan, so these pathogens should be treated by physical removal process such as MF and sand

filtration or UV treatment. However, it was confirmed that suspended solid (SS) of SAT effluent is sufficiently low and they do not need more removal in the SAT effluent. Therefore, the physical removal unit is not necessary in this case. Only disinfection is sufficient and UV disinfection is appropriate to inactivate these protozoa.

Basically, bacteria and protozoa can be easily removed by the soil passage (Clancy and Stendahl, 1997; Au, 2004). It does not necessitate considering bacteria and protozoa in the SAT effluent. The only reason why *Cryptosporidium* and *Giadia* are concerned is because they can be polluted in groundwater. Hence, it is concluded that the combination of UV (high dose 167 mJ/cm^2) and chlorination or the combination of ozonation, UV and chlorination can be effective to remove the pathogens after SAT system in this study.

6.5 Summary

Adenovirus and rotavirus yearly infection risks in reclaimed water via SAT when implemented in the Katsura River Basin were estimated by QMRA. Although the viruses were eliminated by the SAT, the results of the virus infection risk assessment showed that SAT alone is still insufficient to ensure the human safety for drinking purposes. The main findings in this chapter can be summarized as the follows:

- The SAT system implemented in the Katsura River basin is insufficient to remove the AdVF and the RV to achieve the acceptable yearly risk of infection (10^{-4} infection/person/year).
- The Additional water treatment after the SAT is needed. The expected additional water treatment requirement calculation found that the practical case (case 1): 8.07 $\log_{10}$ of AdVF and 7.20 $\log_{10}$ of RV are required to achieve the acceptable level of 10^{-4} infection/person/year, the worst case (case 3): 8.89 of AdVF and 8.10 $\log_{10}$ of RV are required to achieve the acceptable level. The best case (case 7): 2.47 of AdVF and 1.53 $\log_{10}$ of RV are required to achieve the acceptable level.
- The impact of the dose (D) unit affected the yearly infection risk estimation from the uncertainty analysis.
- Chlorination and UV disinfection were selected to be a good combination in the additional treatment after SAT system.

References

Asano T., Burton F. L., Leverenz H., Tsuchihashi R. & Tchobanoglous G. 2007 Water *Reuse: Issues, Technologies, and Applications*, McGraw-Hill, New York. (Comprehensive background on water reuse)

Au, K. K. 2004 *Water treatment and pathogen control: Process efficiency in achieving safe drinking-water*. IWA Publishing.

Chigor V. N., Sibanda T. & Okoh, A. I. 2014 Assessment of the risks for human health of adenoviruses, hepatitis a virus, rotaviruses and enteroviruses in the buffalo river and three source water dams in the eastern cape. *Food and Environmental Virology*, **6**(2), 87-98.

Clancy J. L. & Stendahl, D. 1997 Ground water or surface water—microscopic evaluation of an Ontario River well system. In *Proceedings of the American Water Works Association Water Quality Technology Conference. Denver, CO, American Water Works Association*.

Crabtree K. D., Gerba C. P., Rose, J. B. & Haas C. N. 1997 Waterborne adenovirus: a risk assessment. *Water Science and Technology*, **35**(11), 1-6.

EPA Victoria 2005 Dual pipe water recycling schemes-health and environmental risk. Publication 1015. Guidelines for environmental management. EPA Victoria.

Fongaro G., Do Nascimento M. A., Rigotto C., Ritterbusch G., da Silva A. D. A., Esteves P. A. & Barardi, C. R. 2013 Evaluation and molecular characterization of human adenovirus in drinking water supplies: viral integrity and viability assays. *Journal of Virology*, **10**(1), 1.

Gerba C. P., Rose J. B., Haas C. N. & Crabtree K. D. 1996 Waterborne rotavirus: a risk assessment. *Water Research*, **30**(12), 2929-2940.

Greening G. E., Hewitt J. & Lewis G. D. 2002 Evaluation of integrated cell culture - PCR (C - PCR) for virological analysis of environmental samples. *Journal of Applied Microbiology*, **93**(5), 745-750.

Haas C.N., Rose, J. & Gerba C.P. 1999 Quantitative Microbial Risk Assessment. New York: Wiley.

He J. W. & Jiang S. 2005 Quantification of enterococci and human adenoviruses in environmental samples by real-time PCR. *Applied and Environmental Microbiology*, **71**(5), 2250-2255.

Health Canada 2011 *Guidelines for Canadian drinking water quality: guideline technical document-enteric viruses* (pp. 1-64). Ottawa: Water, Air and Climate Change Bureau, Healthy Environments and Consumer Safety Branch, Health Canada.

Heerden J., Ehlers M. M., Vivier J. C. & Grabow, W. O. K. 2005 Risk assessment of adenoviruses detected in treated drinking water and recreational water. *Journal of Applied Microbiology*, **99**(4), 926-933.

Hijnen W. A. M. 2009 *Elimination of micro-organisms in water treatment*. KWR Watercycle Research Institute.

Itoh S 2015 *How safe is safe? Risk management for indirect potable reuse using soil aquifer treatment*. The First Asian Symposium on Water Reuse-Technology Renovation and Risk Management, Beijing, China, April 23-15, 2015

Japan sewage works association. Plan and design guideline of sewage treatment facility and its explanation (Japanese), (2009).

Ko G., Cromeans, T. L. & Sobsey M. D. 2003 Detection of infectious adenovirus in cell culture by mRNA reverse transcription-PCR. *Applied and Environmental Microbiology*, **69**(12), 7377-7384.

Kotmatsu Y., Kondo, T. & Tagawa K. 2013 Survey and analysis on unboiled water consumption from tap water by a questionnaire on Internet. *Journal of Japan Water Works Association* **82***(3)*:16-25 (in Japanese)

Li D., Gu A. Z., Yang W., He M., Hu X. H. & Shi H. C. 2010 An integrated cell culture and reverse transcription quantitative PCR assay for detection of infectious rotaviruses in environmental waters. *Journal of Microbiological Methods*, **82**(1), 59-63.

McBride G. B., Stott R., Miller W., Bambic D. & Wuertz S. 2013 Discharge-based QMRA for estimation of public health risks from exposure to stormwater-borne pathogens in recreational waters in the United States. *Water Research*, **47**(14), 5282-5297.

Medema G. & Smeets P. 2009 Quantitative risk assessment in the Water Safety Plan: case studies from drinking water practice. *Water Science & Technology: Water Supply*, **9**(2), 127-132.

Mena K. D. & Gerba C. P. 2009 Waterborne adenovirus. In *Reviews of Environmental Contamination and Toxicology* (pp. 133-167). Springer New York.

Microrisk 2006 Microbiological risk assessment: a scientific basis for managing drinking water safety from source to tap. EU project under 5FP. (http://www.microrisk.com/publish/cat_index_11.shtml)(visited 08.08.15)

Olivieri A. W., Seto E., Cooper R. C., Cahn M. D., Colford J., Crook J. & Hultquist R. A. 2014 Risk-Based Review of California's Water-Recycling Criteria for Agricultural Irrigation. *Journal of Environmental Engineering*, **140**(6), 04014015.

Paul C. D., Theresa B. K., Rabin B., Prasanta K K. & Mark S. K. 2013 Investigation of rotavirus survival in different soil fractions and temperature conditions. *Journal of Environmental Protection*, *2013*.

Payne A. F., Binduga-Gajewska I., Kauffman E. B. & Kramer L. D. 2006 Quantitation of flaviviruses by fluorescent focus assay. *Journal of Virological Methods*, **134**(1), 183-189.

Prez V. E., Gil P. I., Temprana C. F., Cuadrado P. R., Martínez L. C., Giordano M. O. & Barril P. A. 2015 Quantification of human infection risk caused by rotavirus in surface waters from Córdoba, Argentina. *Science of The Total Environment*, **538**, 220-229.

Regli S., Rose J.B., Haas C.N. & Gerba C.P. 1991 Modeling the risk from *Giardia* and viruses in drinking-water. *Journal of the American Water Works Association,* **83**,76-84.

Rose J.B. & Gerba C.P. 1991 Use of risk assessment for development of microbial standards. *Water Science and Technology,* **24**:29-34.

Rose J.B. & Sobsey M.D. 1993 Quantitative risk assessment for viral contamination of shellfish and coastal waters. *Journal of Food Protection* **56**(12), 1043-1050.

Sato A., Wang R., Ma H., Hsiao B. S. & Chu B. 2011 Novel nanofibrous scaffolds for water filtration with bacteria and virus removal capability. *Journal of Electron Microscopy*, dfr019.

Soller J. A. 2006 Use of microbial risk assessment to inform the national estimate of acute gastrointestinal illness attributable to microbes in drinking water. *Journal of Water and Health*, **4** (2), 165-186.

Tanaka H., Asano T., Schroeder E. D. & Tchobanoglous G. 1998 Estimating the safety of wastewater reclamation and reuse using enteric virus monitoring data. *Water Environment Research*, **70**(1), 39-51.

Teunis P.F.M. & Havelaar A. 2000 The beta-Poisson model is not a single hit model. *Risk Analysis* **20**(4), 513-520.

Thurston-Enriquez J. A., Haas C. N., Jacangelo J. & Gerba C. P. 2003 Chlorine inactivation of adenovirus type 40 and feline calicivirus. *Applied and Environmental Microbiology*, **69**(7), 3979-3985.

Toze S., Bekele E., Page D., Sidhu J. & Shackleton M. 2010 Use of static quantitative microbial risk assessment to determine pathogen risks in an unconfined carbonate aquifer used for managed aquifer recharge. *Water Research*, **44**(4), 1038-1049.

Ward R. L., Bernstein D. I., Young E. C., Sherwood J. R., Knowlton D. R. & Schiff G. M. 1986 Human rotavirus studies in volunteers: determination of infectious dose and serological response to infection. *Journal of Infectious Diseases*, **154**(5), 871-880.

Wuertz S., Miller W., Bambic D., McBride G. 2011 Quantification of Pathogens and Sources of Microbial Indicators for QMRA in Recreational Waters. IWA Publishing, ISBN 9781843395430, p. 200

Yasukawa T., Asada Y., Kunimoto K., Ojkouchi Y. & Itoh S. 2014 An estimation of disability adjusted life years associated with indirect potable reuse based on the occurrence of *Campylobacter Jejuni*. Journal of Japan society of civil engineering, Ser. G (Environmental research), **70**(7), 285-294. (In Japanese)

Chapter 7

Conclusions and recommendations

7.1 Conclusions

The aims of this study are to simulate the virus concentration profile in the Katsura River Basin, where SAT was applied, and to perform the viral risk assessment of the water treated by the processes.

According to the SAT treatment selected in this study, the virus concentration and its reduction during the treatment is significant. The first purposes of this study are to collect the virus concentrations in the SAT influent and to estimate virus reduction through SAT by using batch experiment and a pilot–scale plant. The second purposes of this study are to simulate the infectious virus output profile by the 2-dimensional virus transport model with advection-dispersion-irreversible removal- inactivation, and to evaluate the viral risk in the reclaimed water from all simulated outputs by using the QMRA. Finally, the requirement of additional water treatment was suggested to overcome the multiple barriers and ensure the water is safe for consumption. The findings of the present study have provided valuable information on the virological control in the reclaimed water and its implementation in the actual land.

The major findings in each chapter are described below:

In Chapter 3, virus adsorption and inactivation experiments in batch mode were performed under various conditions (i.e., different temperature and soil type). The major findings are summarized as follows:

a) The removals of AdVF were 0.6 to 3.2 $\log_{10}$ in sand and 1.5 to 3.9 log in weathered granite soil. The removals of RV were 0.2 to 1.5 $\log_{10}$ in sand and 0.8 to 2.4 in the weathered granite soil.
b) Virus adsorption: AdVF has a higher potential to adsorb to the porous media (sand and weathered granite soil) than RV. Weathered granite soil adsorb more AdVF and RV than sand.
c) The temperature between 4-37 ˚C had no significant effect on AdVF and RV adsorption and inactivation on sand and weathered granite soil at $p>0.05$.

d) The inactivation rate of AdVF in sand was 0.064 to 0.080 day^{-1} and the inactivation rate of RV in sand was 0.075 to 0.114 day^{-1}. Moreover, the inactivation rate of AdVF in weathered granite soil was 0.062 to 0.075 day^{-1} and the inactivation rate of RV in weathered granite soil was 0.091to 0.120 day^{-1}.
e) Sand and weathered granite soil may protect the viruses from inactivation.

In Chapter 4, the fate of viruses in a pilot-scale SAT sand column with a retention time of 1-month was studied to estimate the removal capacity of the viruses through the SAT. The important findings are described as follows:

a) Infectious AdVF was more abundant than RV in the A2O effluent. AdVF concentration in the A2O water was $8x10^3$ to $2x10^6$ copies/L (mean $2x10^5$copies/L) and the infectious AdVF was 10 to $4x10^3$ MPNIU/L (mean 8x102 MPNIU/L). For RV in A2O water, the concentration was $2x10^3$ to $6x10^5$ copies/L (mean $1x10^5$ copies/L) and the infectious RV concentration was 22 to 73 MPNIU/L (mean 51 MPNIU/L)
b) AdVF removal through SAT was 0.09 to 2.24 $\log_{10}$ (mean 0.72-$\log_{10}$) and RV removal was 0 to 1.45 $\log_{10}$ (mean 0.15-$\log_{10}$).
c) AdVF reduction (removal and inactivation) in SAT was 1.28 to 2.03 $\log_{10}$ (mean 1.88 $\log_{10}$) and RV reduction in SAT was 0.43 to 0.96 $\log_{10}$ (mean 0.70 $\log_{10}$).
d) DOC and temperature has no significant effect on AdVF and RV removal in SAT at $p>0.05$.

In Chapter 5, the virus transport model was applied in the Katsura River Basin to simulate the virus reduction profile when the SAT was implemented there. All input parameters collected from Chapters 3 and 4 have been used in a 2-dimensional advection dispersion and inactivation equation. The major findings are shown below:

a) The AdVF and the RV irreversible removal coefficients were validated with one-dimensional transport model and the coefficients were well fit with 0.1 day^{-1} and 0.07 day^{-1} for AdVF and RV, respectively.
b) The most suitable case for implementation in the Katsura River Basin is case 1 with 50 m of distance between the injection and abstraction point and 500

m^3/day because the recovery of reclaimed water is appropriated and the HRT is approximately 23 days, which is acceptable to apply in a limited area such as Japan.

c) The best-case of virus reduction is in case 7 with 200 m of distance between the injection and withdrawal point and 500 m^3/day injection flow rate. The reduction efficiencies were 7.12 and 7.23 $\log_{10}$ of the AdVF and the RV, respectively.

In Chapter 6, the viral risk of the reclaimed water was calculated by QMRA. The major findings from this chapter are highlighted below:

a) The AdVF and RV risk in the reclaimed water treated by the SAT system are higher than the acceptable level, with 10^{-4} infection/person/year in all the simulation cases.

b) The expected additional water treatment requirement (97.5 percentile) calculation found that the practical case (Case 1:HRT 23 days): 8.07 $\log_{10}$ of AdVF and 7.20 $\log_{10}$ of RV are required to achieve the acceptable level of 10^{-4} infection/person/year, the worst case (Case 3:HRT 10 days): 8.89 of AdVF and 8.10 $\log_{10}$ of RV are required to achieve the acceptable level. The best case (Case 7:HRT 183 days): 2.47 of AdVF and 1.53 $\log_{10}$ of RV are required to achieve the acceptable level.

c) Chlorination and UV disinfection was selected to be a good combination in the additional treatment after SAT system to inactivate AdVF and RV.

In conclusions, this study indicated that the numerical transport model and viral risk model are very useful tools to make a decision of implementation of SAT system and additional treatment requirement after SAT system. The results showed that SAT with a short retention time is insufficient for the virus reduction and the combination of chlorination and UV disinfection is essential to ensure the reclaimed water safety after SAT system.

7.2 Future research

This research has shed light on the control of the viral risk assessment in the reclaimed water by SAT.

A future research should be structured as follows:

1) To carry on the infectious virus detection, the ICC-qPCR is the one that should be used, instead of the ICC-PCR, because it is more sensitive than the ICC-PCR and it also can reduce the incubation time for infectious virus detection.
2) It is better to use the inactivation coefficient from the pilot column plant. Thus, the higher volume for virus concentration or other higher virus recovery methods are required.
3) The harmonized unit between new infectious virus detection techniques (such as ICC-PCR or ICC-qPCR) and old techniques ($TCID_{50}$ and FFU) should be compared in the same experimental condition to improve the accuracy of the risk calculation.
4) Other enteric viruses such as noroviruses should be studied in the same pattern of this study.

Appendix A

The results of Adenovirus-40 and Rotativus-Wa strains kinetic adsorption on soils

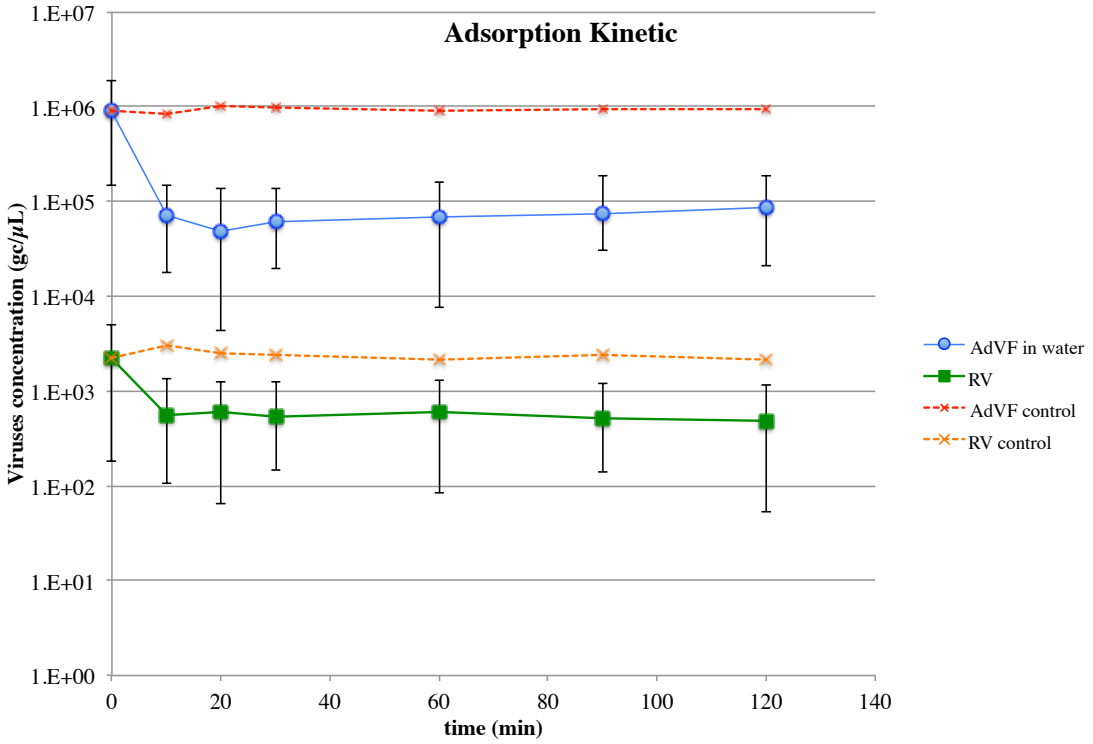

The virus concentrations go to equilibrium with in 10 minutes as shown in the figure above in the both case of AdVF and RV.

Appendix A (II)

The limit of detection of AdVF and RV in SAT effluent

According to the MPN calculation, the lowest value in the MPN table is 3 MPN/100 mL. After harmnonizing the volume of virus inoculation with 720 μL, the calculation will change to 3 MPN/ 720 μL and the concentration of virus volume from 50 L to 2 mL, should be divided by 25000,the recovery rate of the AdVF is 3.58% in average. Thus the calculation becomes 4.76 MPNIU/L of the AdVF.

For the RV, the calculation method is the same but the recovery rate of the RV is 2.5%. Since we started collecting the RV sample in September 2014. The limit of detection of the RV in the SAT effluent is 6.66 MPNIU/L.

Appendix B

The Anova two factor test of virus inactivation experiment was used for statistic analysis. The Two-way ANOVA will test for the main effects of factor A or factor B. The effect of temperature between 4˚C to 37˚C with the virus inactivation was quantified by using the correlation of ANOVA. The results are shown in the table bellow.

AdVF statistic results

The details calculation between the virus concentration in different time and temperature for A2O water with sand

SUMMARY time (days)	*Count*	*Sum*	*Average*	*Variance*
1	4	4	1	0
3	4	4	1	0
7	4	2.891666667	0.722916667	0.01046875
14	4	1.934722222	0.483680556	0.027046521
21	4	0.302638889	0.075659722	0.000292945
28	4	0.386666667	0.096666667	4.44444E-05
35	4	0.355	0.08875	0.000224769
42	4	0.341666667	0.085416667	0.000361806
49	4	0.246083333	0.061520833	0.000811742
Sand 4	9	3.9875	0.443055556	0.184898264
Sand 15	9	3.675083333	0.408342593	0.162840853
Sand 25	9	3.515555556	0.390617284	0.159183001
Sand 37	9	3.280305556	0.364478395	0.173561008

ANOVA analysis of AdVF inactivation in A2O water with sand

ANOVA

Source of Variation	*SS*	*df*	*MS*	*F*	*P-value*	*F crit*
Rows	5.355475991	8	0.669434499	181.7695051	1.45959E-19	2.355081495
Columns	0.029363913	3	0.009787971	2.657697911	0.071207987	3.008786572
Error	0.088389018	24	0.003682876			
Total	5.473228922	35				

ANOVA analysis of AdVF inactivation in A2O water with weathered granite soil

ANOVA

Source of Variation	*SS*	*df*	*MS*	*F*	*P-value*	*F crit*
Rows	4.488004671	8	0.561000584	106.4514883	7.57571E-17	2.355081495
Columns	0.07036792	3	0.010455973	2.450839	0.062707266	3.008786572
Error	0.12648028	24	0.005270012			
Total	4.684852871	35				

ANOVA analysis of AdVF inactivation in only A2O water

ANOVA

Source of Variation	*SS*	*df*	*MS*	*F*	*P-value*	*F crit*
Rows	4.966349947	8	0.620793743	156.9727906	8.16891E-19	2.355081495
Columns	0.031052485	3	0.010350828	2.617291849	0.074202042	3.008786572
Error	0.094914856	24	0.003954786			
Total	5.092317288	35				

The details calculation between the virus concentration in different time and temperature for A2O water with sand would select to describe.
There are two null hypotheses: one for the rows and the other for the columns,
The first rows is
Ho: there is no significant different in yield between the virus concentration and the inactivation time.

Since the p-value for the rows= 1.45E-9 < 0.05 or F = 181.76 > F-crit = 2.35 we reject the null hypothesis, and so at the 95% level of confidence we conclude there is significant different in the yields by the different inactivation time.

The null hypothesis for the column is
Ho: there is no significant difference in yield between the virus concentration and the temperature
Since the p-value for the rows= 0.07 > 0.05 or F = 2.65 < F-crit = 3.01 we accept the null hypothesis, and so at the 95% level of confidence we conclude there is no significant different in the yields by the different temperature of 4-37˚C.
The others cases can be analysed by the same way like AdVF in sand as mentioned above.

RV statistic results

SUMMARY	*Count*	*Sum*	*Average*	*Variance*
1	4	4	1	0
7	4	3.975	0.99375	0.00015625
14	4	1.600555556	0.400138889	0.010217978
21	4	0.391666667	0.097916667	0.000457485
28	4	0.202222222	0.050555556	0.000744907
35	4	0.2035	0.050875	0.002024729
Sand 4	6	2.791944444	0.465324074	0.19347276
Sand 15	6	2.448888889	0.408148148	0.217848076
Sand 25	6	2.619166667	0.436527778	0.210982554
Sand 37	6	2.512944444	0.418824074	0.216865204

ANOVA analysis of RV inactivation in A2O water with sand

ANOVA

Source of Variation	*SS*	*df*	*MS*	*F*	*P-value*	*F crit*
Rows(day)	4.166278967	5	0.833255793	422.7721288	1.3946E-15	2.901294536
Columns(temp)	0.011240045	3	0.003746682	1.900967919	0.172837686	3.287382108
Error	0.029564004	15	0.001970934			
Total	4.207083015	23				

ANOVA analysis of RV inactivation in A2O water with weathered granite soil

ANOVA

Source of Variation	*SS*	*df*	*MS*	*F*	*P-value*	*F crit*
Rows	4.400618673	5	0.880123735	305.2109215	1.56806E-14	2.901294536
Columns	0.009646836	3	0.003215612	1.11511587	0.374059847	3.287382108
Error	0.043254861	15	0.002883657			
Total	4.45352037	23				

ANOVA analysis of RV inactivation in only A2O water

ANOVA

Source of Variation	*SS*	*df*	*MS*	*F*	*P-value*	*F crit*
Rows	3.157807804	4	0.789451951	39.06842201	8.64363E-07	3.259166727
Columns	0.08526653	3	0.028422177	1.406557533	0.288845467	3.490294821
Error	0.242482878	12	0.020206907			
Total	3.485557212	19				

The conclusion of all results is that the temperature between 4˚C to 37˚C has no effect on the virus inactivation at the 95% level of confidence in both cases of AdVF and RV in sand, weathered granite soil and A2O water. However the time is significant for the virus inactivation at a 95% level of confidence in all cases of this study.

Appendix C

1-D model code of AdVF transport in SAT

```
import csv

cin=[]
cout=[]

csvfile = '/Users/thuangsitdenpetkul1/Desktop/AdVF and RV1.csv'
f = open(csvfile, "r")
reader = csv.reader(f)

for line in reader:
    cin.append(float(line[1]))
    cout.append(float(line[2]))

f.close()

# -*- coding: utf-8 -*-
import numpy as np                          #Module for matrix operation
import matplotlib.pyplot as plt             #Modle for plot
import time                                 #Module for time measurement
start = time.time()                         #Time start

#Definition of parameters
d = 2.16*24                                 #Dispersion number
rd = 1.0                                   #Retardation factor
u = 46.0/(150.0*150.0) *60.0*24.0/0.37     #velocity
r =0.3                                     #decay rate constant
L = 217.0                                   #length of the aqifer in meter
T = 565.0                                   #in days
#cin =100000.0                               #input virus conc.

#Definition of mesh (grid)
xn = 40.0
dx =L/(xn-1)
dx2 =dx**2
dt = 0.1

a =dt*d/(rd*dx2)
b = u/rd/2.0/dx*dt
e =dt*r

f =1.0-a*2.0-e
g = a-b
h = a+b

xl = int(xn)
tl = int(T/dt)+1

#initialization
c = np.zeros(xl+1)
ca = np.zeros(xl+1)
c[0] = cin[0]
ca[0] =cin[0]
ctend =[]
ctend.append(0.0)

#main loop
for n in xrange(0, tl-1,1):
        ca[1:xl] = f*c[1:xl] + g*c[2:xl+1]  +h*c[0:xl-1]
        ca[xl] = c[xl-1]
        c[:] =ca[:]
        ctend.append(c[-1])
        c[0]=cin[n+1]

```

```
64
65
66 elapsed_time = time.time() - start
67 print("elapsed_time:{0}".format(elapsed_time))
68
69 dspan = np.linspace(0.0, T, num=tl)
70
71 plt.plot(dspan,ctend)
72 #plt.plot(dspan,cin)
73 plt.plot(dspan,cout)
74 plt.show()
75
76
77 print"Peclet", u*dx/d
78 print"Courant", dt*u/dx/rd
79 print"Neumann", d*dt/dx2/rd
```

2-D model code of virus transport in Katsura River Basin

```
Clear["Global`*"]
start = SessionTime[]
<< JLink`;
InstallJava[];
ReinstallJava[CommandLine → "java", JVMArguments → "-Xmx512m"]
Import["/Users/YUMETO/Desktop/scenario50/scenario50500.xlsx"];
velocity = %[[1]];

(*u is the velocity in i vector in diffierent direction in the area*)
Table[u[Round[velocity[[i]][[1]]], Round[velocity[[i]][[2]]]] = velocity[[i]][[4]] * 60 * 60 * 24, {i, 1, 40748}];

(*v is the velocity in j vector in diffierent direction in the area*)
Table[v[Round[velocity[[i]][[1]]], Round[velocity[[i]][[2]]]] = velocity[[i]][[5]] * 60 * 60 * 24, {i, 1, 40748}];

(*adsolute velocity calculation*)
ul[z, j] = Sqrt[u[z, j]^2 + v[z, j]^2]

(*define parameter*)
s = 14 / 10 (*specific gravity of sand*)
fe = 35 / 100 (*sand porosity*)|
kd = (*2/10*)0
rd = 1 + (1 - fe) * s * kd / fe
λ = (*11*10^(-5)*60*24*)0.17 (*overall redcution rates (μ+kirr)*)

(*the  defined area related to the MODFLOW*)
zori = 254
jori = 130
zter = 155
jter = 229

(*MODFLOW grid width*)
Δx = 5
Δy = 5

(*length and width of the target area in meter*)
lx = (jter - jori + 1) * Δx
ly = (zori - zter + 1) * Δy

(*grid number*)
nx = lx / Δx
ny = ly / Δy
nt = lt / Δt

(*define the withdrawal point*)
mx = (151 - jori) * Δx
my = (zori - 195) * Δy

xl = Sqrt[(x - mx)^2 + (y - my)^2]
(*al=0.0169*xl^1.53*)
(*al=0.32*xl^0.83*)
al = 0.0175 * xl^1.46
ath = 0.01 * xl

dx = (al * u[z, j]^2 + ath * v[z, j]^2) / ul[z, j]
dy = (al * v[z, j]^2 + ath * u[z, j]^2) / ul[z, j]
dxy = ((al - ath) * u[z, j] * v[z, j]) / ul[z, j]
```

```
(*nested grid method with the different grid width*)
b = {5, 5 / 2, 1 / 2, 1 / 10}
pos = b / 2
b[[0]] = 5
pos[[0]] = b[[0]] / 2

q = jori - 1

(*Peclet Number criteria*)
x = -Δx + pos[[1]]
Catch[Do[x = x + Δx; q = q + 1 / (5 / Δx); j = Floor[q]; k = zori + 1; y = -Δy + pos[[1]]; Do[k = k - 1 / (5 / Δy); z = Ceiling[k](*切り上げ*); y = y + Δy;
    Do[
     Δx = b[[i]];
     Δy = b[[i]];
     If[Abs[u[z, j] * Δx / dx] > 1, Continue[]](**);
     If[Abs[v[z, j] * Δy / dy] > 1, Continue[]];
     mesh[z, j] = b[[i]];
     Δx = 5;
     Δy = 5;
     Break[], {i, 1, Length[b]}]
    , {i, ny + 1}], {i, nx + 1}]]

ArrayPlot[Table[mesh[z, j], {z, zter, zori, 1}, {j, jori, jter}], ColorFunction → "Rainbow"]

(*Location of the round-up work*)
siguma = 0
Clear[cmesh]
Do[Clear[me];
 m = 0;
 Do[Do[If[mesh[z, j] == b[[i]], m = m + 1; me[m] = {mesh[z, j], z, j}], {z, zori, zter, -1}], {j, jori, jter}];
 Print[m];
 sigumaf[i] = (m * (5 / b[[i]]))^2;
 siguma = siguma + sigumaf[i];
 zmax[i] = Max[Table[me[i][[2]], {i, 1, m}]];
 zmin[i] = Min[Table[me[i][[2]], {i, 1, m}]];
 jmax[i] = Max[Table[me[i][[3]], {i, 1, m}]];
 jmin[i] = Min[Table[me[i][[3]], {i, 1, m}]];
 Table[cmesh[z, j] = b[[i]], {z, zmax[i], zmin[i], -1}, {j, jmin[i], jmax[i]}], {i, 1, Length[b]}]
siguma

ArrayPlot[Table[cmesh[z, j], {z, zter, zori, 1}, {j, jori, jter}], ColorFunction → "Rainbow"]

totaldivide[0] = 0
Do[Clear[me];
 m = 0;
 Δx = b[[i]];
 Δy = b[[i]];
 x = -Δx + pos[[1]];
 Do[x = x + 5; y = -Δy + pos[[1]];
  Do[y = y + 5;
   Do[Δt = 1 / (2 * 10^(n - 1));
    If[cmesh[z, j] == Δx, If[dx * Δt / Δx^2 + dy * Δt / Δy^2 ≤ 0.5, , Continue[]](*Neuman boundary*);
     If[Abs[u[z, j] * Δt / Δx] ≤ 1, , Continue[]](*Courant Number criteria*);
     If[Abs[v[z, j] * Δt / Δy] ≤ 1, m = m + 1(*クーラン基準*); me[m] = {cmesh[z, j], z, j, Δt}; Break[], Continue[]], Break[]], {n, 1, 10}],
   {z, zori, zter, -1}], {j, jori, jter}];
 time[i] = Min[Table[me[i][[4]], {i, 1, m}]]; Print[time[i]];
 divide[i] = sigumaf[i] / time[i] * lt;
 totaldivide[i] = totaldivide[i - 1] + divide[i];
 Table[tmesh[me[in][[2]], me[in][[3]]] = time[i], {in, 1, m}], {i, 1, Length[b]}]
totaldivide[Length[b]]

ArrayPlot[Table[tmesh[z, j], {z, zter, zori, 1}, {j, jori, jter}], ColorFunction → "Rainbow"]
```

```
Clear[me, m]
Do[Δx = b[[i]];
 Δy = b[[i]];
 Do[Do[z = Ceiling[k]; j = Floor[q];
    If[cmesh[z, j] == b[[i]], c[(q - jori) * 5 + pos[[i]], (zori - k) * 5 + pos[[i]], 0] = 0;
     x = (q - jori) * 5 + pos[[i]];
     y = (zori - k) * 5 + pos[[i]];
     zone[i, x, y] = {, , x, y, dx, dy, u[z, j], v[z, j], c[(q - jori) * 5 + pos[[i]], (zori - k) * 5 + pos[[i]], 0], Δx, Δy, dxy}],
    {k, zmax[i], zmin[i] - 1 + b[[i]] / 5, -b[[i]] / 5}], {q, jmin[i], jmax[i] + 1 - b[[i]] / 5, b[[i]] / 5}], {i, 1, Length[b] - 1}]

(*divided into specific sheets*)
mc = (*initial concentration for AdVF injection*)828
sheetC =
  DeleteCases[Table[zone[i, x, y][[10]], {i, 1, Length[b] - 1},
    {y, (zori - zmax[i]) * 5 + pos[[i]], (zori - (zmin[i] - 1 + b[[i]] / 5)) * 5 + pos[[i]], b[[i]]},
    {x, (jmin[i] - jori) * 5 + pos[[i]], (jmax[i] + 1 - b[[i]] / 5 - jori) * 5 + pos[[i]], b[[i]]}], _Part, -1];
sheetU =
  DeleteCases[Table[zone[i, x, y][[8]], {i, 1, Length[b] - 1},
    {y, (zori - zmax[i]) * 5 + pos[[i]], (zori - (zmin[i] - 1 + b[[i]] / 5)) * 5 + pos[[i]], b[[i]]},
    {x, (jmin[i] - jori) * 5 + pos[[i]], (jmax[i] + 1 - b[[i]] / 5 - jori) * 5 + pos[[i]], b[[i]]}], _Part, -1];
sheetV =
  DeleteCases[Table[zone[i, x, y][[9]], {i, 1, Length[b] - 1},
    {y, (zori - zmax[i]) * 5 + pos[[i]], (zori - (zmin[i] - 1 + b[[i]] / 5)) * 5 + pos[[i]], b[[i]]},
    {x, (jmin[i] - jori) * 5 + pos[[i]], (jmax[i] + 1 - b[[i]] / 5 - jori) * 5 + pos[[i]], b[[i]]}], _Part, -1];
sheetDX =
  DeleteCases[Table[zone[i, x, y][[6]], {i, 1, Length[b] - 1},
    {y, (zori - zmax[i]) * 5 + pos[[i]], (zori - (zmin[i] - 1 + b[[i]] / 5)) * 5 + pos[[i]], b[[i]]},
    {x, (jmin[i] - jori) * 5 + pos[[i]], (jmax[i] + 1 - b[[i]] / 5 - jori) * 5 + pos[[i]], b[[i]]}], _Part, -1];
sheetDY =
  DeleteCases[Table[zone[i, x, y][[7]], {i, 1, Length[b] - 1},
    {y, (zori - zmax[i]) * 5 + pos[[i]], (zori - (zmin[i] - 1 + b[[i]] / 5)) * 5 + pos[[i]], b[[i]]},
    {x, (jmin[i] - jori) * 5 + pos[[i]], (jmax[i] + 1 - b[[i]] / 5 - jori) * 5 + pos[[i]], b[[i]]}], _Part, -1];
sheetX =
  DeleteCases[Table[zone[i, x, y][[4]], {i, 1, Length[b] - 1},
    {y, (zori - zmax[i]) * 5 + pos[[i]], (zori - (zmin[i] - 1 + b[[i]] / 5)) * 5 + pos[[i]], b[[i]]},
    {x, (jmin[i] - jori) * 5 + pos[[i]], (jmax[i] + 1 - b[[i]] / 5 - jori) * 5 + pos[[i]], b[[i]]}], _Part, -1];
sheetY =
  DeleteCases[Table[zone[i, x, y][[5]], {i, 1, Length[b] - 1},
    {y, (zori - zmax[i]) * 5 + pos[[i]], (zori - (zmin[i] - 1 + b[[i]] / 5)) * 5 + pos[[i]], b[[i]]},
    {x, (jmin[i] - jori) * 5 + pos[[i]], (jmax[i] + 1 - b[[i]] / 5 - jori) * 5 + pos[[i]], b[[i]]}], _Part, -1];
sheetΔX =
  DeleteCases[Table[zone[i, x, y][[11]], {i, 1, Length[b] - 1},
    {y, (zori - zmax[i]) * 5 + pos[[i]], (zori - (zmin[i] - 1 + b[[i]] / 5)) * 5 + pos[[i]], b[[i]]},
    {x, (jmin[i] - jori) * 5 + pos[[i]], (jmax[i] + 1 - b[[i]] / 5 - jori) * 5 + pos[[i]], b[[i]]}], _Part, -1];
sheetΔY =
  DeleteCases[Table[zone[i, x, y][[12]], {i, 1, Length[b] - 1},
    {y, (zori - zmax[i]) * 5 + pos[[i]], (zori - (zmin[i] - 1 + b[[i]] / 5)) * 5 + pos[[i]], b[[i]]},
    {x, (jmin[i] - jori) * 5 + pos[[i]], (jmax[i] + 1 - b[[i]] / 5 - jori) * 5 + pos[[i]], b[[i]]}], _Part, -1];
sheetDXY =
  DeleteCases[Table[zone[i, x, y][[13]], {i, 1, Length[b] - 1},
    {y, (zori - zmax[i]) * 5 + pos[[i]], (zori - (zmin[i] - 1 + b[[i]] / 5)) * 5 + pos[[i]], b[[i]]},
    {x, (jmin[i] - jori) * 5 + pos[[i]], (jmax[i] + 1 - b[[i]] / 5 - jori) * 5 + pos[[i]], b[[i]]}], _Part, -1];

Time = SessionTime[] - start

(*Boundary*)
CXP = 0;
CXM = 0;
CYP = Table[0, {x, lx / b[[1]]}];
CYM = Table[0, {x, lx / b[[1]]}];
```

```
(*Boundary Position*)
(*Outside boundary*)
Table[pold1[i, ni] = Intersection[Position[sheetX[[i - 1]], ((jmax[i] + 1) - jori) * 5 + pos[[i - 1]]],
    Position[sheetY[[i - 1]], (zori - zmax[i]) * 5 + Floor[ni * (b[[i]] / b[[i - 1]])] * b[[i - 1]] + pos[[i - 1]]]], {i, 2, Length[b] - 1},
  {ni, 0, (zmax[i] - (zmin[i] - 1 + b[[i]] / 5)) / (b[[i]] / 5)}];
Table[pnew1[i, ni] = Intersection[Position[sheetX, (jmax[i] + 1 - b[[i]] / 5 - jori) * 5 + pos[[i]]],
    Position[sheetY, (zori - zmax[i]) * 5 + ni * b[[i]] + pos[[i]]]], {i, 2, Length[b] - 1}, {ni, 0, (zmax[i] - (zmin[i] - 1 + b[[i]] / 5)) / (b[[i]] / 5)}];
(*inner leftside boundary*)
Table[pold2[i, ni, w] = Intersection[Position[sheetX[[i + 1]], (jmin[i + 1] - jori) * 5 + pos[[i + 1]]],
    Position[sheetY[[i + 1]], (zori - zmax[i + 1]) * 5 + w * b[[i + 1]] + ni * b[[i]] + pos[[i + 1]]]], {i, 1, Length[b] - 2},
  {ni, 0, (zmax[i + 1] - (zmin[i + 1] - 1 + b[[i]] / 5)) / (b[[i]] / 5)}, {w, 0, b[[i]] / b[[i + 1]] - 1}];
Table[pnew2[i, ni] = Intersection[Position[sheetX, (jmin[i + 1] - jori) * 5 - pos[[i]]],
    Position[sheetY, (zori - zmax[i + 1]) * 5 + ni * b[[i]] + pos[[i]]]], {i, 1, Length[b] - 2},
  {ni, 0, (zmax[i + 1] - (zmin[i + 1] - 1 + b[[i]] / 5)) / (b[[i]] / 5)}];
Table[pnew2l[ni] = Intersection[Position[sheetX, (jmin[Length[b] - 1 + 1] - jori) * 5 - pos[[Length[b] - 1]]],
    Position[sheetY, (zori - zmax[Length[b] - 1 + 1]) * 5 + ni * b[[Length[b] - 1]] + pos[[Length[b] - 1]]]],
  {ni, 0, (zmax[Length[b] - 1 + 1] - (zmin[Length[b] - 1 + 1] - 1 + b[[Length[b] - 1]] / 5)) / (b[[Length[b] - 1]] / 5)}];
(*Outside at the left side boundary*)
Table[pold3[i, ni] = Intersection[Position[sheetX[[i - 1]], ((jmin[i] - b[[i - 1]] / 5) - jori) * 5 + pos[[i - 1]]],
    Position[sheetY[[i - 1]], (zori - zmax[i]) * 5 + Floor[ni * (b[[i]] / b[[i - 1]])] * b[[i - 1]] + pos[[i - 1]]]], {i, 2, Length[b] - 1},
  {ni, 0, (zmax[i] - (zmin[i] - 1 + b[[i]] / 5)) / (b[[i]] / 5)}];
Table[pnew3[i, ni] = Intersection[Position[sheetX, (jmin[i] - jori) * 5 + pos[[i]]], Position[sheetY, (zori - zmax[i]) * 5 + ni * b[[i]] + pos[[i]]]],
  {i, 2, Length[b] - 1}, {ni, 0, (zmax[i] - (zmin[i] - 1 + b[[i]] / 5)) / (b[[i]] / 5)}];
 (*Inner right side boundary*)
Table[pold4[i, ni, w] = Intersection[Position[sheetX[[i + 1]], ((jmax[i + 1] + 1 - b[[i + 1]] / 5) - jori) * 5 + pos[[i + 1]]],
    Position[sheetY[[i + 1]], (zori - zmax[i + 1]) * 5 + w * b[[i + 1]] + ni * b[[i]] + pos[[i + 1]]]], {i, 1, Length[b] - 2},
  {ni, 0, (zmax[i + 1] - (zmin[i + 1] - 1 + b[[i]] / 5)) / (b[[i]] / 5)}, {w, 0, b[[i]] / b[[i + 1]] - 1}];
Table[pnew4[i, ni] = Intersection[Position[sheetX, ((jmax[i + 1] + 1) - jori) * 5 + pos[[i]]],
    Position[sheetY, (zori - zmax[i + 1]) * 5 + ni * b[[i]] + pos[[i]]]], {i, 1, Length[b] - 2},
  {ni, 0, (zmax[i + 1] - (zmin[i + 1] - 1 + b[[i]] / 5)) / (b[[i]] / 5)}];
Table[pnew4l[ni] = Intersection[Position[sheetX, (jmax[Length[b]] + 1 - jori) * 5 + pos[[Length[b] - 1]]],
    Position[sheetY, (zori - zmax[Length[b]]) * 5 + ni * b[[Length[b] - 1]] + pos[[Length[b] - 1]]]],
  {ni, 0, (zmax[Length[b] - 1 + 1] - (zmin[Length[b] - 1 + 1] - 1 + b[[Length[b] - 1]] / 5)) / (b[[Length[b] - 1]] / 5)}];
(*Outside top side boundary*)
i = 1;
ypc1 = Intersection[Position[sheetX[[i]], (jmin[i + 1] - jori) * 5 + pos[[i]]], Position[sheetY[[i]], (zori - (zmin[i + 1] - 1)) * 5 + pos[[i]]]][[
    1]][[1]];
from1 = Intersection[Position[sheetX[[i]], (jmin[i + 1] - jori) * 5 + pos[[i]]], Position[sheetY[[i]], (zori - (zmin[i + 1] - 1)) * 5 + pos[[i]]]][[
    1]][[2]];
to1 =
  Intersection[Position[sheetX[[i]], (jmax[i + 1] + 1 - b[[i]] / 5 - jori) * 5 + pos[[i]]],
    Position[sheetY[[i]], (zori - (zmin[i + 1] - 1)) * 5 + pos[[i]]]][[1]][[2]];
Table[pold5[i, ni] = Intersection[Position[sheetX[[i - 1]], (jmin[i] - jori) * 5 + Floor[ni * (b[[i]] / b[[i - 1]])] * b[[i - 1]] + pos[[i - 1]]],
    Position[sheetY[[i - 1]], (zori - (zmin[i] - 1)) * 5 + pos[[i - 1]]]], {i, 2, Length[b] - 1},
  {ni, 0, ((jmax[i] + 1 - b[[i]] / 5) - jmin[i]) / (b[[i]] / 5)}];
Table[
  ypc2[i] =
   Intersection[Position[sheetX[[i]], (jmin[i + 1] - jori) * 5 + pos[[i]]], Position[sheetY[[i]], (zori - (zmin[i + 1] - 1)) * 5 + pos[[i]]]][[1]][[
    1]], {i, 2, Length[b] - 1}];
Table[
  from2[i] =
   Intersection[Position[sheetX[[i]], (jmin[i + 1] - jori) * 5 + pos[[i]]], Position[sheetY[[i]], (zori - (zmin[i + 1] - 1)) * 5 + pos[[i]]]][[1]][[
    2]], {i, 2, Length[b] - 1}];
Table[
  to2[i] =
   Intersection[Position[sheetX[[i]], (jmax[i + 1] + 1 - b[[i]] / 5 - jori) * 5 + pos[[i]]],
     Position[sheetY[[i]], (zori - (zmin[i + 1] - 1)) * 5 + pos[[i]]]][[1]][[2]], {i, 2, Length[b] - 1}];


(*inside down side boundary*)
Table[pold6[i, ni, w] = Intersection[Position[sheetX[[i + 1]], (jmin[i + 1] + w * b[[i + 1]] / 5 - jori) * 5 + ni * b[[i]] + pos[[i + 1]]],
    Position[sheetY[[i + 1]], (zori - zmax[i + 1]) * 5 + pos[[i + 1]]]], {i, 1, Length[b] - 2},
  {ni, 0, ((jmax[i + 1] + 1 - b[[i]] / 5) - jmin[i + 1]) / (b[[i]] / 5)}, {w, 0, b[[i]] / b[[i + 1]] - 1}];
Table[ypo3[i] = Position[sheetY[[i]], (zori - zmax[i + 1]) * 5 - pos[[i]]], {i, 1, Length[b] - 2}];
Table[from3[i] = Position[sheetX[[i]], (jmin[i + 1] - jori) * 5 + pos[[i]]][[1]][[2]], {i, 1, Length[b] - 2}];
bcon = Table[mc, {ni, 0, ((jmax[Length[b] - 1 + 1] + 1 - b[[Length[b] - 1]] / 5) - jmin[Length[b] - 1 + 1]) / (b[[Length[b] - 1]] / 5)}];
ypo3l = Position[sheetY[[Length[b] - 1]], (zori - zmax[Length[b] - 1 + 1]) * 5 - pos[[Length[b] - 1]]];
from3l = Position[sheetX[[Length[b] - 1]], (jmin[Length[b] - 1 + 1] - jori) * 5 + pos[[Length[b] - 1]]][[1]][[2]];
(*outside down side boundary*)
i = 1;
ypc4 = Intersection[Position[sheetX[[i]], (jmin[i + 1] - jori) * 5 + pos[[i]]], Position[sheetY[[i]], (zori - zmax[i + 1]) * 5 - pos[[i]]]][[1]][[
   1]];
from4 = Intersection[Position[sheetX[[i]], (jmin[i + 1] - jori) * 5 + pos[[i]]], Position[sheetY[[i]], (zori - zmax[i + 1]) * 5 - pos[[i]]]][[1]][[
   2]];
to4 =
  Intersection[Position[sheetX[[i]], (jmax[i + 1] + 1 - b[[i]] / 5 - jori) * 5 + pos[[i]]], Position[sheetY[[i]], (zori - zmax[i + 1]) * 5 - pos[[i]]]][[
    1]][[2]];
Table[pold7[i, ni] = Intersection[Position[sheetX[[i - 1]], (jmin[i] - jori) * 5 + Floor[ni * (b[[i]] / b[[i - 1]])] * b[[i - 1]] + pos[[i - 1]]],
    Position[sheetY[[i - 1]], (zori - zmax[i]) * 5 - pos[[i - 1]]]], {i, 2, Length[b] - 1}, {ni, 0, ((jmax[i] + 1 - b[[i]] / 5) - jmin[i]) / (b[[i]] / 5)}];
Table[
  ypc5[i] = Intersection[Position[sheetX[[i]], (jmin[i + 1] - jori) * 5 + pos[[i]]], Position[sheetY[[i]], (zori - zmax[i + 1]) * 5 - pos[[i]]]][[
    1]][[1]], {i, 2, Length[b] - 1}];
Table[
  from5[i] = Intersection[Position[sheetX[[i]], (jmin[i + 1] - jori) * 5 + pos[[i]]], Position[sheetY[[i]], (zori - zmax[i + 1]) * 5 - pos[[i]]]][[
    1]][[2]], {i, 2, Length[b] - 1}];
Table[
  to5[i] =
   Intersection[Position[sheetX[[i]], (jmax[i + 1] + 1 - b[[i]] / 5 - jori) * 5 + pos[[i]]],
     Position[sheetY[[i]], (zori - zmax[i + 1]) * 5 - pos[[i]]]][[1]][[2]], {i, 2, Length[b] - 1}];
(*inside top side boundary*)
Table[pold8[i, ni, w] = Intersection[Position[sheetX[[i + 1]], (jmin[i + 1] + w * b[[i + 1]] / 5 - jori) * 5 + ni * b[[i]] + pos[[i + 1]]],
    Position[sheetY[[i + 1]], (zori - (zmin[i + 1] - 1 + b[[i + 1]] / 5)) * 5 + pos[[i + 1]]]], {i, 1, Length[b] - 2},
  {ni, 0, ((jmax[i + 1] + 1 - b[[i]] / 5) - jmin[i + 1]) / (b[[i]] / 5)}, {w, 0, b[[i]] / b[[i + 1]] - 1}];
Table[ypo6[i] = Position[sheetY[[i]], (zori - (zmin[i + 1] - 1)) * 5 + pos[[i]]], {i, 1, Length[b] - 2}];
Table[from6[i] = Position[sheetX[[i]], (jmin[i + 1] - jori) * 5 + pos[[i]]][[1]][[2]], {i, 1, Length[b] - 2}];
ypo6l = Position[sheetY[[Length[b] - 1]], (zori - (zmin[Length[b] - 1 + 1] - 1)) * 5 + pos[[Length[b] - 1]]];
from6l = Position[sheetX[[Length[b] - 1]], (jmin[Length[b] - 1 + 1] - jori) * 5 + pos[[Length[b] - 1]]][[1]][[2]];

t = 0;
Δt = 1 / 200
lt = Δt * 200 * 50
(*re[0]={t,0};*)

Time = SessionTime[] - start
re[t] = {t, sheetC[[2]][[7]][[27]]}
```

```
Do[
 Do[
  t = t + Δt;

  sheetCXP = Table[Map[Append[#, CXP] &, sheetC[[i]]], {i, 1, Length[b] - 1}];
  sheetCXP = Table[Map[Rest[#] &, sheetCXP[[i]]], {i, 1, Length[b] - 1}];
  Do[
   Do[
    bc = Extract[sheetC[[i - 1]], pold1[i, ni]];
    sheetCXP = ReplacePart[sheetCXP, pnew1[i, ni] → bc[[1]]]
    , {ni, 0, (zmax[i] - (zmin[i] - 1 + b[[i]] / 5)) / (b[[i]] / 5)}], {i, 2, Length[b] - 1}];

  Do[
   Do[
    bc = Mean[Table[Extract[sheetC[[i + 1]], pold2[i, ni, w]][[1]], {w, 0, b[[i]] / b[[i + 1]] - 1}]];
    sheetCXP = ReplacePart[sheetCXP, pnew2[i, ni] → bc], {ni, 0, (zmax[i + 1] - (zmin[i + 1] - 1 + b[[i]] / 5)) / (b[[i]] / 5)}]
   , {i, 1, Length[b] - 2}];
  Do[
   sheetCXP = ReplacePart[sheetCXP, pnew21[ni] → mc],
   {ni, 0, (zmax[Length[b] - 1 + 1] - (zmin[Length[b] - 1 + 1] - 1 + b[[Length[b] - 1]] / 5)) / (b[[Length[b] - 1]] / 5)}];


  sheetCXM = Table[Map[Prepend[#, CXM] &, sheetC[[i]]], {i, 1, Length[b] - 1}];
  sheetCXM = Table[Map[Most[#] &, sheetCXM[[i]]], {i, 1, Length[b] - 1}];
  Do[
   Do[
    bc = Extract[sheetC[[i - 1]], pold3[i, ni]];
    sheetCXM = ReplacePart[sheetCXM, pnew3[i, ni] → bc[[1]]]
    , {ni, 0, (zmax[i] - (zmin[i] - 1 + b[[i]] / 5)) / (b[[i]] / 5)}], {i, 2, Length[b] - 1}];

  Do[
   Do[
     bc = Mean[Table[Extract[sheetC[[i + 1]], pold4[i, ni, w]][[1]], {w, 0, b[[i]] / b[[i + 1]] - 1}]];
     sheetCXM = ReplacePart[sheetCXM, pnew4[i, ni] → bc], {ni, 0, (zmax[i + 1] - (zmin[i + 1] - 1 + b[[i]] / 5)) / (b[[i]] / 5)}];
   , {i, 1, Length[b] - 2}];
  Do[
   sheetCXM = ReplacePart[sheetCXM, pnew41[ni] → mc],
   {ni, 0, (zmax[Length[b] - 1 + 1] - (zmin[Length[b] - 1 + 1] - 1 + b[[Length[b] - 1]] / 5)) / (b[[Length[b] - 1]] / 5)}];


sheetCYP = Insert[sheetC, CYP, {1, -1}];
  sheetCYP = Table[Rest[sheetCYP[[i]]], {i, 1, Length[b] - 1}];
  i = 1;
  bc = Drop[sheetCYP[[i]][[ypc1 - 1]], {from1, to1}];
  sheetCYP = ReplacePart[sheetCYP, {i, ypc1 - 1} → bc];
  Do[
   bc = Table[Extract[sheetC[[i - 1]], pold5[i, ni]][[1]], {ni, 0, ((jmax[i] + 1 - b[[i]] / 5) - jmin[i]) / (b[[i]] / 5)}];
   sheetCYP = Insert[sheetCYP, bc, {i, -1}];
   bc = Drop[sheetCYP[[i]][[ypc2[i] - 1]], {from2[i], to2[i]}];
   sheetCYP = ReplacePart[sheetCYP, {i, ypc2[i] - 1} → bc]
   , {i, 2, Length[b] - 1}];

  Do[
   bc = Table[Mean[Table[Extract[sheetC[[i + 1]], pold6[i, ni, w]][[1]], {w, 0, b[[i]] / b[[i + 1]] - 1}]],
     {ni, 0, ((jmax[i + 1] + 1 - b[[i]] / 5) - jmin[i + 1]) / (b[[i]] / 5)}];
   sheetCYP = Insert[sheetCYP, bc, {i, ypo3[i][[1]][[1]], from3[i]}];
   sheetCYP = FlattenAt[sheetCYP, {i, ypo3[i][[1]][[1]], from3[i]}], {i, 1, Length[b] - 2}];
  sheetCYP = Insert[sheetCYP, bcon, {Length[b] - 1, ypo31[[1]][[1]], from31}];
  sheetCYP = FlattenAt[sheetCYP, {Length[b] - 1, ypo31[[1]][[1]], from31}];
```

```
sheetCYM = Insert[sheetC, CYM, {1, 1}];
sheetCYM = Table[Most[sheetCYM[[i]]], {i, 1, Length[b] - 1}];
i = 1;
bc = Drop[sheetCYM[[i]][[ypc4 + 1]], {from4, to4}];
sheetCYM = ReplacePart[sheetCYM, {i, ypc4 + 1} → bc];
Do[
 bc = Table[Extract[sheetC[[i - 1]], pold7[i, ni]][[1]], {ni, 0, ((jmax[i] + 1 - b[[i]] / 5) - jmin[i]) / (b[[i]] / 5)}];
 sheetCYM = Insert[sheetCYM, bc, {i, 1}];
 bc = Drop[sheetCYM[[i]][[ypc5[i] + 1]], {from5[i], to5[i]}];
 sheetCYM = ReplacePart[sheetCYM, {i, ypc5[i] + 1} → bc]
 , {i, 2, Length[b] - 1}];

Do[
 bc = Table[Mean[Table[Extract[sheetC[[i + 1]], pold8[i, ni, w]][[1]], {w, 0, b[[i]] / b[[i + 1]] - 1}]],
   {ni, 0, ((jmax[i + 1] + 1 - b[[i]] / 5) - jmin[i + 1]) / (b[[i]] / 5)}];
 sheetCYM = Insert[sheetCYM, bc, {i, ypo6[i][[1]][[1]], from6[i]}];
 sheetCYM = FlattenAt[sheetCYM, {i, ypo6[i][[1]][[1]], from6[i]}], {i, 1, Length[b] - 2}];
sheetCYM = Insert[sheetCYM, bcon, {Length[b] - 1, ypo61[[1]][[1]], from61}];
sheetCYM = FlattenAt[sheetCYM, {Length[b] - 1, ypo61[[1]][[1]], from61}];
(*cxpyp*)
sheetCXPYP = Table[Map[Append[#, CXP] &, sheetCYP[[i]]], {i, 1, Length[b] - 1}];
sheetCXPYP = Table[Map[Rest[#] &, sheetCXPYP[[i]]], {i, 1, Length[b] - 1}];
Do[
 Do[
  bc = Extract[sheetCYP[[i - 1]], pold1[i, ni]];
  sheetCXPYP = ReplacePart[sheetCXPYP, pnew1[i, ni] → bc[[1]]]
  , {ni, 0, (zmax[i] - (zmin[i] - 1 + b[[i]] / 5)) / (b[[i]] / 5)}], {i, 2, Length[b] - 1}];

Do[
 Do[
  bc = Mean[Table[Extract[sheetCYP[[i + 1]], pold2[i, ni, w]][[1]], {w, 0, b[[i]] / b[[i + 1]] - 1}]];
  sheetCXPYP = ReplacePart[sheetCXPYP, pnew2[i, ni] → bc], {ni, 0, (zmax[i + 1] - (zmin[i + 1] - 1 + b[[i]] / 5)) / (b[[i]] / 5)}]
 , {i, 1, Length[b] - 2}];
Do[
 sheetCXPYP = ReplacePart[sheetCXPYP, pnew21[ni] → mc],
 {ni, 0, (zmax[Length[b] - 1 + 1] - (zmin[Length[b] - 1 + 1] - 1 + b[[Length[b] - 1]] / 5)) / (b[[Length[b] - 1]] / 5) - 1}];
bc1 = Extract[sheetC[[Length[b] - 1]], {ypc2[Length[b] - 1], from2[Length[b] - 1]}];
sheetCXPYP =
 ReplacePart[sheetCXPYP, pnew21[(zmax[Length[b] - 1 + 1] - (zmin[Length[b] - 1 + 1] - 1 + b[[Length[b] - 1]] / 5)) / (b[[Length[b] - 1]] / 5)] → bc1];

(*cxmyp*)
sheetCXMYP = Table[Map[Prepend[#, CXM] &, sheetCYP[[i]]], {i, 1, Length[b] - 1}];
sheetCXMYP = Table[Map[Most[#] &, sheetCXMYP[[i]]], {i, 1, Length[b] - 1}];
Do[
 Do[
  bc = Extract[sheetCYP[[i - 1]], pold3[i, ni]];
  sheetCXMYP = ReplacePart[sheetCXMYP, pnew3[i, ni] → bc[[1]]]
  , {ni, 0, (zmax[i] - (zmin[i] - 1 + b[[i]] / 5)) / (b[[i]] / 5)}], {i, 2, Length[b] - 1}];

Do[
 Do[
   bc = Mean[Table[Extract[sheetCYP[[i + 1]], pold4[i, ni, w]][[1]], {w, 0, b[[i]] / b[[i + 1]] - 1}]];
   sheetCXMYP = ReplacePart[sheetCXMYP, pnew4[i, ni] → bc], {ni, 0, (zmax[i + 1] - (zmin[i + 1] - 1 + b[[i]] / 5)) / (b[[i]] / 5)}];
 , {i, 1, Length[b] - 2}];
Do[
 sheetCXMYP = ReplacePart[sheetCXMYP, pnew41[ni] → mc],
 {ni, 0, (zmax[Length[b] - 1 + 1] - (zmin[Length[b] - 1 + 1] - 1 + b[[Length[b] - 1]] / 5)) / (b[[Length[b] - 1]] / 5) - 1}];
bc2 = Extract[sheetC[[Length[b] - 1]], {ypc2[Length[b] - 1], to2[Length[b] - 1]}];
sheetCXPYP =
 ReplacePart[sheetCXPYP, pnew41[(zmax[Length[b] - 1 + 1] - (zmin[Length[b] - 1 + 1] - 1 + b[[Length[b] - 1]] / 5)) / (b[[Length[b] - 1]] / 5)] → bc2];
```

```
(*cxpym*)
sheetCXPYM = Table[Map[Append[#, CXP] &, sheetCYM[[i]]], {i, 1, Length[b] - 1}];
sheetCXPYM = Table[Map[Rest[#] &, sheetCXPYM[[i]]], {i, 1, Length[b] - 1}];
Do[
 Do[
  bc = Extract[sheetCYM[[i - 1]], pold1[i, ni]];
  sheetCXPYM = ReplacePart[sheetCXPYM, pnew1[i, ni] → bc[[1]]]
  , {ni, 0, (zmax[i] - (zmin[i] - 1 + b[[i]] / 5)) / (b[[i]] / 5)}], {i, 2, Length[b] - 1}];

Do[
 Do[
  bc = Mean[Table[Extract[sheetCYM[[i + 1]], pold2[i, ni, w]][[1]], {w, 0, b[[i]] / b[[i + 1]] - 1}]];
  sheetCXPYM = ReplacePart[sheetCXPYM, pnew2[i, ni] → bc], {ni, 0, (zmax[i + 1] - (zmin[i + 1] - 1 + b[[i]] / 5)) / (b[[i]] / 5)}]
 , {i, 1, Length[b] - 2}];
Do[
 sheetCXPYM = ReplacePart[sheetCXPYM, pnew2l[ni] → mc],
 {ni, 1, (zmax[Length[b] - 1 + 1] - (zmin[Length[b] - 1 + 1] - 1 + b[[Length[b] - 1]] / 5)) / (b[[Length[b] - 1]] / 5)}];
bc3 = Extract[sheetC[[Length[b] - 1]], {ypc5[Length[b] - 1], from5[Length[b] - 1]}];
sheetCXPYP = ReplacePart[sheetCXPYP, pnew2l[0] → bc3];


(*cxmym*)
sheetCXMYM = Table[Map[Prepend[#, CXM] &, sheetCYM[[i]]], {i, 1, Length[b] - 1}];
sheetCXMYM = Table[Map[Most[#] &, sheetCXMYM[[i]]], {i, 1, Length[b] - 1}];
Do[
 Do[
  bc = Extract[sheetCYM[[i - 1]], pold3[i, ni]];
  sheetCXMYM = ReplacePart[sheetCXMYM, pnew3[i, ni] → bc[[1]]]
  , {ni, 0, (zmax[i] - (zmin[i] - 1 + b[[i]] / 5)) / (b[[i]] / 5)}], {i, 2, Length[b] - 1}];

Do[
 Do[
   bc = Mean[Table[Extract[sheetCYM[[i + 1]], pold4[i, ni, w]][[1]], {w, 0, b[[i]] / b[[i + 1]] - 1}]];
   sheetCXMYM = ReplacePart[sheetCXMYM, pnew4[i, ni] → bc], {ni, 0, (zmax[i + 1] - (zmin[i + 1] - 1 + b[[i]] / 5)) / (b[[i]] / 5)}];
 , {i, 1, Length[b] - 2}];
Do[
 sheetCXMYM = ReplacePart[sheetCXMYM, pnew4l[ni] → mc],
 {ni, 1, (zmax[Length[b] - 1 + 1] - (zmin[Length[b] - 1 + 1] - 1 + b[[Length[b] - 1]] / 5)) / (b[[Length[b] - 1]] / 5)}];
bc4 = Extract[sheetC[[Length[b] - 1]], {ypc5[Length[b] - 1], to5[Length[b] - 1]}];
sheetCXPYP = ReplacePart[sheetCXPYP, pnew4l[0] → bc4];

(*advection dispersion inactivation irriversible removal equation*)
sheetC =
 Δt * (sheetDX / rd * (sheetCXP - 2 * sheetC + sheetCXM) / sheetΔX^2 - sheetU * (sheetCXP - sheetCXM) / (2 * sheetΔX) +
      sheetDY / rd * (sheetCYP - 2 * sheetC + sheetCYM) / sheetΔY^2 - sheetV * (sheetCYP - sheetCYM) / (2 * sheetΔY) +
      sheetDXY / rd * (sheetCXPYP - sheetCXPYM - sheetCXMYP + sheetCXMYM) / (2 * sheetΔX * sheetΔY) - λ * sheetC) + sheetC;


re[t] = {t, sheetC[[2]][[7]][[27]]}

, {o, lt / Δt}];

If[Abs[re[t][[2]] - re[t - lt][[2]]] < 0.05 * re[t - lt][[2]], Break[]], {or, 1000}]

MemoryInUse[];
Time = SessionTime[] - start ;
(*plot graph*)
outX = Flatten[sheetX];
outY = Flatten[sheetY];
outC = Flatten[sheetC];
m = Length[Flatten[sheetX]];
Do[outC[[i]] = If[outC[[i]] < 0, 0, outC[[i]]], {i, 1, m}];
output = Table[{outX[[i]], outY[[i]], outC[[i]]}, {i, 1, m}];
ListContourPlot[output, PlotRange → {{0, lx}, {0, ly}, {0, mc}}, ContourLabels → {All, FontSize → 15}, PlotLegends → Automatic]
ListLinePlot[Table[re[i], {i, 0, t, Δt}]]
sheetC[[2]][[7]][[27]]

Export["/Users/YUMETO/Desktop/dsinario50500.xlsx", sheetC]
Export["/Users/YUMETO/Desktop/esinario50500.xlsx", Table[re[i], {i, 0, t, Δt}]]

MemoryInUse[]
Time = SessionTime[] - start
```

Appendix D

AdVF simulation profile after 2-D transport model in Katsuragawa basin with 0.164 day^{-1} reduction rate coefficient; I is the injection point, W is the withdrawal point.

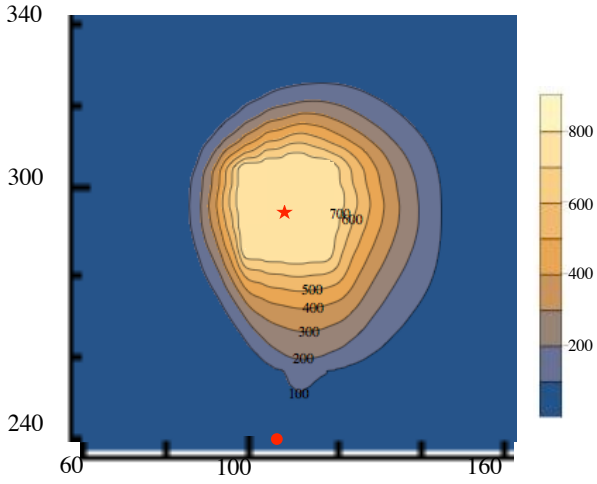

case 1

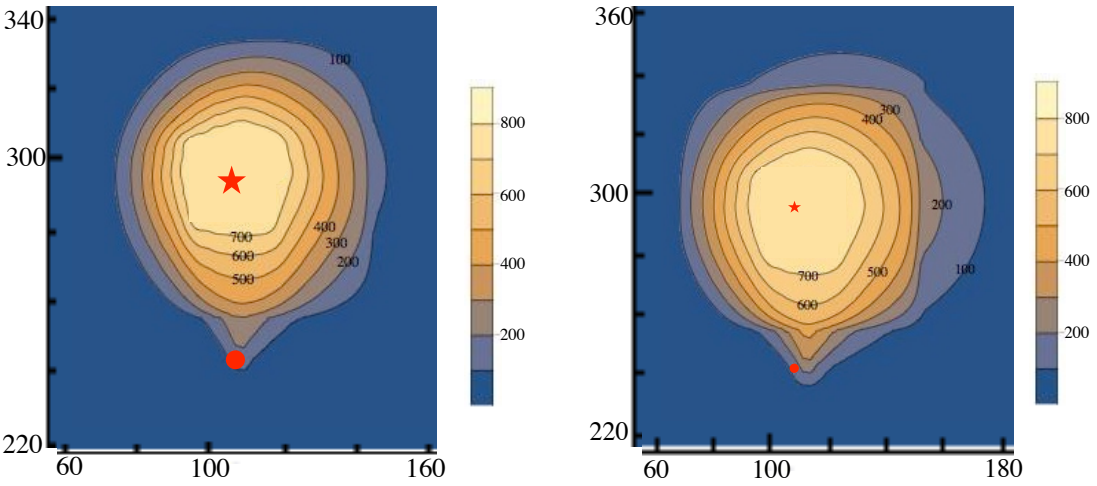

case 2 case 3

A: the simulation in case1 with 50 meters between the injection and withdrawal point and the injection rate of 500 m^3/day (I = 828 MPNIU/L, W=25.1 MPNIU/L)
B: the simulation in case1 with 50 meters between the injection and withdrawal point and the injection rate of 1000 m^3/day (I = 828 MPNIU/L, W=103.9 MPNIU/L)
C: the simulation in case1 with 50 meters between the injection and withdrawal point and the injection rate of 2000 m^3/day (I = 828 MPNIU/L, W=188.9 MPNIU/L)

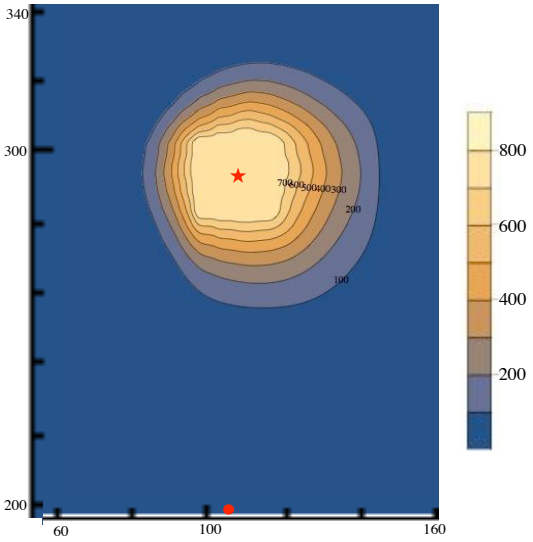

case 4

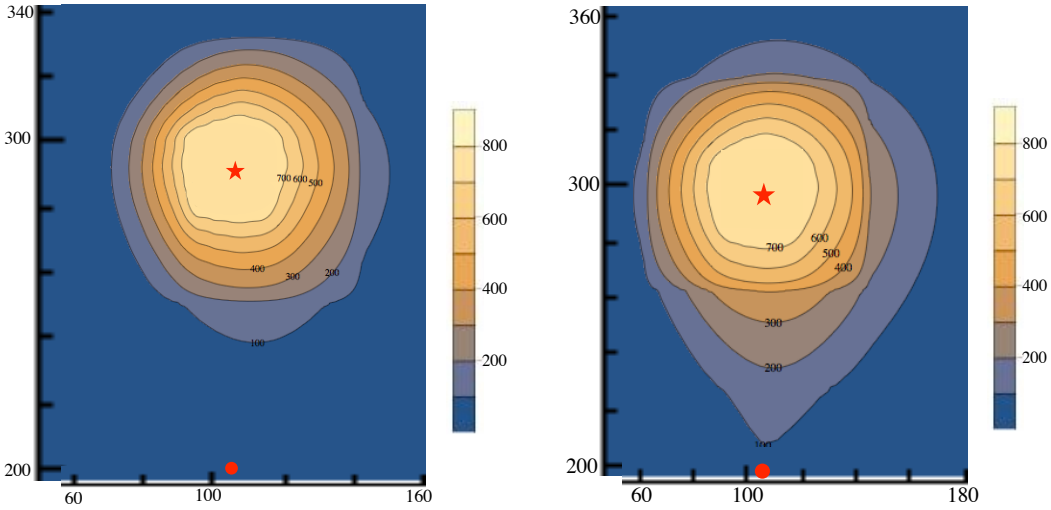

case 5 case 6

D: the simulation in case1 with 50 meters between the injection and withdrawal point and the injection rate of 500 m^3/day (I = 828 MPNIU/L, W=0.49 MPNIU/L)
E: the simulation in case1 with 50 meters between the injection and withdrawal point and the injection rate of 1000 m^3/day (I = 828 MPNIU/L, W=9.61 MPNIU/L)
F: the simulation in case1 with 50 meters between the injection and withdrawal point and the injection rate of 2000 m^3/day (I = 828 MPNIU/L, W=52.6 MPNIU/L)

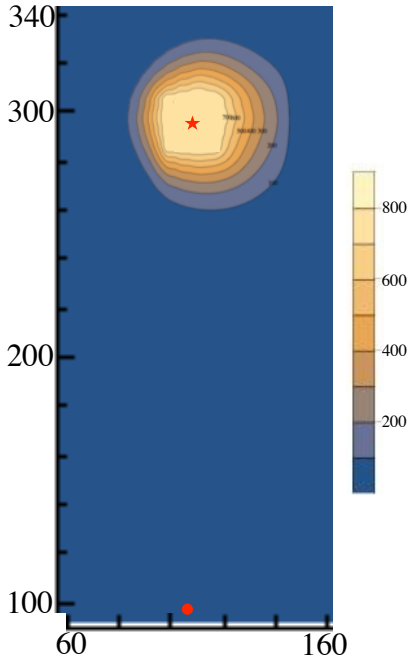

case 7

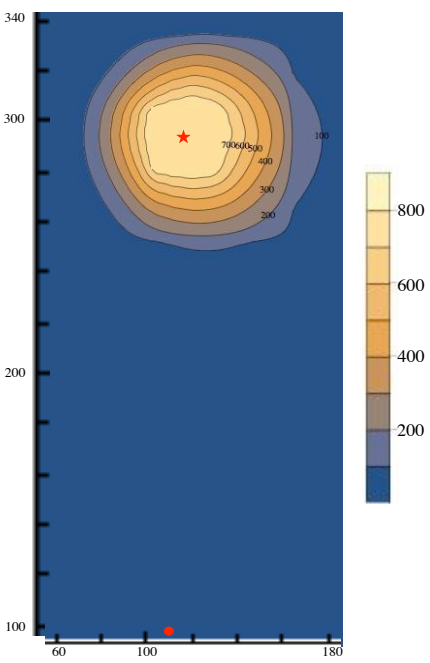

case 8

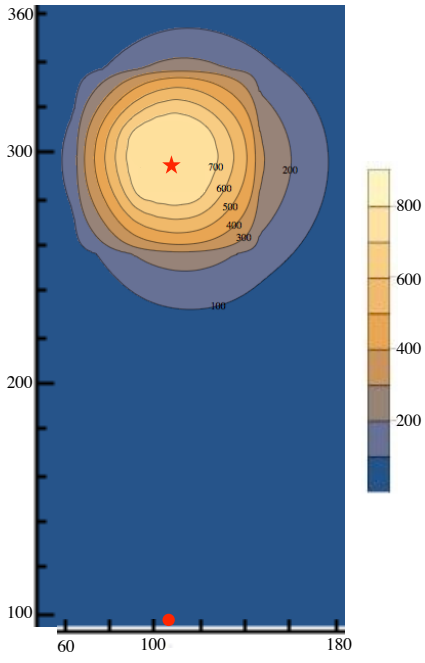

case 9

G: the simulation in case1 with 50 meters between the injection and withdrawal point and the injection rate of 500 m^3/day (I = 828 MPNIU/L, W=0.000062 MPNIU/L)
H: the simulation in case1 with 50 meters between the injection and withdrawal point and the injection rate of 1000 m^3/day (I = 828 MPNIU/L, W=0.031 MPNIU/L)
I: the simulation in case1 with 50 meters between the injection and withdrawal point and the injection rate of 2000 m^3/day (I = 828 MPNIU/L, W=1.18 MPNIU/L)

RV simulation profile after 2D transport model in Katsuragawa basin with 0.168 day^{-1} reduction rate coefficient; I is the injection point, W is the withdrawal point.

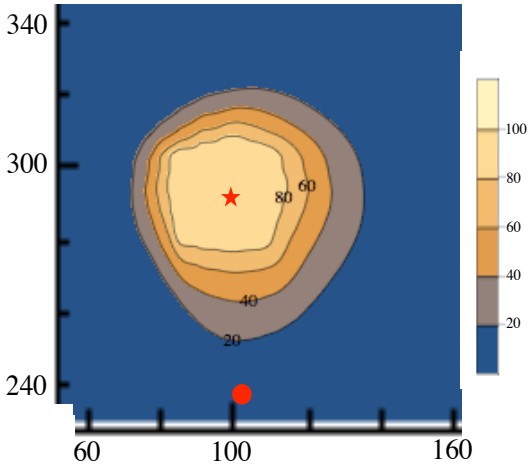

case 1

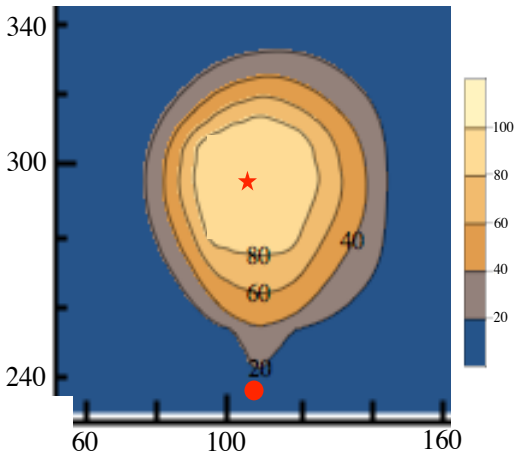

case 2

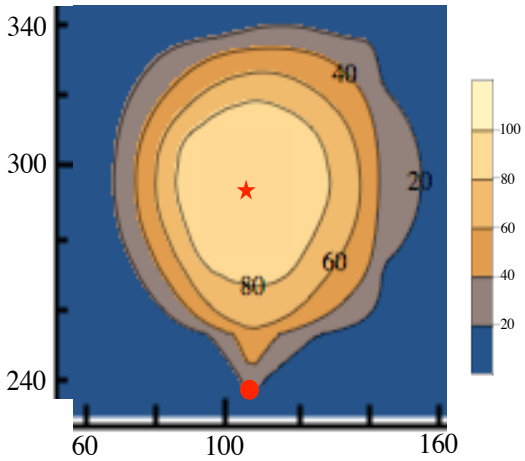

case 3

A: the simulation in case1 with 50 meters between the injection and withdrawal point and the injection rate of 500 m^3/day (I = 103 MPNIU/L, W=6.9 MPNIU/L)
B: the simulation in case1 with 50 meters between the injection and withdrawal point and the injection rate of 1000 m^3/day (I = 103 MPNIU/L, W=20.54 MPNIU/L)
C: the simulation in case1 with 50 meters between the injection and withdrawal point and the injection rate of 2000 m^3/day (I = 103 MPNIU/L, W=57.9 MPNIU/L)

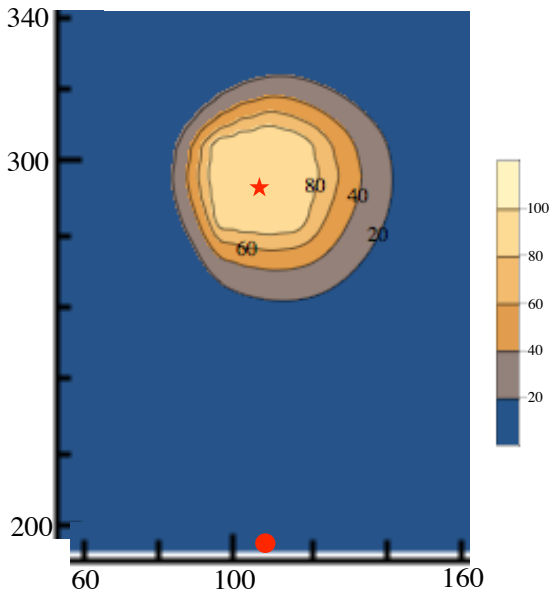

case 4

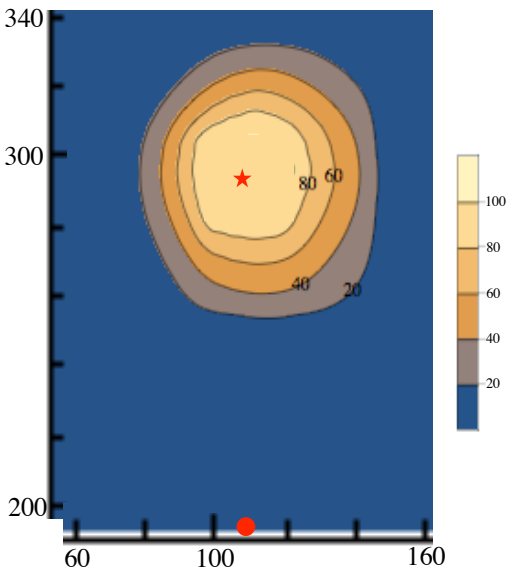

case 5

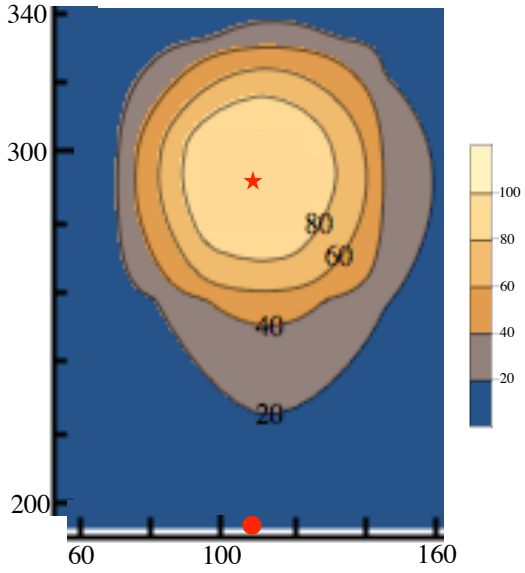

case 6

D: the simulation in case1 with 50 meters between the injection and withdrawal point and the injection rate of 500 m^3/day (I = 103 MPNIU/L, W=0.42 MPNIU/L)
E: the simulation in case1 with 50 meters between the injection and withdrawal point and the injection rate of 1000 m^3/day (I = 103 MPNIU/L, W=3.93 MPNIU/L)
F: the simulation in case1 with 50 meters between the injection and withdrawal point and the injection rate of 2000 m^3/day (I = 103 MPNIU/L, W=13.3 MPNIU/L)

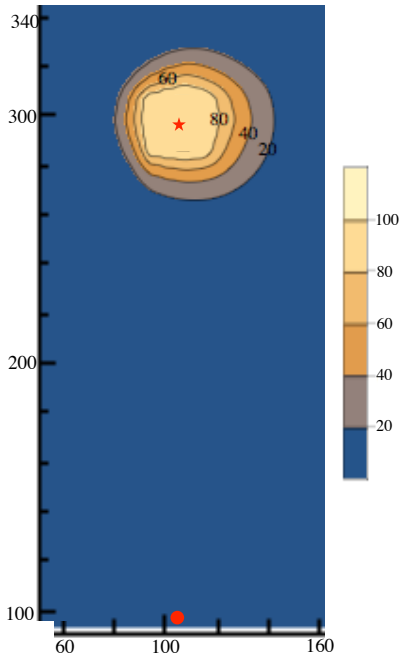

case 7

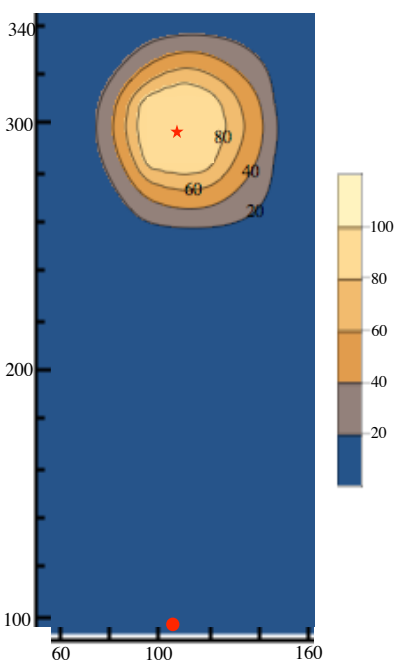

case 8

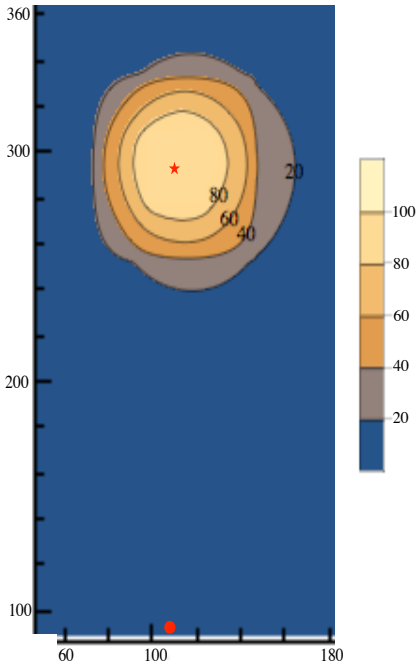

case 9

G: the simulation in case1 with 50 meters between the injection and withdrawal point and the injection rate of 500 m^3/day (I = 103 MPNIU/L, W=0.00042 MPNIU/L)
H: the simulation in case1 with 50 meters between the injection and withdrawal point and the injection rate of 1000 m^3/day (I = 103 MPNIU/L, W=0.056 MPNIU/L)
I: the simulation in case1 with 50 meters between the injection and withdrawal point and the injection rate of 2000 m^3/day (I = 103 MPNIU/L, W=0.85 MPNIU/L)

Appendix E

The ratio of the virus detection between ICC-(RT)-qPCR and ICC-(RT)-PCR

The ICC-PCR and ICC-qPCR was compared for AdVF and RV.

The results of AdVF sensitivity between ICC-PCR and qPCR
The ratio between ICC-PCR and ICC-qPCR of AdVF was calculated by the results as shown in Figure E1. The ICC-PCR result was calculated in MPNIU/μL with 2.3 MPNIU/μL (3:0:0). However, the concentration detected by ICC-qPCR is 100 copies/μL. Thus, the ratio between ICC-qPCR and ICC-PCR is approximately 1:50.

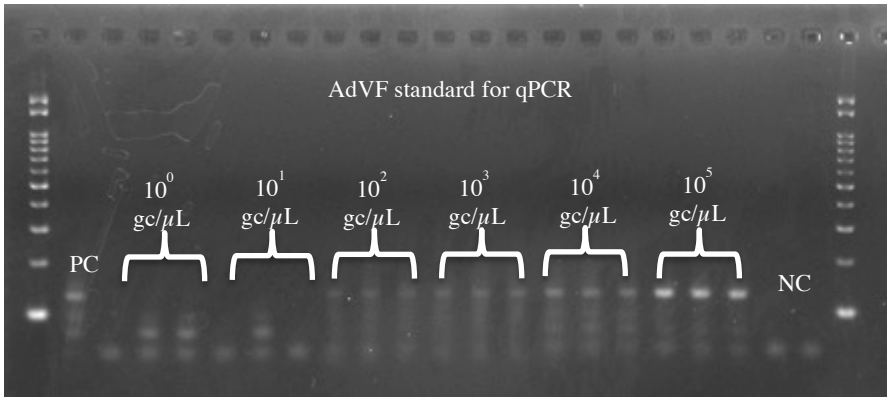

Figure E1: the sensitivity of AdVF between ICC-PCR and ICC-qPCR

The results of RV sensitivity between ICC-PCR and qPCR
The ratio between ICC-RT-PCR and ICC-RT-qPCR of RV was calculated by the results as shown in Figure E2. The ICC-PCR result was calculated in MPNIU/μL with 2.3 MPNIU/μL (3:0:0). However, the concentration detected by ICC-RT-qPCR is 1000 copies/μL. Thus, the ratio between ICC-qPCR and ICC-PCR is approximately 1:500.

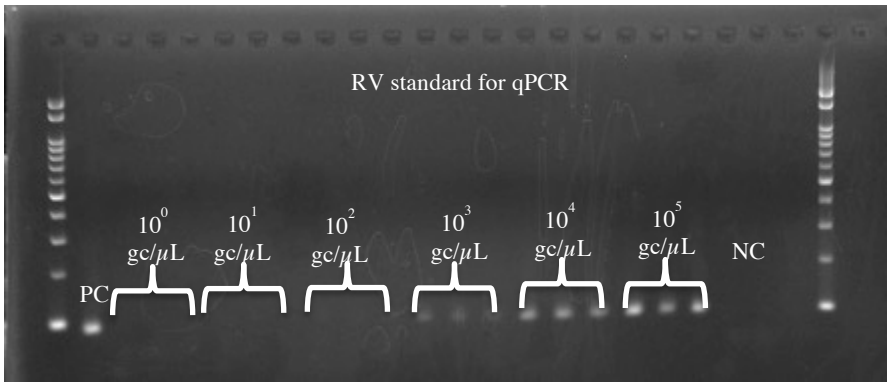

Figure E2: the sensitivity of RV between ICC-PCR and ICC-qPCR